

AN ABSTRACT OF THE THESIS OF

Anthony William Sorentino for the degree of Master of Science in Civil Engineering
presented on March 20, 2012.

Title: Behavior and Analysis of Pile Caps with Poor Anchorage Details.

Abstract approved: _____

Christopher C. Higgins

Pile caps are structural elements used to transmit loads from structural columns into pile groups. A pile cap is generally constructed of reinforced concrete and contains only minimal flexural reinforcing steel. Using modern design methods, the anchorage of the flexural steel may limit the design capacity of existing pile caps. To develop new data on performance of existing pile caps with poorly detailed flexural reinforcing steel, four pile cap specimens were constructed and tested. The specimens were full-size representations of in-situ pile caps used in a mid-rise hospital building. Materials used to construct the specimens were selected to represent those of the in-situ pile caps. Tests were conducted until failure or the maximum capacity of the hydraulic loading system was achieved. Design methods were used to compare the predicted design strength with the measured experimental strength of the specimens. Based on the observed experimental

response, specimens exhibited either two-way punching shear or one-way shear failure modes. Widespread yielding and little relative slip of the embedded reinforcing steel were observed. The modern design methods were sometimes conservative and sometimes unconservative in predicting the strength of the specimens.

©Copyright by Anthony Sorentino

March 20, 2012

All Rights Reserved

BEHAVIOR and ANALYSIS of PILE CAPS with POOR ANCHORAGE DETAILS

by

Anthony William Sorentino

A THESIS

Submitted to

Oregon State University

In partial fulfillment of

the requirements for the

degree of

Master of Science

Presented March 20, 2012

Commencement June 2012

Master of Science thesis of Anthony William Sorentino presented on March 20, 2012

APPROVED:

Major Professor, representing Civil Engineering

Head of the School of Civil and Construction Engineering

Dean of the Graduate School

I understand that my thesis will become part of the permanent collection of Oregon State University libraries. My signature below authorizes release of my thesis to any reader upon request.

Anthony William Sorentino, Author

ACKNOWLEDGEMENTS

Susan Sorentino: For the never-ending love and support, I could have never made it this far without you.

Christopher C. Higgins, PhD: Providing guidance throughout my career at Oregon State University.

Degenkolb Engineers: Providing Funding as well as assistance in the experimental design and procedure.

CONTRIBUTIONS OF AUTHORS

TABLE OF CONTENTS

	<u>Page</u>
1.0 INTRODUCTION and BACKGROUND	1
2.0 LITERATURE REVIEW	2
2.1 Experimental Studies	2
2.2 Design and Analysis Methods	5
2.3 Current Design Provisions	10
3.0 EXPERIMENTAL PROGRAM	11
3.1 Construction and Materials	12
4.2 Instrumentation	16
3.3 Testing Methodology	18
4.0 EXPERIMENTAL RESULTS	37
4.1 Pile Cap #3	38
4.2 Pile Cap #4	39
4.3 Pile Cap #5	39
4.4 Pile Cap #7	41
4.5 Experimental Conclusions	42
5.0 ANALYSIS	64
5.1 Finite Element Models	64
5.1.1 Element Section Properties	65

TABLE OF CONTENTS (Continued)

	<u>Page</u>
5.1.2 Material Properties	65
5.1.3 Boundary Conditions and Loading	66
5.1.4 Assembly	67
5.1.5 Finite Element Modeling Results	67
5.2 Strut and Tie Models	74
5.2.1 S&T Results.....	75
5.3 One-way and Two-Way Shear Models.....	77
6.0 SUMMARY and CONCLUSIONS	82
REFERENCES	85
APPENDICES	87
APPENDIX A – Original Design Drawings	88
APPENDIX B – Shop Drawings of In situ Pile Caps.....	92
APPENDIX C – Concrete Mix Design for In situ Pile Caps.....	97
APPENDIX D – Concrete Core Strengths for In Situ Pile Caps.....	103
APPENDIX E – Concrete Mix Design for Pile Cap Specimens	107
APPENDIX F – Experimental Data for All Pile Cap Specimens.....	111

LIST OF FIGURES

<u>Figure</u>	<u>Page</u>
Figure 3.1.1a: Reference location for pipe bearing plates in Figure 2.1b.....	20
Figure 3.1.1: b) Side view and c) top view of bearing plate with reinforcing details at top of pipe pile	20
Figure 3.1.2a: Plan View – Pile Cap #3.....	21
Figure 3.1.2b: Reinforcement placement and formwork for Pile Cap #3.....	21
Figure 3.1.2c: Elevation View - Pile Cap #3	22
Figure 3.1.2d: Elevation view of completed specimen on strong floor – Pile Cap #3	22
Figure 3.1.3a: Plan view for Pile Cap #4.....	23
Figure 3.1.3b: Reinforcement placement and formwork for Pile Cap #4.....	23
Figure 3.1.3c: Elevation plan – Pile Cap #4	24
Figure 3.1.3d: Elevation view of completed specimen on strong floor – Pile Cap #4	24
Figure 3.1.4a: Plan View – Pile Cap #5.....	25
Figure 3.1.4b: Reinforcement placement and formwork for Pile Cap #5.....	25
Figure 3.1.4c: Elevation View – Pile Cap #5	26
Figure 3.1.4d: Elevation view of completed specimen on strong floor – Pile Cap #5	26
Figure 3.1.5a: Plan view – Pile Cap #7.....	27
Figure 3.1.5b: Reinforcement placement and formwork for Pile Cap #7.....	27
Figure 3.1.5c: Elevation View – Pile Cap #7	28
Figure 3.1.5d: Elevation view of completed specimen on strong floor – Pile Cap #7	28

LIST OF FIGURES (Continued)

<u>Figure</u>	<u>Page</u>
Figure 3.2.1: Example strain gage location on reinforcing bar near bearing plate of pipe pile	29
Figure 3.2.2: Example reinforcing steel slip displacement sensor.....	29
Figure 3.2.3 Example vertical displacement measurements of specimen relative to strong floor (yellow arrows) and pipe motion relative to concrete (red arrow).....	30
Figure 3.2.4: Instrumentation plan for specimen #3	31
Figure 3.2.5: Instrumentation plan for specimen #4.....	32
Figure 3.2.6: Instrumentation plan for specimen #5	33
Figure 3.2.7: Instrumentation plan for specimen #7	34
Figure 3.3.1: Schematic of test setup	35
Figure 3.3.2: Experimental setup with specimen #5.....	35
Figure 3.3.3: W14x99 profile attached to 3 in. bearing plate (note: white material is hydrostone used to grout baseplate).....	36
Figure 3.3.4: Hydraulic Cylinder and Load cell for center pile control with specimen #5	36
Figure 4.1: Example of spurious slip data due to concrete cracking affecting the instrumentation mount.	44
Figure 4.3: Column load vs. Centerline vertical displacement – Pile Cap #3	45
Figure 4.4: Crack maps – Pile Cap #3	46
Figure 4.5: Failure of Pile Cap #3	47

LIST OF FIGURES (Continued)

<u>Figure</u>	<u>Page</u>
Figure 4.6: Slip of reinforcement – Pile Cap #3	47
Figure 4.7: Conditions at failure for Pile Cap #3.....	48
Figure 4.8: Column load vs. Time – Pile Cap #4	49
Figure 4.9: Column load vs. Centerline vertical displacement – Pile Cap #4	49
Figure 4.10: Crack maps – Pile Cap #4	50
Figure 4.11a: Failure of Pile Cap #4.....	51
Figure 4.11b: Punching of 3 in. thick bearing plate at failure of Pile Cap #4	51
Figure 4.12: Slip of reinforcement – Pile Cap #4.....	52
Figure 4.13: Conditions at failure for Pile Cap #4.....	53
Figure 5.14: Column load vs. Time – Pile Cap #5	54
Figure 4.15: Column load vs. Centerline vertical displacement – Pile Cap #5	54
Figure 4.16: Crack maps – Pile Cap #5	55
Figure 5.17a: Failure of Pile Cap #5.....	56
Figure 4.17b: Punching of 3 in. thick bearing plate at failure of Pile Cap #5	56
Figure 4.18: Slip of reinforcement – Pile Cap #5.....	57
Figure 4.19: Conditions at failure for Pile Cap #5.....	58
Figure 4.20: Column load vs. Time – Pile Cap #7	59
Figure 4.21: Column load vs. Centerline vertical displacement – Pile Cap #7 (note: displacement was reset to zero for different configurations).....	59
Figure 4.22: Crack maps – Pile Cap #7	60

LIST OF FIGURES (Continued)

<u>Figure</u>	<u>Page</u>
Figure 4.23: Slip of Reinforcement for Pile Cap #7 with 7 and 6 piles intact	61
Figure 4.24: Pile Cap #7 after testing with piles 1, 4 and the center pile removed	61
Figure 4.25: Slip of Reinforcement for Pile Cap #7 with 4 piles.	62
Figure 4.26: Conditions at maximum load for Pile Cap #7	63
Figure 5.3a: Principal stress tensor Strut A (see Fig. 6.12) in Pile Cap #3.....	68
Figure 5.3b: Principal compression Strut A (see Fig. 6.12) in Pile Cap #3	68
Figure 5.3c: Principal stress tension Strut A (see Fig. 6.12) in Pile Cap #3	69
Figure 5.3d: Principal stress tensor Strut B (see Fig. 6.12) in Pile Cap #3.....	69
Figure 5.3e: Principal compression Strut B (see Fig. 6.12) in Pile Cap #3	69
Figure 5.3f: Principal tension Strut B (see Fig. 6.10) in Pile Cap #3	70
Figure 5.4a: Principal stress tensors cut along strut in Pile Cap #4	70
Figure 5.4b: Principal compression cut along strut in Pile Cap #4.....	70
Figure 5.4c: Principal tension stress cut along strut in Pile Cap #4.....	71
Figure 5.5a: Principal stress tensors cut along strut in Pile Cap #5	71
Figure 5.5b: Principal compression stresses cut along strut in Pile Cap #5.....	71
Figure 5.5c: Principal tension cut along strut in Pile Cap #5.....	72
Figure 5.7a: Principal compression Strut A (see Fig. 6.14) in Pile Cap #7	72
Figure 5.7b: Principal tension Strut A (see Fig. 6.14) in Pile Cap #7	72
Figure 5.7c: Principal stress tensor Strut B (see Fig. 6.14) in Pile Cap #7	73
Figure 5.7d: Principal compression Strut B (see Fig. 6.14) in Pile Cap #7	73

LIST OF FIGURES (Continued)

<u>Figure</u>	<u>Page</u>
Figure 5.7e: Principal tension Strut B (see Fig. 6.14) in Pile Cap #7	73
Figure 5.8: Pile Cap #3 Normalized reinforcement strain	79
Figure 5.9: Pile Cap #3 Normalized reinforcement strain	80
Figure 5.10: Pile Cap #4 Normalized reinforcement strain	80
Figure 5.11: Pile Cap #5 Normalized reinforcement strain	80
Figure 5.12: Pile Cap #3 assumed S&T geometry.....	81
Figure 5.13: Pile Cap #4 and #5 assumed S&T geometry.....	81
Figure 5.14: Pile Cap #7 assumed S&T geometry.....	82

LIST OF TABLES

<u>Table</u>	<u>Page</u>
Table 3.1 : Reinforcing steel material properties.....	14
Table 3.2a: Concrete compressive properties.	15
Table 3.2b: Concrete tensile properties.	16
Table 4.1: Key data from all tests.	43
Table 5.1: Analysis Results	79

LIST OF APPENDIX FIGURES

<u>Figure</u>	<u>Page</u>
Figure A.1: Original Design Drawing (1 of 3)	89
Figure A.2: Original Design Drawing (2 of 3)	90
Figure A.3: Original Design Drawing (3 of 3)	91
Figure B.1: Shop Drawings of In-Situ Pile Caps (1 of 4).....	93
Figure B.2: Shop Drawings of In-Situ Pile Caps (2 of 4).....	94
Figure B.3: Shop Drawings of In-Situ Pile Caps (3 of 4).....	95
Figure B.4: Shop Drawings of In-Situ Pile Caps (4 of 4).....	96
Figure C.1: Concrete Mix Design for In-Situ Pile Caps (1 of 5).....	98
Figure C.2: Concrete Mix Design for In-Situ Pile Caps (2 of 5).....	99
Figure C.3: Concrete Mix Design for In-Situ Pile Caps (3 of 5).....	100
Figure C.4: Concrete Mix Design for In-Situ Pile Caps (4 of 5).....	101
Figure C.5: Concrete Mix Design for In-Situ Pile Caps (5 of 5).....	102
Figure D.1: Concrete Core Strengths for In-Situ Pile Caps (1 of 3).....	104
Figure D.2: Concrete Core Strengths for In-Situ Pile Caps (2 of 3).....	105
Figure D.3: Concrete Core Strengths for In-Situ Pile Caps (3 of 3).....	106
Figure E.1: Concrete Mix Design for Pile Cap Specimens (1 of 3)	108
Figure E.2: Concrete Mix Design for Pile Cap Specimens (2 of 3)	109
Figure E.3: Concrete Mix Design for Pile Cap Specimens (3 of 3)	110
Figure F3.1: Column Loading – Pile Cap #3.....	112
Figure F3.2: Column load vs. Strain (1 of 4) – Pile Cap #3	112
Figure 3.3: Column load vs. Strain (2 of 4) – Pile Cap #3	113

LIST OF APPENDIX FIGURES (Continued)

<u>Figure</u>	<u>Page</u>
Figure F3.4: Column load vs. Strain (3 of 4) – Pile Cap #3	113
Figure F3.5: Column load vs. Strain (4 of 4) – Pile Cap #3	114
Figure F3.6: Column load vs. Displacement (1 of 2) – Pile Cap #3.....	114
Figure F3.7: Column load vs. Displacement (2 of 2) – Pile Cap #3.....	115
Figure F3.8: Column load vs. Slip (1 of 2) – Pile Cap #3	115
Figure F3.9: Column load vs. Slip (2 of 2) – Pile Cap #3	116
Figure F4.1: Loading – Pile Cap #4.....	116
Figure F4.2: Column load vs. Strain (1 of 4) – Pile Cap #4	117
Figure F4.3: Column load vs. Strain (2 of 4) – Pile Cap #4	117
Figure F4.4: Column load vs. Strain (3 of 4) – Pile Cap #4	118
Figure F4.5: Column load vs. Strain (4 of 4) – Pile Cap #4	118
Figure F4.6: Column load vs. Displacement (1 of 2) – Pile Cap #4.....	119
Figure F4.7: Column load vs. Displacement (2 of 2) – Pile Cap #4.....	119
Figure F4.8: Column load vs. Slip (1 of 2) – Pile Cap #4	120
Figure F5.1: Loading – Pile Cap #5.....	121
Figure F5.2: Column load vs. Strain (1 of 4) - Pile Cap #5 (5 piles).....	121
Figure F5.3: Column load vs. Strain (2 of 4) – Pile Cap #5 (5 piles).....	122
Figure F5.4: Column load vs. Strain (3 of 4) – Pile Cap #5	122
Figure F5.5: Column load vs. Strain (4 of 4) – Pile Cap #5	123
Figure F5.6: Column load vs. Displacement (1 of 2) – Pile Cap #5.....	123
Figure F5.7: Column load vs. Displacement (2 of 2) – Pile Cap #5.....	124

LIST OF APPENDIX FIGURES (Continued)

<u>Figure</u>	<u>Page</u>
Figure F5.8: Column load vs. Slip (1 of 2) – Pile Cap #5	124
Figure F5.9: Column load vs. Slip (2 of 2) – Pile Cap #5	125
Figure F7.1: Column Load vs. Time – Pile Cap # 7	126
Figure F7.2: Column load vs. Strain (1 of 4) – Pile Cap #7 (7 and 6 piles)	126
Figure F7.3: Column load vs. Strain (2 of 4) – Pile Cap #7 (7 and 6 piles)	127
Figure F7.4: Column load vs. Strain (3 of 4) – Pile Cap #7 (7 and 6 piles)	127
Figure F7.5: Column load vs. Strain (4 of 4) – Pile Cap #7 (7 and 6 piles)	128
Figure F7.6: Column load vs. Strain (1 of 4) – Pile Cap #7 (4 Piles).....	128
Figure F7.7: Column load vs. Strain (2 of 4) – Pile Cap #7 (4 Piles).....	129
Figure F7.8: Column load vs. Strain (3 of 4) – Pile Cap #7 (4 Piles).....	129
Figure 7.9: Column load vs. Strain (4 of 4) – Pile Cap #7 (4 Piles).....	130
Figure F7.10: Column load vs. Displacements (1 of 2) – Pile Cap #7 (7 and 6 Piles)	130
Figure F7.11: Column load vs. Displacement (2 of 2) – Pile Cap #7 (7 and 6 Piles)	131
Figure F7.12: Column load vs. Displacement (1 of 2) – Pile Cap #7 (4 Piles)	131
Figure F7.13: Column load vs. Displacement (2 of 2) – Pile Cap #7 (4 Piles)	132
Figure F7.14: Column load vs. Slip (1 of 3) – Pile Cap #7 (7 and 6 Piles)	132
Figure F7.15: Column load vs. Slip (2 of 3) – Pile Cap #7 (7 and 6 Piles)	133
Figure F7.16: Column load vs. Slip (3 of 3) – Pile Cap #7 (7 and 6 Piles)	133
Figure F7.17: Column load vs. Slip (1 of 3) – Pile Cap #7 (4 Piles).....	134

LIST OF APPENDIX FIGURES (Continued)

<u>Figure</u>	<u>Page</u>
Figure F7.18: Column load vs. Slip (2 of 3) – Pile Cap #7 (4 Piles).....	134
Figure F7.19: Column load vs. Slip (3 of 3) – Pile Cap #7 (4 Piles).....	135

1.0 INTRODUCTION and BACKGROUND

Pile caps are structural elements used to transmit loads from structural columns into pile groups. A pile group consists of a number of piles driven into soil within relatively close proximity to each other. The piles resist applied vertical forces through skin friction and/or end bearing. Pile caps link the pile group together and distribute the column load to them. A pile cap is generally constructed of reinforced concrete. They often do not use transverse reinforcing steel and contain only minimal flexural reinforcing steel. The geometry of pile caps can vary widely depending on the number of piles, the relative locations of the piles to each other, and the column reaction force. However, pile caps generally have aspect ratios that would lead them to be considered as deep beams with shear dominated response.

Modern design provisions for pile caps require adequate anchorage of reinforcing steel with hooks and bends at the terminated ends. These details ensure that the reinforcing steel can achieve the yield stress. Earlier designs, such as those prior to the 1980's, commonly used straight bar terminations for the flexural steel. The effectiveness of flexural reinforcing steel with straight-bar terminations in large-sized pile caps is uncertain. When using modern design provisions, such as strut-and-tie methods for evaluation, the poorly detailed flexural steel may limit the strength of the cap. This was a concern in a recent building renovation study for the Veterans Affairs Medical Center (VA) in Portland, OR.

To provide for increasing demand for services, the hospital is considering adding floors to one of the buildings on the medical campus. The ability of the existing

foundations to support higher column axial loads could limit the opportunity to add more stories to the building. The steel columns in the VA Hospital are supported on foundations made up of end-bearing steel pipe piles with reinforced concrete pile caps. Pile cap geometry varies depending on the number of piles in the particular pile cap. Each pipe pile is designed to resist 195 kips of vertical force. A feasibility study conducted by an engineering firm to evaluate the potential for adding an additional story level found that four different pile group arrangements would potentially be overstressed under additional gravity loads associated with the building expansion. To minimize potential costly and disruptive pile cap remediation, full-scale tests of each potentially deficient pile cap were conducted to determine their maximum vertical load carrying capacities. These tests, the results, and findings are reported in this thesis.

2.0 LITERATURE REVIEW

A review of the available technical literature on the behavior and strength of pile caps was performed. The review considered past experimental studies as well as analysis and design methodologies and the findings are summarized below.

2.1 Experimental Studies

Pile caps were first looked at by Blevot *et al.* [1967]. The focus of this study was the influence of different reinforcement arrangements on the strength of pile caps. Approximately 100 tests were performed on what were mostly half-scale specimens. Specimens contained multiple pile arrangements. For the common four pile symmetric cap it was found that the most effective reinforcement arrangement was to bunch the

reinforcement between piles. This arrangement provided an approximate 20 percent increase in failure strength. For a three pile cap it was found that spreading the reinforcement decreased strength by 50 percent.

Clarke [1973] became the next to do significant pile cap testing. A total of 15 half-scale tested were performed to examine four pile caps. Also looking at arrangement Clarke [1973] found that concentrating the reinforcement over the piles provided a 14 percent increase in strength compared to spreading the reinforcement.

The next to look at reinforcement distribution as a scope of their study were Adebar *et al.* [1990]. The main scope of this study was overall performance of the pile cap and will be discussed in more detail later; however reinforcement distribution was also examined. The study included six full-scale pile caps and results showed an increase in strength of 18.6 percent when bunched reinforcement was used over uniformly distributed reinforcement.

Suzuki *et al.* [1998] was the next to document studies that looked at the effect of reinforcement layout. In this test 28 specimens were used to determine the effect of bar arrangement as well as edge distance. Specimens were not full-scale, averaging approximately 88.9cm (35 in.) on each side and about 20 to 30 cm (8 to 12 in.) thick. Three main reinforcement layouts were used: uniform bar arrangement, bunched square arrangement, and edge distance varied arrangement. It was found that bunched reinforcement does provide for greater strength.

Edge distance is another factor of pile cap design that affects the behavior of the cap under loading. Minimal testing has been done on the effects of edge distance. Edge distance is defined as the distance from the pile to the outside edge of the pile cap.

Suzuki *et al.* [1998] found that increased edge distance provides greater yield strength and greater ultimate strength. Shorter edge distances tend to lead to shear failure quickly after initial flexural yield. Full-scale specimens may provide different failure modes, as aggregate size was not scaled in this test and the overall depth of the cap may provide for more linear stress distribution than in full scale testing.

Suzuki *et al.* [2000] establishes a similar approach as Suzuki *et al.* [1998]; this time focusing mainly on edge distance. This testing included 30 specimens similar in size to test done by Suzuki *et al.* [1998], with the exception of a few specimens as thick as 40cm (16 in.). All specimens were designed with respect to reinforcement, in an attempt to produce flexural failure. The main variance in specimens of same size was edge distance. Almost all specimens showed sudden increases in deflection at the estimated point of reinforcement yield. The following conclusions were drawn: the greater the edge distance the greater the cracking load, yield load, and maximum load and in the case of the thick pile caps the edge distance influenced both cracking and strain relationships in the specimens. This illustrates that the depth of concrete sections does affect the specimens' response.

Based on the literature review of the available experimental studies, pile caps are historically lightly reinforced elements. Shear reinforcement is almost never used and flexural reinforcement is often placed in a single layer. The amount and distribution of

reinforcement affects the pile cap strength. Two main types of flexural reinforcement are commonly used: 1) bunched reinforcement that places reinforcement groups over piles and 2) uniform reinforcement that distributes reinforcement uniformly across the pile plan dimensions. Past experimental studies have also focused on reduced-scale models consisting of a symmetrical four pile group.

2.2 Design and Analysis Methods

Clarke [1973] was also concerned with cause of failure and the best way to model the behavior of pile caps. Two main theories existed at that time. First, bending theory where the cap was modeled like a deep beam. The second was a truss analogy, which is the foundation of strut and tie modeling. Results showed that the truss model was the best way to model strength of pile caps with four or more piles.

Gogate *et al.* [1980] also examined the adequacy of the current state of design. At the time of testing in 1980 the ACI 318-77 proposed a design of the pile caps in shear similar to thin slabs. The shear limits provided in the code were found to be accurate only for slender specimens with aspect ratios greater than approximately six. Gogate *et al.* [1980] was the first to express the need for revisions to the current code in an attempt to better reflect the behavior of deep pile caps.

Adebar *et al.* [1990] attempted to model the behavior of pile caps using strut and tie. At the time the current ACI code 318-83 used a two part design method. ACI 318-83 simplified design to providing enough depth to account for shear using just the concrete

contribution and then provided reinforcement based on beam design. The experiment included 6 full scale pile caps with varying shape and reinforcement layouts. Approximate specimen size was 230cm wide by 180cm wide by 64cm deep (90 in x 70 in x 25in), making these some of the largest tested specimens to date. The specimens included four identical geometries with four piles, and two unique geometries. The four similar specimens A,B,D and E received varying amounts of reinforcement in grouped, uniform or a combination of placements. Pile cap F had the same pile spacing however any excess concrete that was not considered part of a strut was removed. The result of this was a cross or “+” shaped pile cap. The last pile cap (C) was cast with six piles with a rectangular cap. Failure loads were then compared with current codes as well as a proposed S&T model. The authors provided multiple findings. Increased reinforcement did provide greater strengths. The removal of excess concrete for cap F did not greatly affect ultimate strength, just 6% less. Specimen F was more brittle than the full specimen. Adebar *et al.* [1990] associated splitting of the compression struts as a source of failure. This occurs when the compression stress spreads horizontally and creates tension in the concrete which can lead to failure. This type of spreading occurs in what is referred to as “bottle-struts”. It is concluded that bearing stress can be an indicator of possible compression strut failure and by limiting bearing stress it is possible to limit this failure. Adebar *et al.* [1990] concluded that four of the six pile caps failed due to splitting of the struts before reinforcement yielding.

In an effort to examine his 1990 theory that bearing stress can control strut strengths in a pile cap, Adebar *et al.* [1993] tested 40 cylinders ranging from approximately 6 to 8 inch (15 to 20 cm) diameter. Maximum aggregate size for testing was 19mm (3/4

in). The results of this testing suggest that bearing ACI Building code 318-89 may not be conservative when regarding large structures such as pile caps. Results provided a maximum bearing stress limit dependent on the aspect ratio of the compression strut, amount of confinement, as well as geometry of the compression zone.

Adebar *et al.* [1996] published work on how to design pile caps using strut and tie models. This work includes an in-depth discussion on what the current design methods are. The authors did not test any pile caps exclusively but instead used data gathered by earlier works including Deutsche and Walker [1963], Blevot *et al.* [1967], Clarke [1973], Gogate *et al.* [1980] and Adebar *et al.* [1990]. A total of 48 pile caps are compared in this study. Each is predicted using ACI '77, ACI '83, ACI (11-8), the CRSI handbook as well as the authors S&T model. The results do not show the S&T to be more effective when comparing experimental to predicted strengths however the coefficient of variation is slightly smaller. An important conclusion is that all methods are still conservative Adebar *et al.* [1996] based his S&T model on Adebar *et al.* [1993] and limits the bearing stress based on confinement of the strut as well as its aspect ratio. A conclusion is reached that by combining the authors bearing stress limit with ACI Code shear design procedure it is possible to cover a wide range of slenderness; ACI procedure controlling more slender caps while the authors check limiting deep caps. It is concluded that any pile shear force within a critical section (d or $d/2$) from the face can be ignored because in these instances bearing will control.

Park *et al.* [2008] did a comparative study of existing data from previous pile cap testing. No original data was presented in this report. Analysis of 6 different design methods was used. Data from Clarke [1973], Suzuki *et al.* [1998], [1999], [2000], Otuski

[2002], and Gogate *et al.* [1980] were selected, a total of 116 mostly scaled pile cap tests were selected. In this study six design methods were used, special provisions for slabs and footings of ACI 318-99, CRSI design handbook [2002], and strut and tie methods in ACI 318-05, CSA [2004], Adebar *et al.* [1996], and Park *et al.* [2008]. Initial investigations were selected to find the accuracy (ultimate test load over predicted load) and variation of the different methods. Results were as follows: ACI318-99 mean 1.97 COV 0.17, CRSI mean 1.96 COV 0.17, ACI318-05 mean 1.73 COV .24, CSA mean 1.74 COV 0.20, Adebar *et al.* [1996] mean 1.44 COV 0.18, and authors mean 1.41 COV 0.18. Initial results showed that the most accurate methods were Adebar *et al.* [1996] and Park *et al.* [2008]. Initial results were based on the limiting failure mode of each method versus the failure load. When considering failure type the authors found more accurate representations. Park *et al.* [2008] reported that the limiting load for the majority of the ACI 318-99 and CRSI results was flexural strength. However, many of the tested specimens were reported to fail in shear. The authors compared the results of the reported shear failures with the shear predictions for these methods. It was found that over half of the shear failures were less than the predicted shear strengths. Therefore, in many cases ACI 318-99 and CRSI appear to underestimate flexural strength and over predict the shear strengths. ACI 318-05 and CSA 2002 show some similar results. When these methods were used to predict the strength of piles caps reported to fail in shear, it was found that they underestimated the flexural strength of the ties and in some cases overestimated the strength in shear of the strut or nodal zones. Adebar *et al.* [1996] was found to predict conservative values for all tests, however most were controlled by the flexural prediction. Adebar *et al.* [1996] used bearing capacity as an indicator of strut strength. As in the other methods it was found that

specimens that failed in shear had a predicted shear strength greater than failure. Results of this report suggest that Adebar *et al.* [1996] bearing strength limit is not a good indicator of pile cap strength as suggested also by Fenton *et al.* [2004]. The Park *et al.* [2008] method was capable of predicting conservative shear values for the pile caps that fit a particular range. Shear span to depth ratios between 0.49 and 1.8 and a concrete strength less than 5900 psi (41 MPa). The work done by Park *et al.* [2008] suggests that S&T methods are the best tool we have for estimating pile cap strengths.

Ahmad *et al.* [2009] provided more evaluation of S&T modeling used in pile cap analysis. In this study six four-pile caps were cast and tested. Uniform reinforcement was used. The authors provide a quick description of past works but do not use any borrowed data. The model used by the authors is a two-dimensional representation of pile caps. The authors attribute failure of the specimens to shear and conservatively predicted failure to approximately 90% the ultimate load. From provided figures it would appear that one-way shear was the failure mode. The authors agree with earlier works that S&T is the best tool for estimating capacity. It is also concluded that because S&T is open to variation by the designer as to the geometry of the assumed truss, thus predicted loads can be greatly affected by designer assumptions. Ahmad *et al.* [2009] urges more research be done in an attempt to generalize an S&T model for pile caps.

Souza *et al.* [2009] attempted to developed a three dimensional (3D) S&T model for four-pile caps. In this work, the authors use data from previous researchers Blevot *et al.* [1967], Clarke [1973], Suzuki *et al.* [1998], [1999], [2000], and develop a 3D S&T model for predicting strength of pile caps as well as failure mode. The proposed model is based on a four-pile cap. Failure is based on shear strength or flexural strength and equations

were developed based on geometry of the assumed S&T model. The model is shown to accurately predict failure to 87% for the 129 four-pile caps tested with an average test load to predicted failure of 1.01 and coefficient of variation of 23%. For cracking and yielding predictions only 67 and 69 specimens respectively were used due to limiting data, however predictions for these specimens were also very accurate. The model uses empirical coefficients for cracking, yielding, and failure that were developed from this data set. These coefficients greatly affected the accuracy of the model and it is unseen how good they represent specimens that were not a part of the test group.

2.3 Current Design Provisions

The American Concrete Institute (ACI) regulates concrete design in the United States of America. The current code, ACI 318-08, developed by committee 318 was issued in 2008. ACI 318-08 has multiple approaches to pile cap design. The code provides that foundations supported by piles be designed to satisfy moment and shear. Flexural requirements including reinforcement layout requirements are prescribed based on a maximum moment demand. ACI 318-08 bases shear demand on location of piles relative to the column. For shallow pile caps, when the distance between the axis of the pile cap and axis of the column is more than two times the distance from the top of the pile cap to the top of the pile, ACI 318-08 requires the pile cap satisfies both requirements for shear in footings and slabs. For foundations on piles that do not satisfy the above criteria, ACI 318-08 requires either the cap is designed to satisfy the same requirements as if it did meet the criteria or it is designed using an S&T approach. The alternative S&T approach was introduced into the ACI code in 2002.

2.4 Summary and Needs

Based on the literature review, past experimental studies have focused on reduced-scale models consisting of a symmetrical four pile group. The applicability of results from reduced-scale models to large-sized pile caps is uncertain considering the disturbed strain fields and possible scale effects. The current state of design is the strut-and-tie (S&T) approach. S&T modeling allows the designer to simplify the behavior into an equivalent truss. The struts are the compression elements usually concrete, and the ties are the reinforcement providing tension. The anchorage of the ties is essential to the model outcomes and is uncertain for pile caps with poor reinforcing details at nodal regions. These uncertainties warrant more detailed study and development of experimental evidence on performance of large-sized pile caps with poorly detailed flexural reinforcing steel. To produce new data and compare with available design and analysis methods, an experimental program was undertaken as described in the next section.

3.0 EXPERIMENTAL PROGRAM

In order to address the conservative pile cap strengths discussed above, an experimental program was developed. The program consists of full scale testing of replica pile caps representing the in-situ piles supporting the VA Hospital. The program consisted of material selection, specimen design, instrumentation, testing, data reduction, and reporting.

Four pile caps were considered in the present project and are identified as Pile Cap #3, #4, #5, and #7 according to the original design drawings, where the number indicates

the number of steel pipe piles in the cap. The specimens were full-size representations of those presently supporting steel columns in the VA Hospital. The pile cap specimens were constructed according to the available original design drawings and reinforcing steel shop drawings (Appendix A and B, respectively) for the VA Hospital. Specimen designs and instrumentation plans were reviewed and approved by Degenkolb Engineers prior to construction. These following sub-sections describe specimen construction, testing methods, and experimental results of the four full-scale pile cap tests.

3.1 Construction and Materials

The specimens were constructed in the Structural Engineering Research Laboratory at Oregon State University. Specimens were designated as Pile Cap #3, Pile Cap #4, Pile Cap #5, and Pile Cap #7, according to the number of pipe piles in each pile cap and correspond to the naming convention described in the original design drawings. Pile Cap #3 was triangular, Pile Caps #4 and #5 were square, and Pile Cap #7 was hexagonal. The first test was of Pile Cap #4, which was performed on April 22, 2011. The second test was of Pile Cap #3, which was performed on May 23, 2011. The third test was of Pile Cap #5, conducted on July 14th, 2011. The last specimen, Pile Cap #7, was tested August 30th, 2011.

The pile cap specimens included an upper portion of the pipe piles, a layer of reinforcing steel, and anchor rods with confining ties to permit attachment to a column base plate. To represent the pipe piles in the present tests, only a short upper portion of the pipe was used. The simulated pipe piles were short sections of 24.4 cm (9-5/8 in.) diameter round pipe with 1.2 cm (0.472 in.) nominal wall thickness. This is that same as that

specified for the driven pipe piles in the VA Hospital. Four pieces of 24 in. long #4 reinforcing steel were welded to the pipes and 2.5 cm (1 in.) thick, 30.5 cm (12 in.) square steel bearing plates with holes corresponding to the reinforcing bar locations were placed on the tops of the pipe piles as illustrated in Fig. 3.1.1a. These represent the in situ details. Original construction drawings indicated that the top of the pile was to be cut flush to obtain 50% minimum bearing. However, the laboratory pipes were saw cut and thus the plates sit flush on the full cross section of the pipes. The pipes extended 4 in. into the bottom of the pile caps. For specimens #3 and #4, a pipe pile length of 25.4 cm (10 in.) was selected to provide sufficient room under the pile cap for placement of instrumentation. For specimens #5 and #7 longer pipe lengths (75 cm (29.5 in.)) were used to allow placement of a hydraulic cylinder and load cell under the center pile (this is described in more detail in the Testing Methodology). For each of the specimens, a layer of ASTM A615-Grade 60 reinforcing steel was fabricated and placed according to the reinforcing steel fabrication shop drawings (shown in Appendix B). The reinforcing steel was held above the pipe bearing plates with 1.5 in. chairs. The geometric and reinforcing details for the specimens are shown along with photographs of the reinforcing layouts and completed specimens in Figs. 3.1.2a to 3.1.5d and Figs 3.1.1b to 3.1.1c. To establish the material properties of the reinforcing steel, tensile tests were performed in accordance with ASTM E8. The measured mechanical properties are shown in Table. 3.1. Data shown in Table 1 are the average of two samples with 2 in. gage lengths.

Table 3.1 : Reinforcing steel material properties.

Property	Pile Cap #3	Pile Cap #4	Pile Cap #5	Pile Cap #7
Bar Size	#7	#7	#8	#8
f_y (ksi)	69.5	69.3	66.4	66.6
f_u (ksi)	97.0	96.8	96.9	93.5
% Elongation	19%	24%	28%	24%
Heat Number	221409	416910	-	120411
Supplier	Cascade	Cascade	Cascade	Cascade

The concrete mix design used during construction of the in situ pile caps was provided in the construction documents and is reported in Appendix C. Because the pile caps represented by the present specimens have been in service for over 20 years, they have gained significant compressive strength above the specified design strength. Cores taken for Degenkolb Engineers from the in-service pile caps were tested by an outside testing service (Appendix D) and the reported compressive strengths for three cores were 46, 46, 42.8 MPa (6670, 6670, and 6210 psi). The average strength was 44.9 MPa (6517 psi). A single core was tested to establish the split tensile strength as 3.8 MPa (550 psi). To reasonably represent the in-situ pile cap concrete materials, a concrete mix was developed to provide reasonably representative compressive and tensile strengths based on data from cores taken from the in situ pile caps. The mix design used for the present experimental study is shown in Appendix E. A key aim of the mix was to achieve relatively high compressive strength in a short period of time (two weeks) yet retain the aggregate size, type, and distribution representative of the in situ materials. For this project, both cores and cylinder molds were used to assess the concrete properties. The cores were tested

according to ASTM C42 and the cylinders according to ASTM C39. The concrete material properties are reported in Table 3.2a and 3.2b. As seen here, the compressive strength of the concrete used in three of the four specimens was below the average strength from cores removed from the in situ pile caps. For specimen #3, the cored strengths were less than the in situ strength, while the samples taken from molds were higher. The average of these is approximately equal to the in situ strength.

Table 3.2a: Concrete compressive properties.

Specimen ID	Sample ID	Relative Test Day*	Type	Nominal Diameter (in.)	f _c (psi)	Average (psi)	St. Dev. (psi)
#3	1	0	Mold	4	6748	6860	145
	2	0	Mold	4	6806		
	3	0	Mold	4	7022		
	4	+2	Core	4	7245	6170	971
	5	+2	Core	4	5903		
	6	+2	Core	4	5359		
#4	1	+2	Core	4	5363	5100	445
	2	+2	Core	4	4821		
	3	+2	Core	4	5588		
	4	+2	Core	4	4643		
#5	1	0	Mold	4	6271	5940	291
	2	0	Mold	4	5792		
	3	0	Mold	4	5746		
#7	1	0	Mold	4	6147	5820	779
	2	0	Mold	4	5472		
	3	0	Mold	4	5828		

* Number of days after pile cap failure that cores were tested

Table 3.2b: Concrete tensile properties.

Specimen ID	Sample ID	Type	Nominal Diameter (in.)	fct (psi)	Average (psi)	St. Dev. (psi)
#3	1	Mold	4	659	650	17
	2	Mold	4	635		
	3	Mold	4	667		
#4	1	Core	4	615	630	25
	2	Core	4	649		
#5	1	Mold	4	542	570	49
	2	Mold	4	538		
	3	Mold	4	624		
#7	1	Mold	4	594	590	37
	2	Mold	4	554		
	3	Mold	4	629		

During construction, concrete was placed in three lifts and consolidated with vibrators. The concrete strength was achieved within approximately two weeks of casting based on cylinder tests made during the time of concrete placement. After curing, the specimens were moved onto a strong floor for testing. To allow the specimens to be lifted into place on the strong floor, lifting inserts were placed in the concrete over the pile locations in regions of the specimens that were considered to be outside the stress fields when column loads were applied.

4.2 Instrumentation

All specimens were instrumented prior to testing. Sensors were placed to measure the applied loads, strains in the reinforcement, slip of the reinforcing steel relative to the concrete, and vertical displacements of the pile cap relative to the strong floor. Summary

instrumentation for each test is as follows: Pile Cap #3 received 32 strain gages, 10 displacement sensors and 16 slip sensors. The gages or gage wires are sometimes damaged as a resultant of concrete placement. When this occurs, the sensor can no longer be used to collect data. For the specimens in this study, the number of gages damaged was relatively small. Only 1 strain gage was damaged during construction of Pile cap #3. Pile Cap #4 received 34 strain gages, 13 displacement sensors and 16 slip displacement sensors. Three of the 34 strain gages in Pile Cap #4 were damaged during construction. Pile Cap #5 received 38 strain gages, 13 displacement sensors and 18 slip displacement sensors. Three strain gages were damaged during construction. Pile Cap #7 was instrumented with 34 strain gages, 13 displacement sensors and 21 slip sensors. Three strain gages were damaged during construction of Pile Cap #7.

To measure strain in the reinforcement, general purpose strain gages were bonded at selected locations on the reinforcement as illustrated in Fig. 3.2.1. These were located near the bearing plates and in between the pipe piles as detailed in the instrumentation plans. The selected gage size was sufficiently small as to fit between the deformation ribs on the rebar. The gages were protected from the wet concrete with mastic, multiple nitrile butyl coatings, and then covered with aluminum foil tape.

Possible slip of the reinforcing bars was measured relative to the exterior surface of concrete at selected reinforcing steel locations. After building the forms, holes were drilled through the forms at the desired slip measurement locations. Short lengths of polyvinyl chloride (PVC) pipe were placed through the holes in the forms and onto the ends of the reinforcing bars. This allowed access to the ends of the reinforcement after the

concrete cured and the forms were removed. Displacement sensors were mounted on an exterior bracket that was bonded to the concrete surface. The tip of the sensor was placed in contact with the end of the reinforcing bars to enable direct measurement of slip of the bar relative to the concrete. An example reinforcing bar slip instrument location is shown in Fig. 3.2.2.

In addition to reinforcement slip, displacement sensors were placed on the specimens to measure vertical displacement relative to the strong floor at selected locations as illustrated in Fig. 3.2.3. Instrumentation plans for all 4 pile caps can be found in Figs. 3.2.4 to 3.2.7.

3.3 Testing Methodology

A reaction frame was fabricated to conduct the tests. The frame consisted of two W40X431 cross beams and eight 3.5 cm (1-3/8 in.) diameter Dywidag bars on each side. The Dywidag hold downs were anchored into a strong floor. The testing frame is illustrated schematically in Fig. 3.3.1 and shown in Fig. 3.3.2.

Load was applied using two 3559 kN (800 kip) nominal capacity hydraulic cylinders. Load was measured directly with load cells placed in series with the hydraulic cylinders. The applied load was transmitted to a spreader beam which reacted against a W14x99 profile attached to a 7.6 cm (3 in.) thick steel bearing plate (Fig. 3.3.3). The bearing plate was placed on the concrete pile cap surface and grouted with hydrostone.

Pile caps #5 and #7 were outfitted with an additional hydraulic cylinder and load cell placed in series with the center pile, as shown in Fig. 3.3.4, to manually control the magnitude of load transmitted to the center pile. The force distribution to the pipes was established in previous studies by the engineering consultant to the hospital considering the typical pile lengths in the pile groups considered. The center pipe pile was assigned 10% more load than the adjacent piles. Load transmitted to the center pile of Pile Caps #5 and #7 was monitored and manually controlled using a separate hydraulic cylinder actuated by a manual hydraulic pump. To conduct the tests for Pile Caps #5 and #7, the center pile was loaded first to near the target value and then the column load was increased to the target value. Adjustments were made to either the applied column load or applied center pile load to achieve the prescribed distribution of pile forces.

The tests were conducted by manually increasing the pressure applied to the hydraulic cylinders to apply load to the column base plate on the surface of the pile caps. Data from sensors were continuously acquired using a commercially available data acquisition system. Load was monotonically increased until failure of the specimen or the capacity of the hydraulic cylinders was reached. Throughout the tests, specimens were monitored to identify cracking and other visible distress. At set load intervals, the loading was suspended and visible cracking was mapped on the concrete surface and recorded. Digital images and video were also collected to document the tests.

All data were collected, stored, and reduced, and are reported here. Data reduction included zeroing initial sensor values, removing spurious artifacts, and correcting sensor offsets that occurred during testing. No data averaging or smoothing was performed.

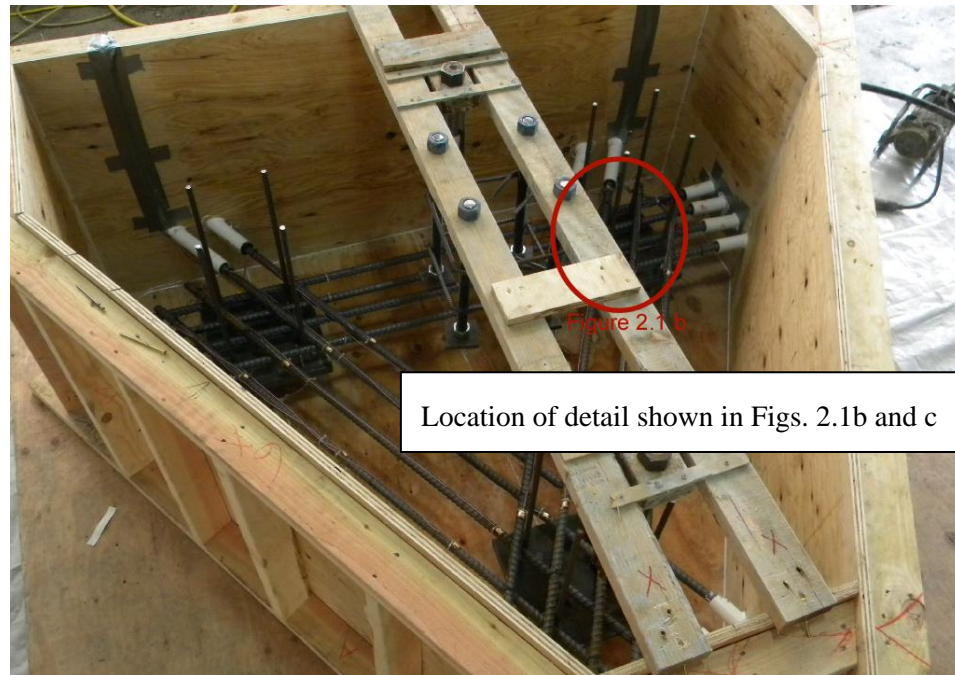


Figure 3.1.1a: Reference location for pipe bearing plates in Figure 2.1b

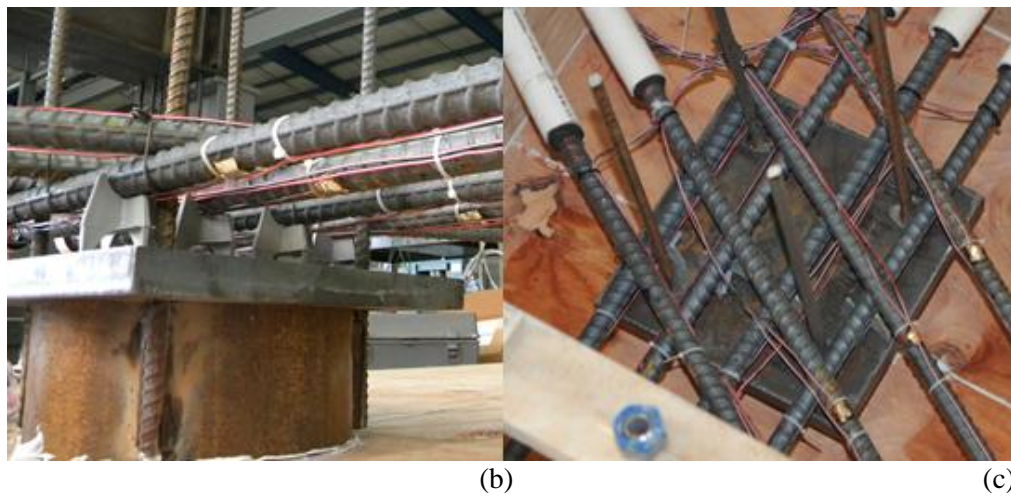


Figure 3.1.1: b) Side view and c) top view of bearing plate with reinforcing details at top of pipe pile

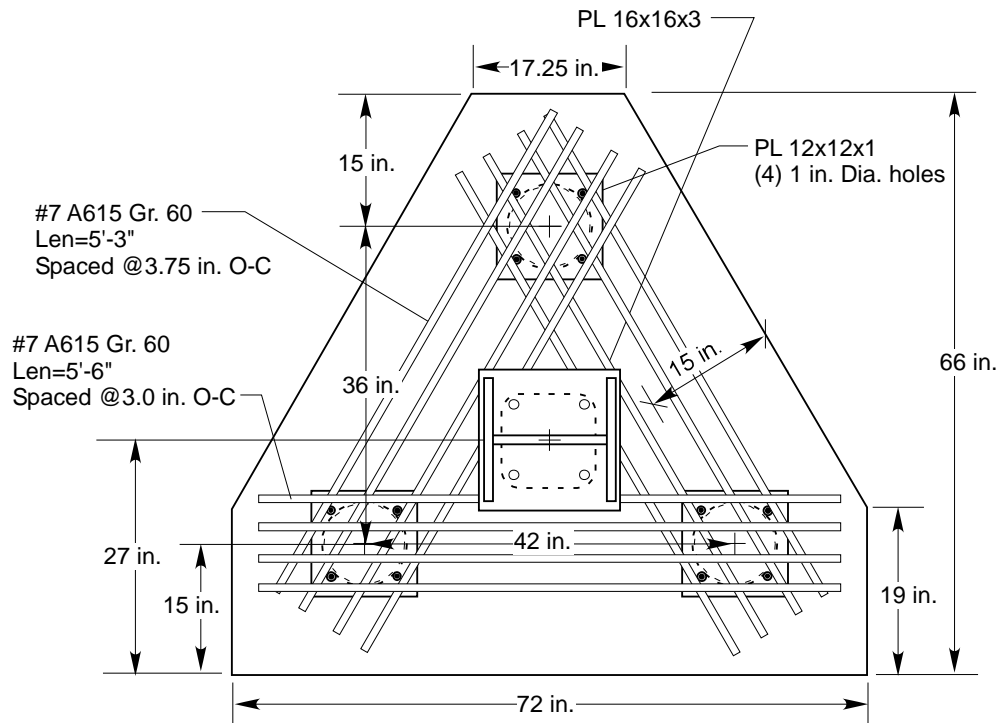


Figure 3.1.2a: Plan View – Pile Cap #3



Figure 3.1.2b: Reinforcement placement and formwork for Pile Cap #3

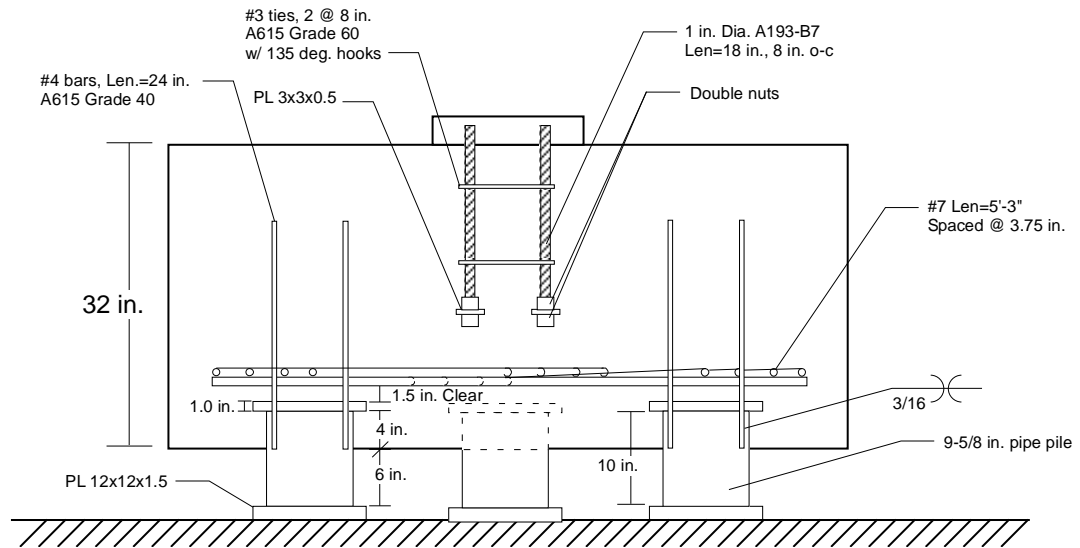


Figure 3.1.2c: Elevation View - Pile Cap #3



Figure 3.1.2d: Elevation view of completed specimen on strong floor – Pile Cap #3

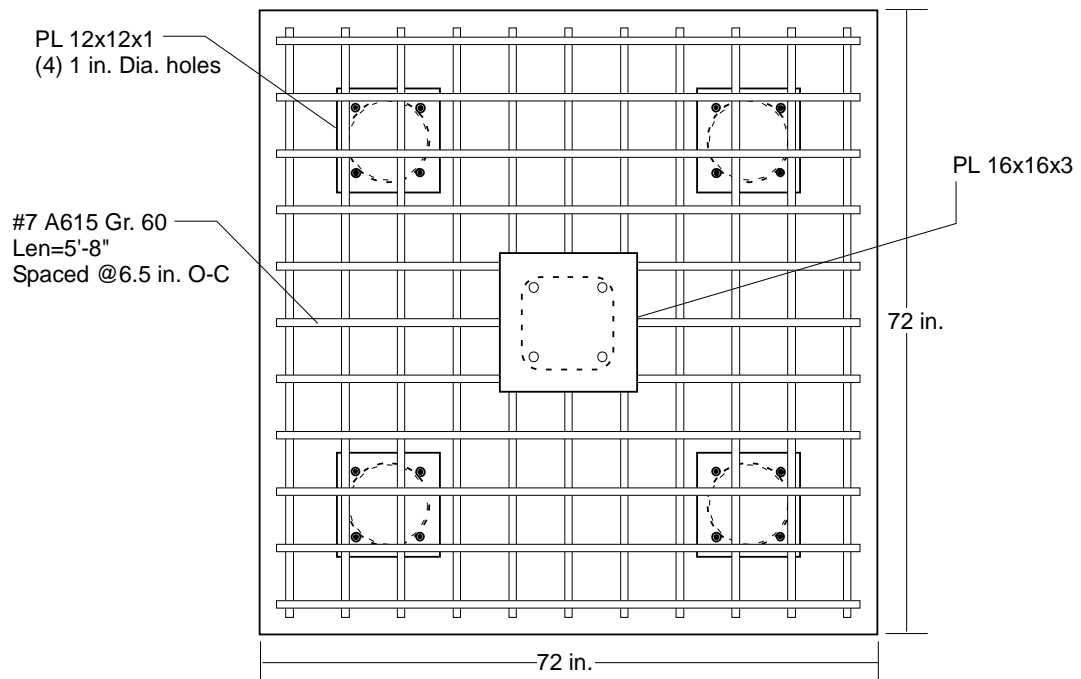


Figure 3.1.3a: Plan view for Pile Cap #4



Figure 3.1.3b: Reinforcement placement and formwork for Pile Cap #4

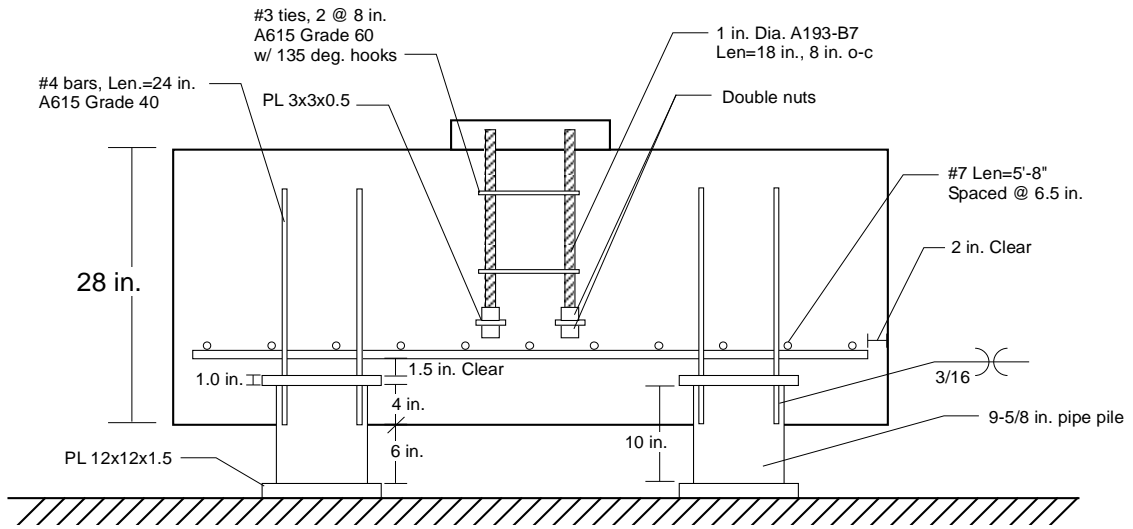


Figure 3.1.3c: Elevation plan – Pile Cap #4



Figure 3.1.3d: Elevation view of completed specimen on strong floor – Pile Cap #4

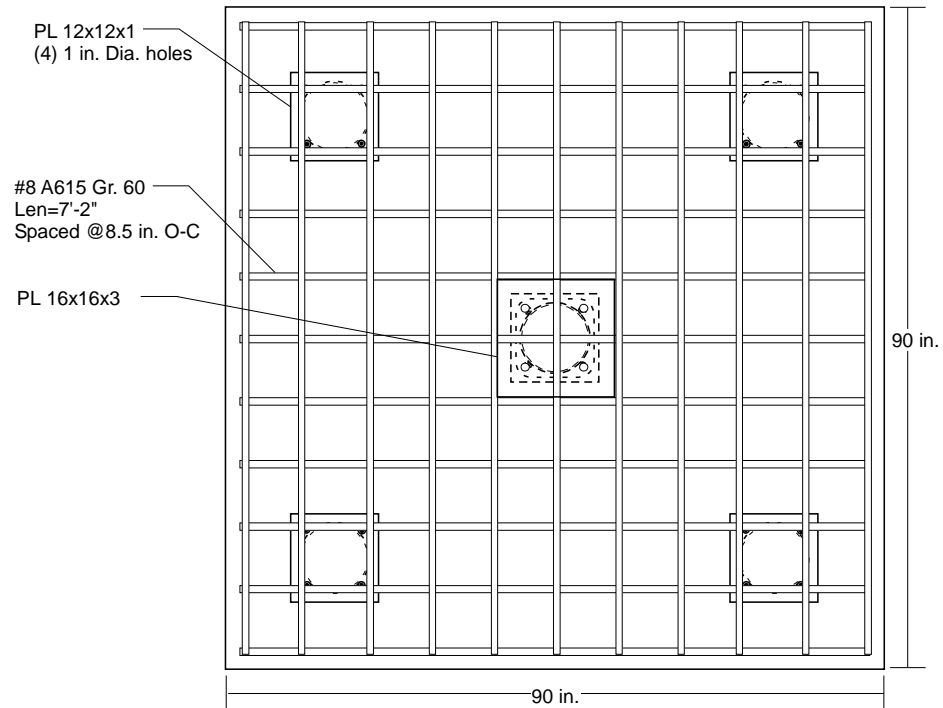


Figure 3.1.4a: Plan View – Pile Cap #5



Figure 3.1.4b: Reinforcement placement and formwork for Pile Cap #5

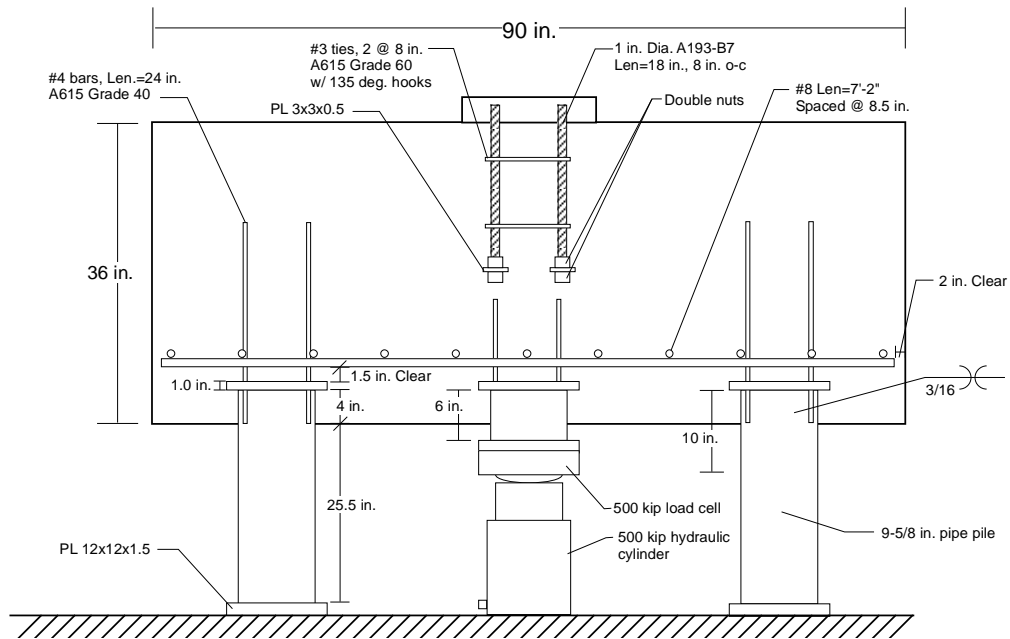


Figure 3.1.4c: Elevation View – Pile Cap #5



Figure 3.1.4d: Elevation view of completed specimen on strong floor – Pile Cap #5

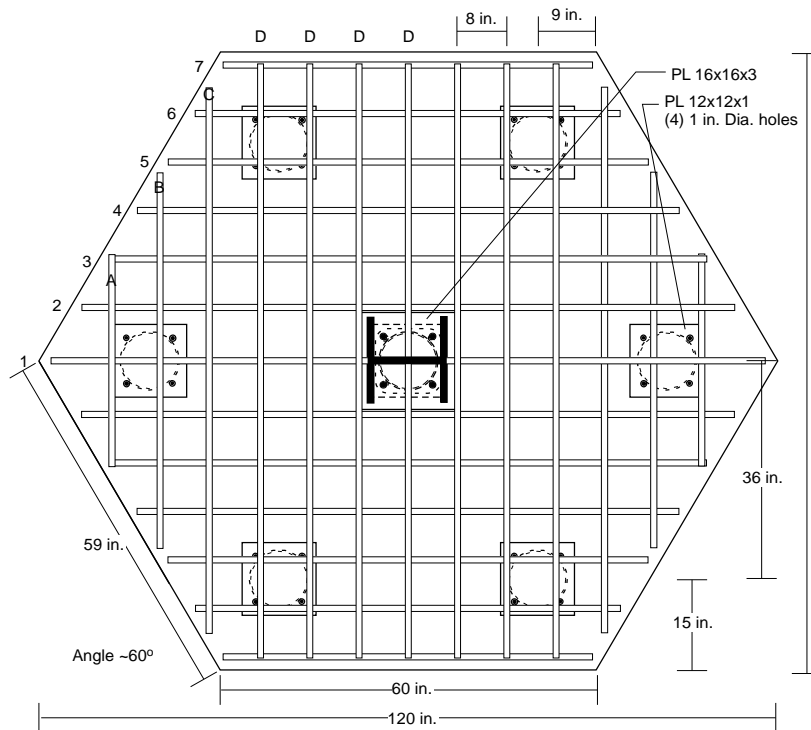


Figure 3.1.5a: Plan view – Pile Cap #7



Figure 3.1.5b: Reinforcement placement and formwork for Pile Cap #7

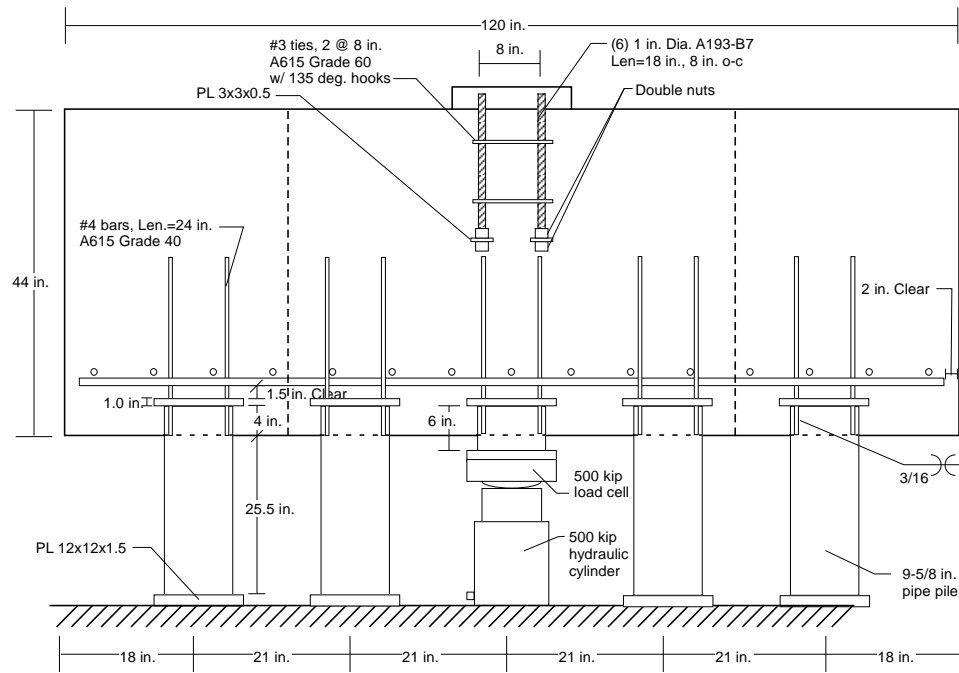


Figure 3.1.5c: Elevation View – Pile Cap #7



Figure 3.1.5d: Elevation view of completed specimen on strong floor – Pile Cap #7

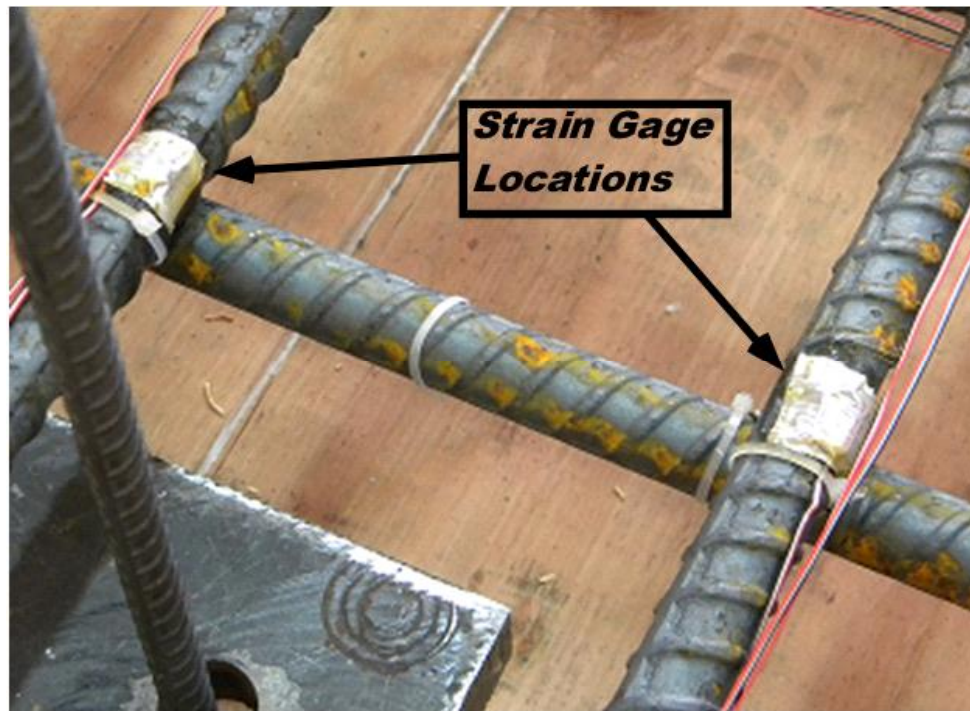


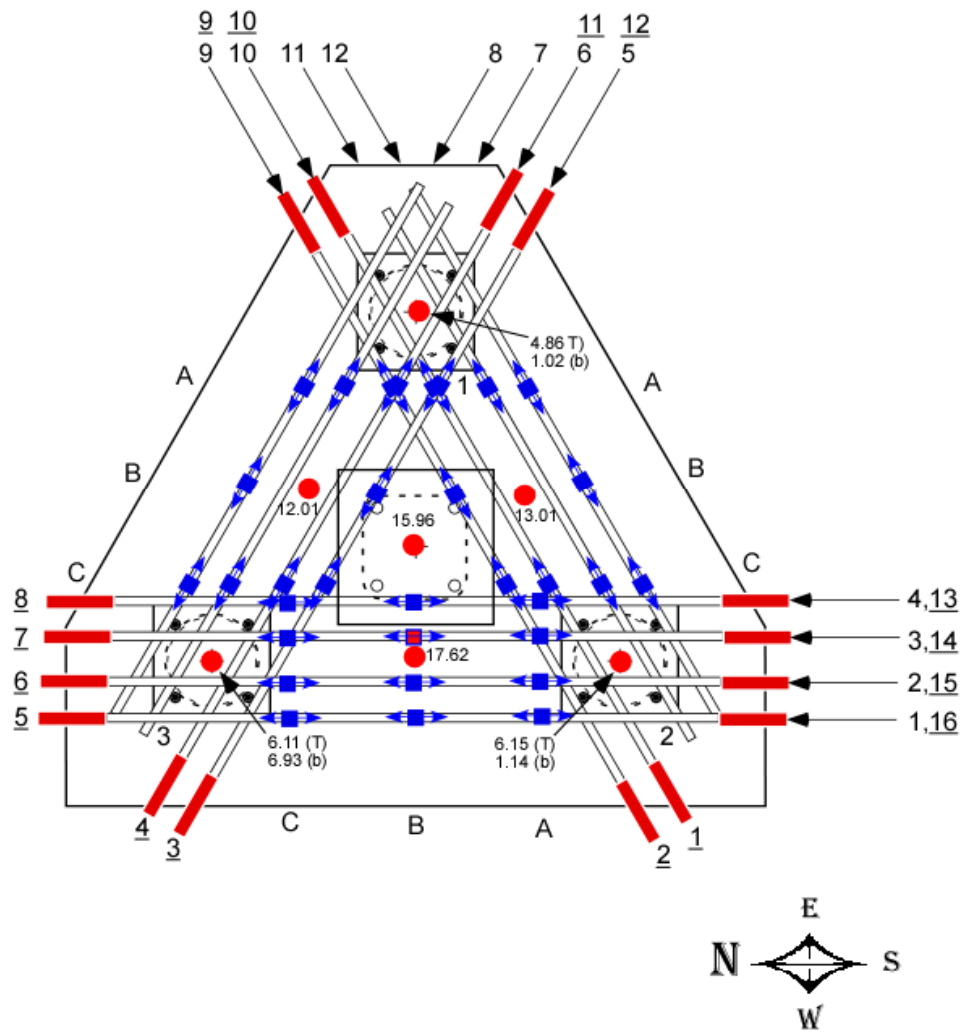
Figure 3.2.1: Example strain gage location on reinforcing bar near bearing plate of pipe pile



Figure 3.2.2: Example reinforcing steel slip displacement sensor



Figure 3.2.3 Example vertical displacement measurements of specimen relative to strong floor (yellow arrows) and pipe motion relative to concrete (red arrow)



*Bars designated by plain numbering, underlined numbers represent instrumentation locations

- Displacements (10 total, 7 relative to strong floor, 3 on piles)
- Reinforcing bar end slip (16 relative to concrete surface)
Designation - Underlined number
- Uniaxial strain gages on reinforcing bars (28 totals, arrow shows orientation)
Designation- Bar then location relative to A,B,C (when only two, A and B only)
- Damaged during Construction

Figure 3.2.4: Instrumentation plan for specimen #3

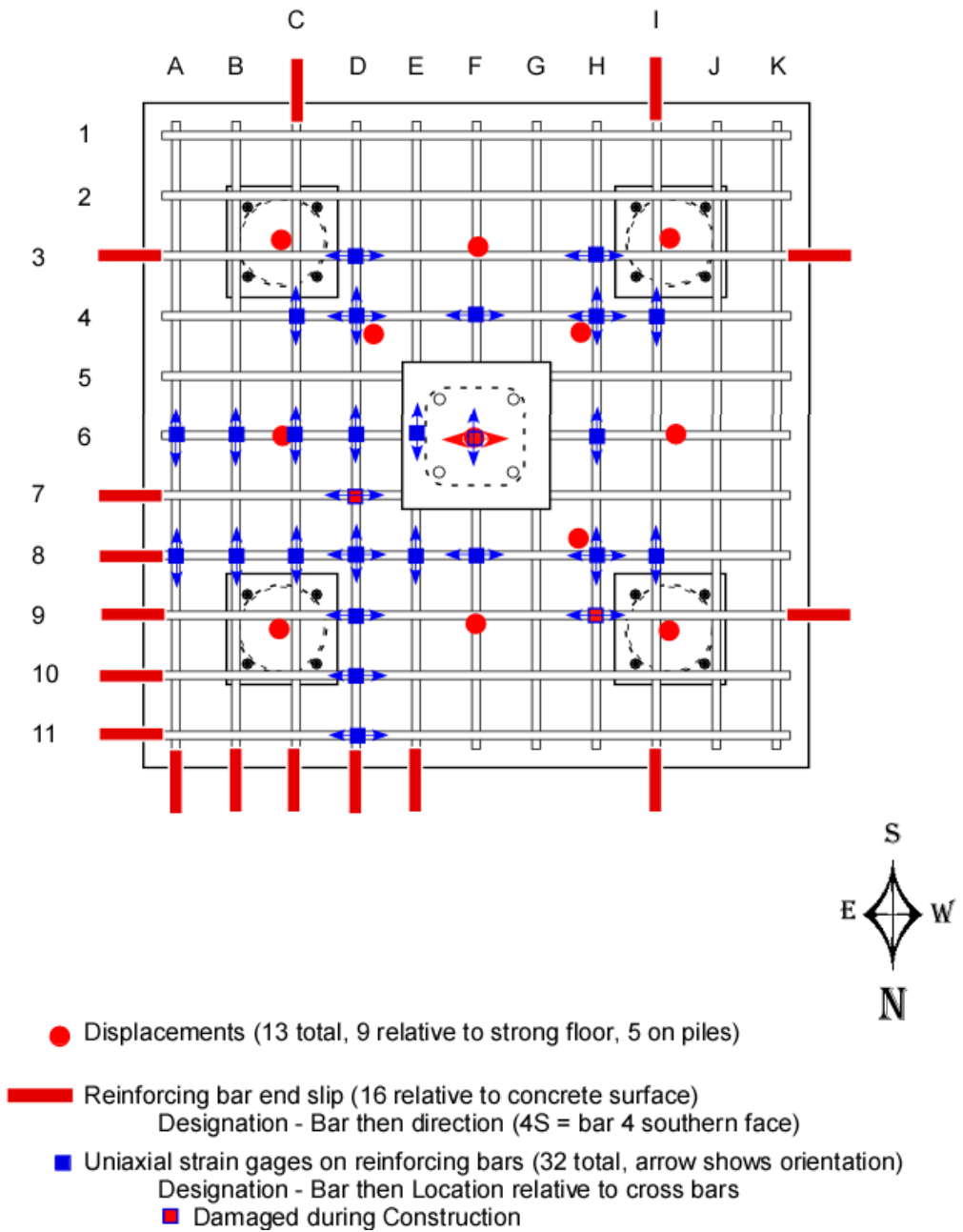
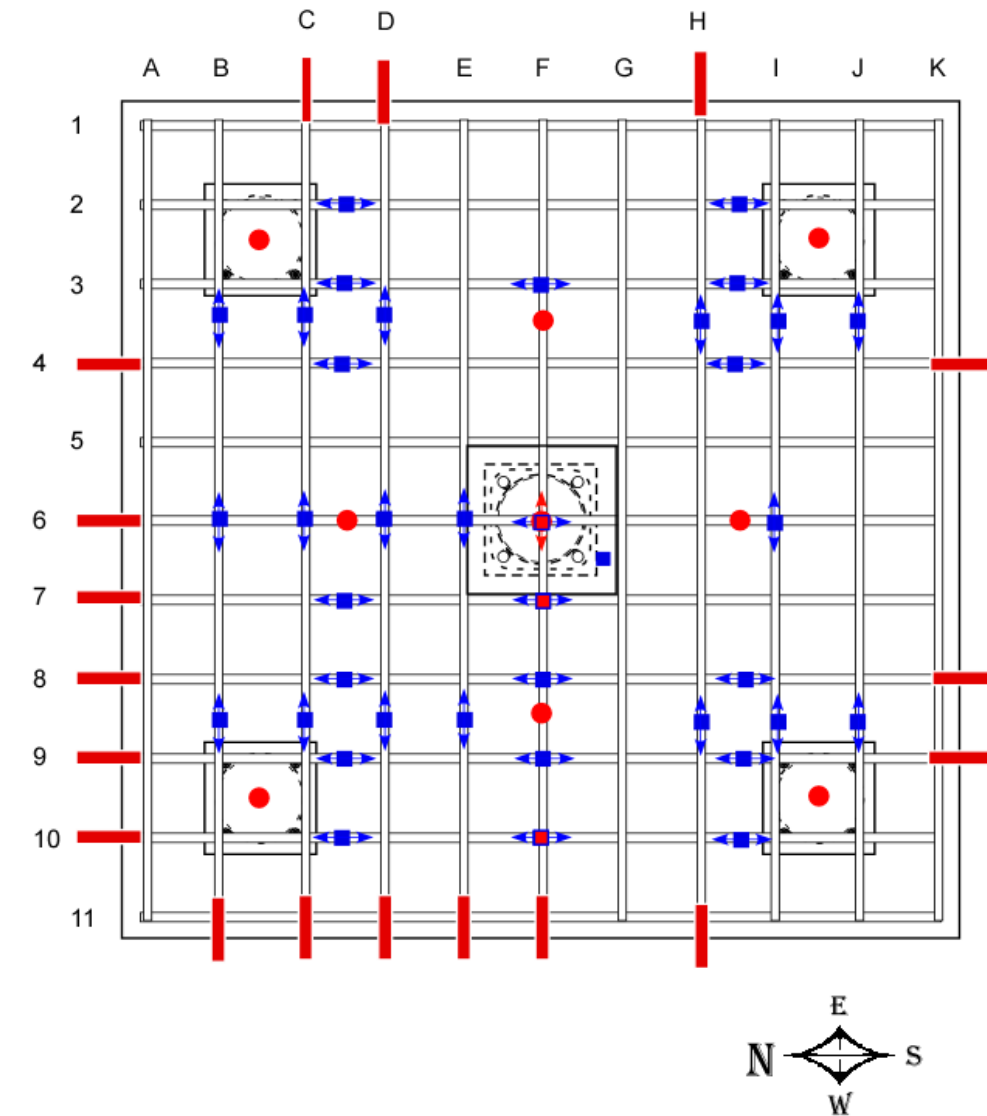


Figure 3.2.5: Instrumentation plan for specimen #4



● Displacements (13 total, 9 relative to strong floor, 4 on piles)

■ Reinforcing bar end slip (18 relative to concrete surface)
Designation - Bar then direction (4S = bar 4 southern face)

■ Uniaxial strain gages on reinforcing bars (38 total, arrow shows orientation)
Designation - Bar then Location relative to cross bars
■ Damaged During Construction

Figure 3.2.6: Instrumentation plan for specimen #5

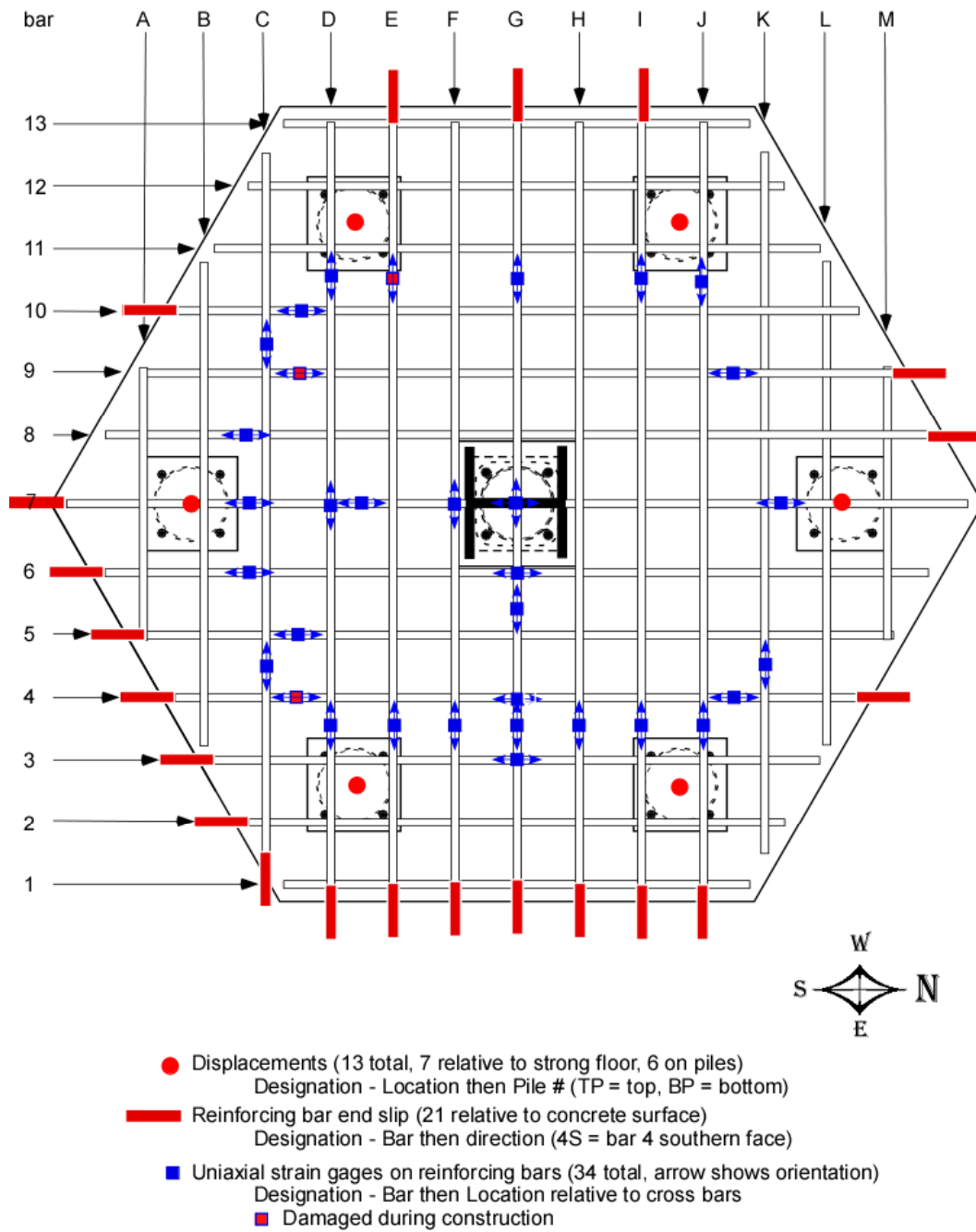


Figure 3.2.7: Instrumentation plan for specimen #7

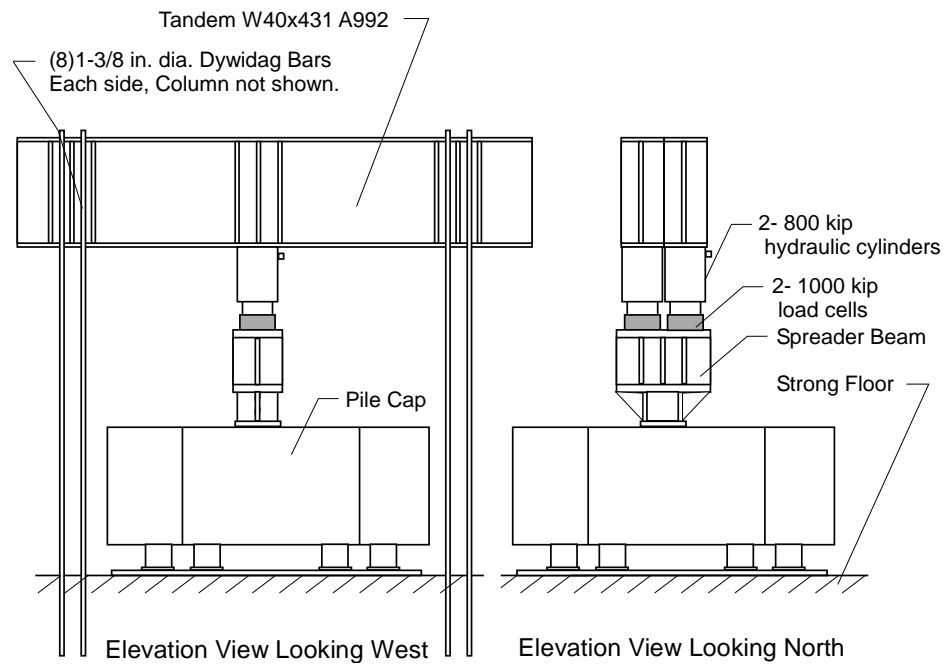


Figure 3.3.1: Schematic of test setup



Figure 3.3.2: Experimental setup with specimen #5



Figure 3.3.3: W14x99 profile attached to 3 in. bearing plate (note: white material is hydrostone used to grout baseplate)



Figure 3.3.4: Hydraulic Cylinder and Load cell for center pile control with specimen #5

4.0 EXPERIMENTAL RESULTS

In this section, the experimental results for each specimen are reported. These include failure load and mode, as well as measured reinforcement slip data, vertical displacement data and visually observed crack patterns. The full data sets are included in Appendix F3, F4, F5, and F7 for specimens #3, #4, #5, and #7, respectively. Selected data are included in the main body of this report to highlight the observed behavior and performance of the specimens.

Reinforcement slip was monitored for several reinforcement bars in each specimen. Some measurable slip was observed for each of the specimens as described subsequently. To describe the slip and bond behavior of reinforcing steel, early studies commonly reported test results as the slip of the reinforcing bar at maximum load or stress, or the force or stress in the bar at a particular slip value. The common slip value used in the archival literature was 2.54 mm (0.01 in.) and was taken either at the loaded or unloaded end of the bar. It is important to recognize that much of the archival work was concerned with working stress conditions and the 2.54 mm (0.01 in.) slip value may not correspond to any particular limit state. However it does serve as an historical reference value and thus was chosen for use in this report as a reference value to distinguish slip at the ends of the reinforcing bars relative to the concrete surface. There were some instances where concrete cracking disturbed the instrument mounting and caused a jump in the sensor output. An example of this is shown in Fig. 4.1. As seen in this figure, after the observed jump the reinforcing bar does not show further slip even as the applied load increases. There were other instances where the sensors debonded from the concrete surface during testing. These

were reattached with testing in progress and the data were post-processed to remove the offset and make the data continuous.

Another important feature of the tests was to assess if yielding occurred in the reinforcement. To establish this, a theoretical yield stress of 413.7 MPa (60 ksi) and modulus of elasticity of 200 GPa (29,000 ksi) were used. For these values, the theoretical yield strain is approximately 2100 microstrain ($10^{-6}/10$) for the nominal Grade 60 reinforcing steel. The locations with strains above nominal yield and the vertical displacements at failure are shown for each specimen.

4.1 Pile Cap #3

Pile Cap #3 was tested on May 23, 2011. The applied load history is shown in Fig. 4.2. The load- vertical displacement of the specimen (under the column load) is shown in Fig. 4.3. The specimen developed cracks at approximately 2891 kN (650 kips) and was loaded to the capacity of the hydraulic system, approximately 1530 kips. Failure was not reached at this load. The specimen was then unloaded. Upon unloading the specimen, additional cracks were observed at the top surface of the concrete pile cap. A map showing the progression of cracks is shown in Fig. 4.4. The specimen was then reloaded. It was able to achieve and briefly sustain a load of 6805 kN (1513 kips) before failure. At failure, the bottom center point of the pile was displaced 0.16 inches relative to the strong floor. The observed failure mode for Pile Cap #3 was one-way shear associated with one of the corner piles as shown in Fig. 4.5. Several locations indicated small amounts of reinforcing slip as seen in Fig. 4.6. The first reinforcing steel slip was observed at a load of 4003 kN (900 kips). None of the slip locations achieved the reference reinforcing bar slip of 2.54 mm

(0.01 in.) The locations of instrumented reinforcing bars at yield when the specimen failed are shown in Fig. 4.7. As seen in the figure, the small amount of rebar slip did not adversely affect the ability of the reinforcing steel to achieve yield across the specimen.

4.2 Pile Cap #4

Pile Cap #4 was tested on April 22, 2011. The applied load history is shown in Fig. 4.8. The load-centerline vertical displacement of the specimen is shown in Fig. 4.9. Initial cracking was observed at an applied load of approximately 2224 kN (500 kips) and cracks were observed on all four sides of the specimen. The load was increased until failure a peak load of 5530 kN (1243 kips). At failure, the bottom center point of the pile was displaced 50.8 mm (0.20 inches) relative to the strong floor. The observed failure mode for Pile Cap #4 was punching shear of the column base plate through the specimen as shown in Fig. 4.11. Several locations indicated small amounts of reinforcing slip as seen in Fig. 4.12. The slip was first observed at a load of (2224 kN) 500 kips. Only four locations achieved the reference slip of 2.54 mm (0.01 in.), the earliest at a load of 4450 kN (1000 kips). The locations of instrumented reinforcing bars at yield when the specimen failed are shown in Fig. 4.13. As seen here, the small amount of rebar slip did not adversely affect the ability of the reinforcing steel to achieve yield across the specimen.

4.3 Pile Cap #5

Pile Cap #5 was tested on July 14th, 2011. This specimen has a pipe pile located directly under the column base plate. As described earlier, the center pile was actively controlled with a separate hydraulic cylinder. To include the center pile influence, this test

was conducted in two parts: 1) the center pile was active and 2) the center pile was removed. The applied load history is shown in Fig. 4.14 with the center pile load also shown in this figure. The load-centerline vertical displacement of the specimen is shown in Fig. 4.15. During part 1, the specimen did not fail and the limits of the hydraulic loading system were reached at a maximum load of 6859 kN (1542 kips). The center displacement observed at this load was 27.4 mm (0.108 in.) at around 2224 kN (500 kips), initial cracking was observed on the southern face however it wasn't until approximately 4003 kN (900 kips) that cracking was observed on all 4 sides of the specimen. Observed crack patterns and corresponding loads are shown in Fig. 4.16. The first slip readings were recorded at 5960 kN (890 kips) however it wasn't until 6228 kN (1400 kips) that the reference slip of 2.54 mm (0.01 in.) was reached.

After reaching the limits of the hydraulic loading system, the applied load was taken off the specimen and the center pile was removed. Then the test repeated. The applied load history for this part is also shown at the end of Fig. 4.13. The applied load-vertical deformation at the center of the pile cap is also included in Fig. 4.14. The load was increased until failure at a peak load of 5511 kN (1239 kips). The specimen was softer and exhibited more distributed and wider cracking with the center pile removed as seen in Fig. 4.16. At failure, the bottom center point of the pile was displaced 40.6 mm (0.16 in.) relative to the strong floor. The observed failure mode for Pile Cap #5 with the center pile removed was punching shear of the column base plate through the specimen as shown in Fig. 4.17. The same reinforcing bar that indicated small amounts of reinforcing slip with the center pile active showed higher amounts of slip when the pile was removed as seen in Fig. 4.18. The locations of instrumented reinforcing bars at yield are shown in Fig. 4.19.

As seen here, the small amount of rebar slip did not adversely affect the ability of the reinforcing steel to achieve yield across the specimen.

4.4 Pile Cap #7

The last specimen was Pile Cap #7 and it was tested on August 30th, 2011. This specimen also had a pipe pile located directly under the column base plate that was actively controlled with a separate hydraulic cylinder. To include the center pile influence, this test was conducted in three parts: 1) the center pile was active and 2) the center pile was removed, 3) the center pile was removed and two additional piles (northernmost and southernmost) were removed. Failure was not achieved for any of these configurations. The applied load history for Parts 1, 2, and 3 is shown in Fig. 4.20 with the center pile load also shown in this figure. The load-centerline vertical displacement of the specimen in all three parts is shown in Fig. 4.21 (the displacements were reset to zero for each part). For Part 1, initial cracking was observed at an applied load of 5783 kN to 6228 kN (1300 to 1400 kips). The observed crack patterns and corresponding loads are shown in Fig. 5.22. The reinforcing bars exhibiting slip response are shown in Fig. 4.23. Initial slip of the reinforcement was measured at 5693 kN (1280 kips) in Part 1, however the reference slip of 2.54 mm (0.01 in.) was never reached for the 7 pile configuration. There were only 2 locations that indicated yielding of the reinforcing steel at the maximum applied load. During Part 1, the specimen did not fail and the limits of the hydraulic loading system were reached at a maximum load of 6860 kN (1542 kips). The center displacement observed at this load was 9.1 mm (0.036 in.). The capacity of Pile Cap #7 exceeded the hydraulic loading capacity of the system and so the load was removed, the center pile was taken out,

and the test repeated as Part 2. The data for Part 2 are shown in the same figures as those in Part 1. Additional cracking and deformations were observed for the specimen during Part 2 of the test as seen in Fig. 4.22. Again the maximum capacity of the hydraulic loading system was reached and the specimen did not fail. At the maximum applied force of 6810 kN (1531 kips), the center displacement was 16 mm (0.063 in.) (initial point was reset to zero). In this configuration, the reference slip was reached in 2 bars at approximately 6228 kN (1400 kips). After reaching the limits of the hydraulic loading system, the load was again removed and then two piles were cut off as seen in Fig. 4.24. These were the northern most and southernmost piles (labeled 1 and 4 in Fig. 3.7). This was Part 3 of the test and the load was again applied to the specimen. The limit of the hydraulic loading system was again reached without specimen failure. The maximum applied force was 6788 kN (1526 kips) and the center pile cap displacement was 29 mm (0.115 in.) (initial displacement value was reset to zero). The displacements vs. load for all three cases are shown in Fig. 4.21 and the response of the reinforcing bars exhibiting slip is shown in Fig. 4.25. Failure was never reached and thus the failure mode is unknown. The locations of instrumented reinforcing bars at yield during the different parts of the test are shown in Fig. 4.26.

4.5 Experimental Conclusions

Table 4.1 provides the key experimental data from the testing. A reference slip of 2.54 mm (0.01 in.) is considered along with a nominal yield stress of 413.7 MPa (60 ksi). Further discussions are found in section 8.0.

Table 4.1: Key data from all tests.

Specimen ID	Max. Load (kips)	Failure Mode	Load at first cracking (kips)	Load at first reference slip ^a (kips)	Number of bars with slip at failure ^a	Number of bars to reach yield ^b
#3	1513 ^c	one-way shear	650	Not observed	0	30/31
#4	1243	punching shear	500	1000	4	29/31
#5	1239 ^d	punching shear	500	1400	4	15/35*
#7	1542 ^e	n/a	1400	1380	3	2/31*

a. Reference slip of 0.01 inches

b. Yield based on 60 ksi nominal strength upon maximum load or failure with all piles active. *At maximum available force (~1540 kips) without failure

c. Failure upon 2nd load cycle

d. Failure after center pile removed and reloaded

e. Specimen did not fail, maximum applied load reported

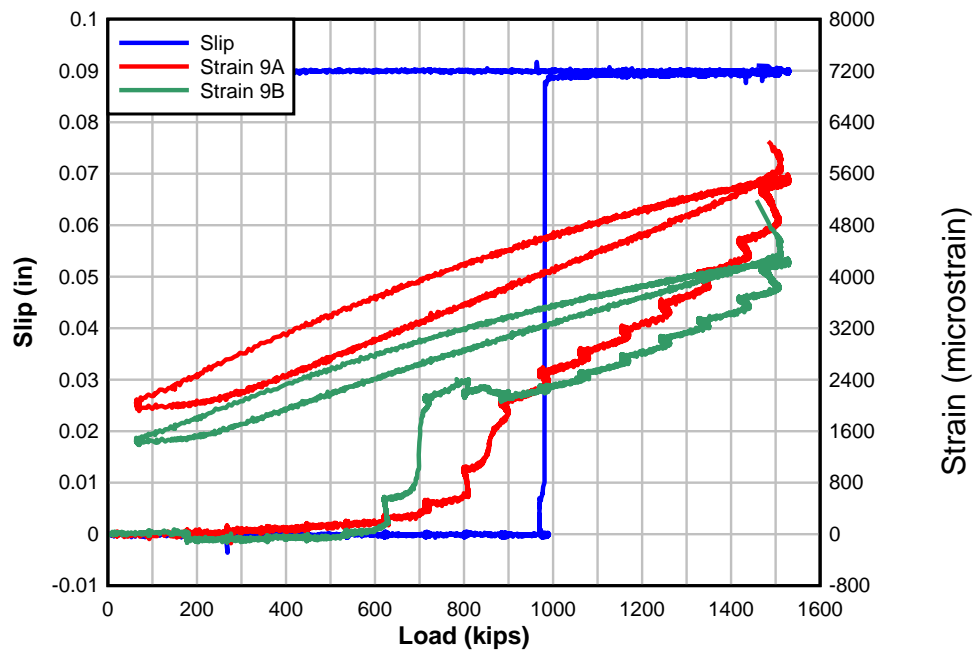


Figure 4.1: Example of spurious slip data due to concrete cracking affecting the instrumentation mount.

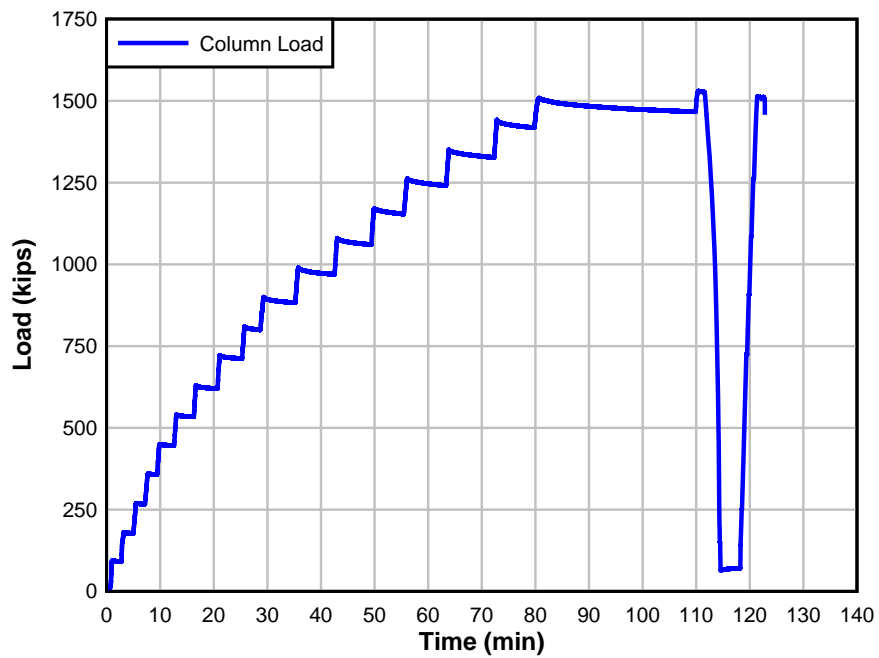


Figure 4.2: Column load vs. Time – Pile Cap #3

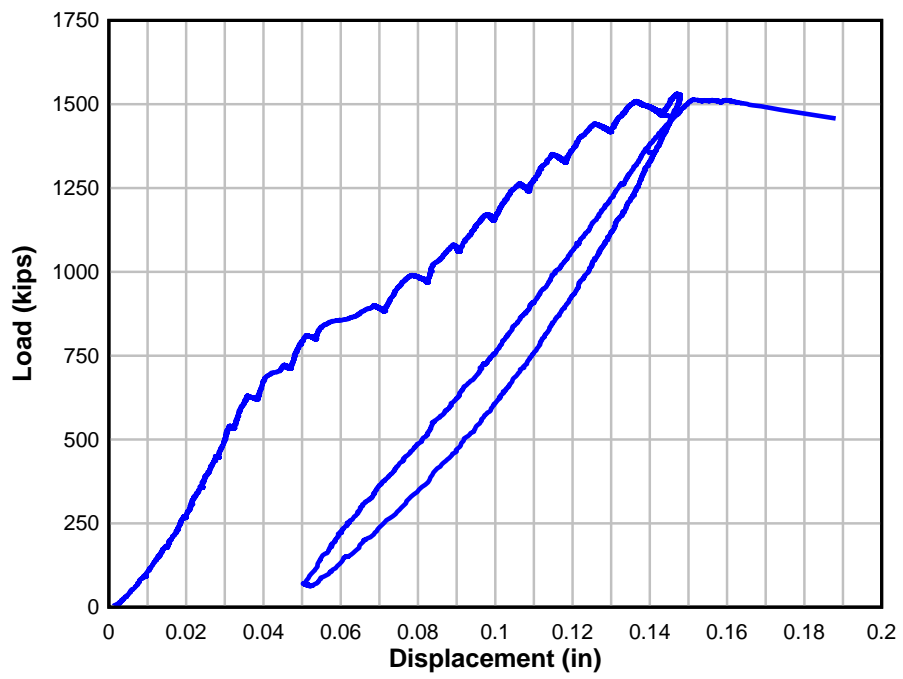


Figure 4.3: Column load vs. Centerline vertical displacement – Pile Cap #3

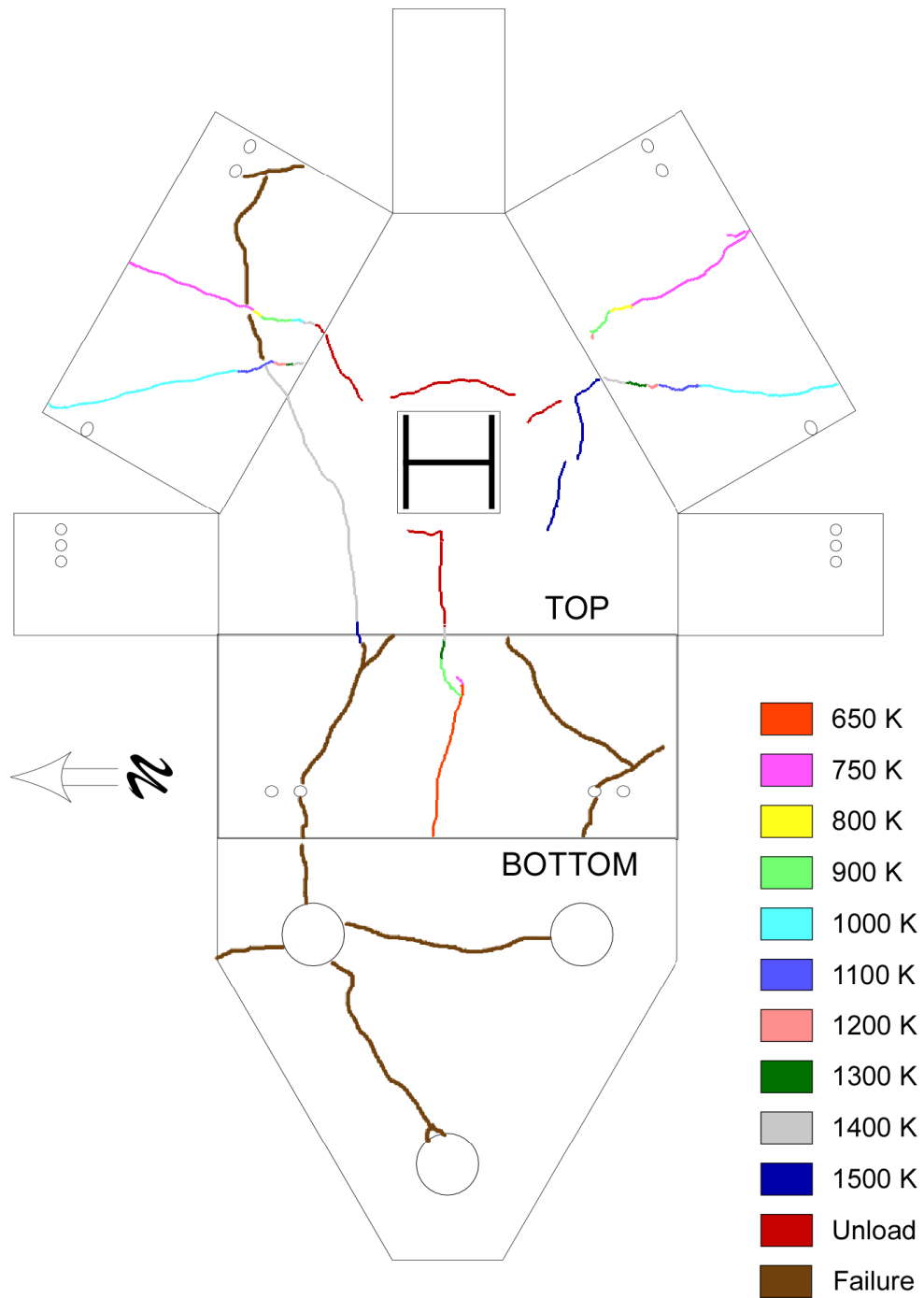


Figure 4.4: Crack maps – Pile Cap #3



Figure 4.5: Failure of Pile Cap #3

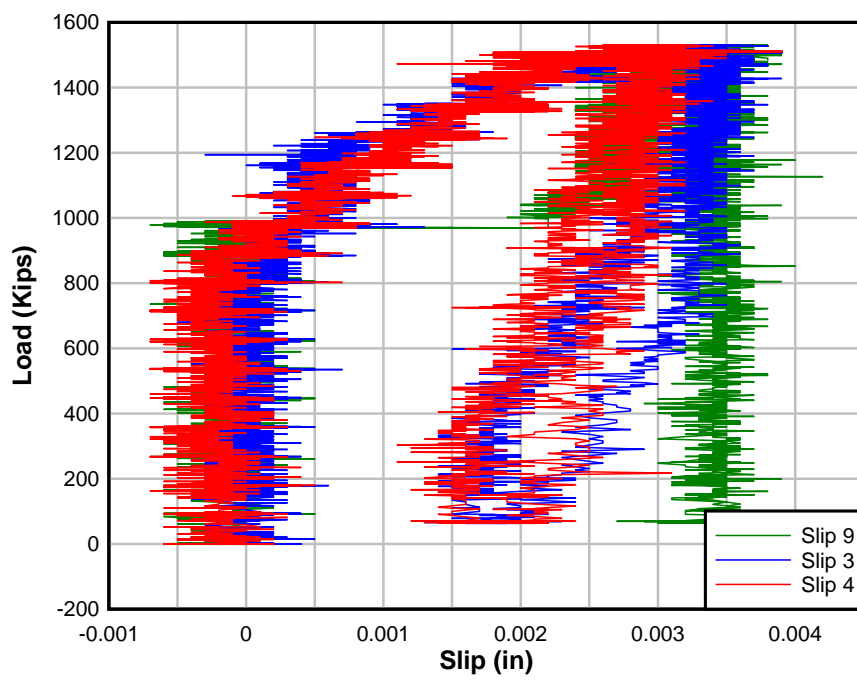
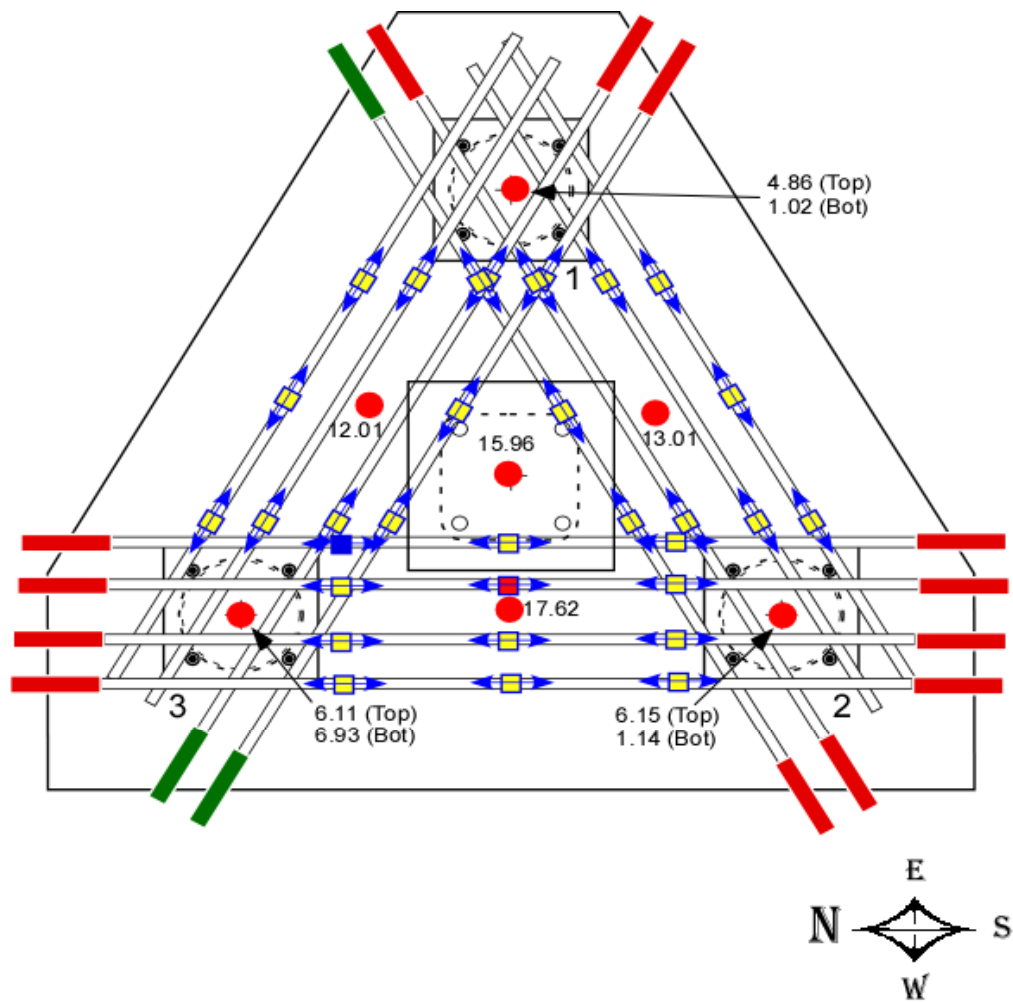


Figure 4.6: Slip of reinforcement – Pile Cap #3



- Displacements just prior to failure (1/100 inches)
- Reinforcing bar end without slip
- Reinforcing bar end with slip
- Uniaxial strain gages on reinforcing bars
 - Damaged during Construction
 - Yielded

Figure 4.7: Conditions at failure for Pile Cap #3

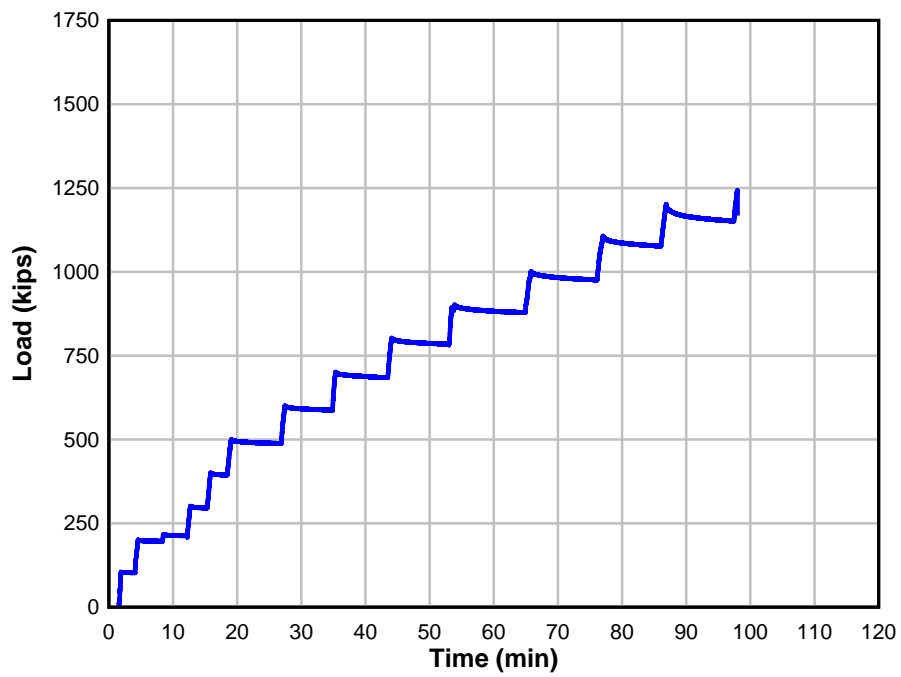


Figure 4.8: Column load vs. Time – Pile Cap #4

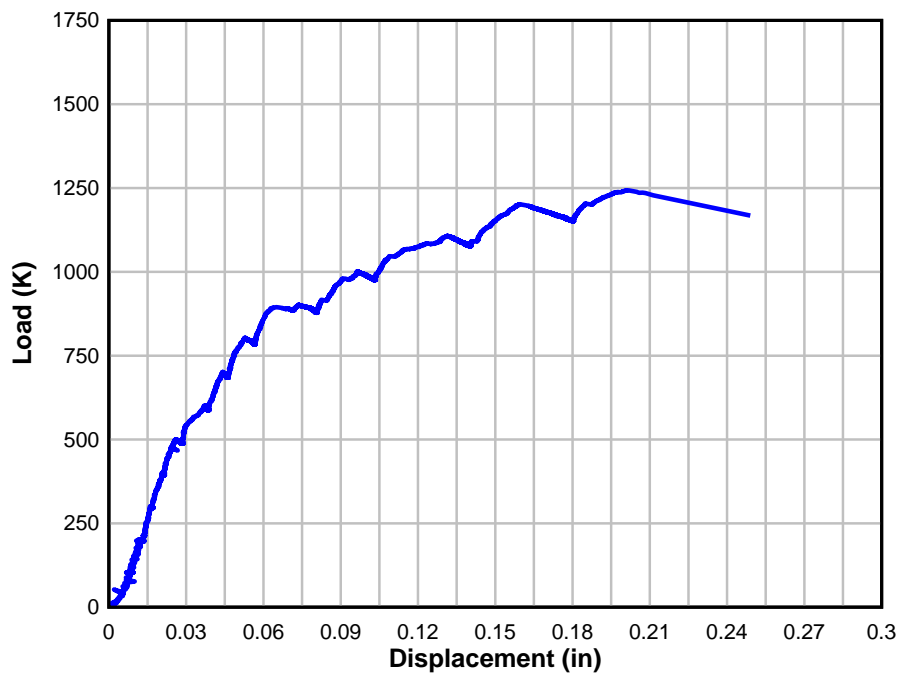


Figure 4.9: Column load vs. Centerline vertical displacement – Pile Cap #4

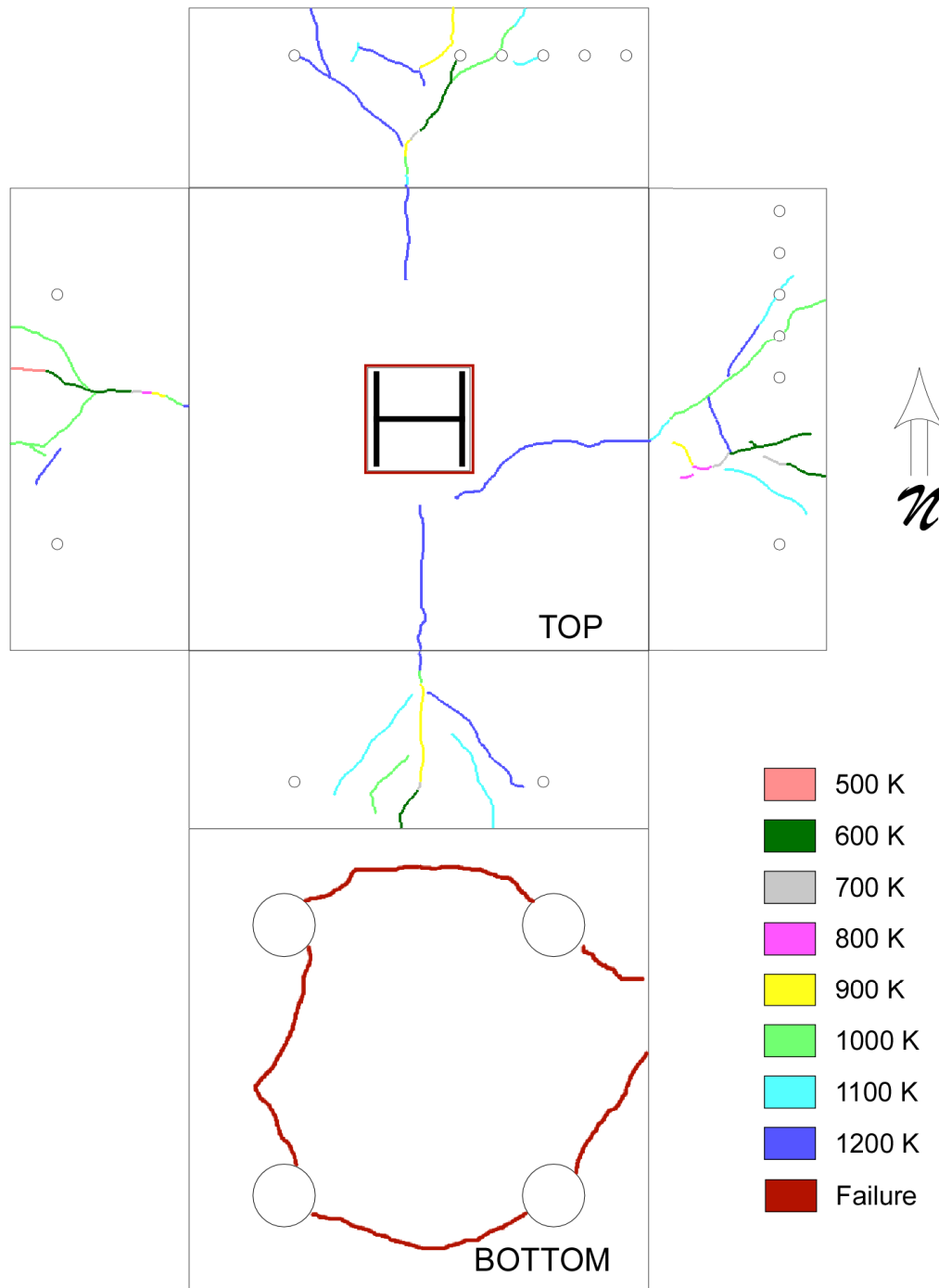


Figure 4.10: Crack maps – Pile Cap #4



Figure 4.11a: Failure of Pile Cap #4



Figure 4.11b: Punching of 3 in. thick bearing plate at failure of Pile Cap #4

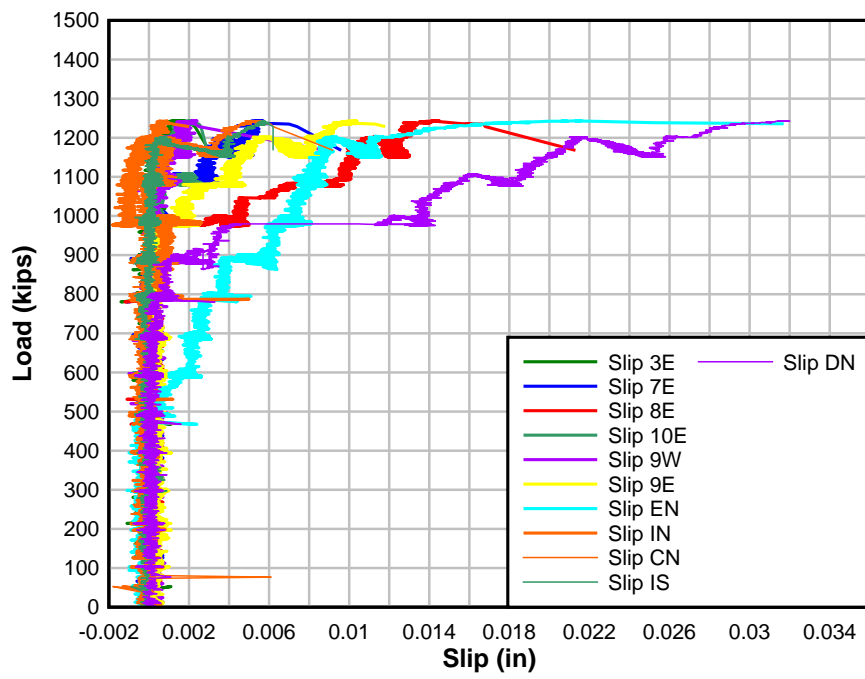


Figure 4.12: Slip of reinforcement – Pile Cap #4

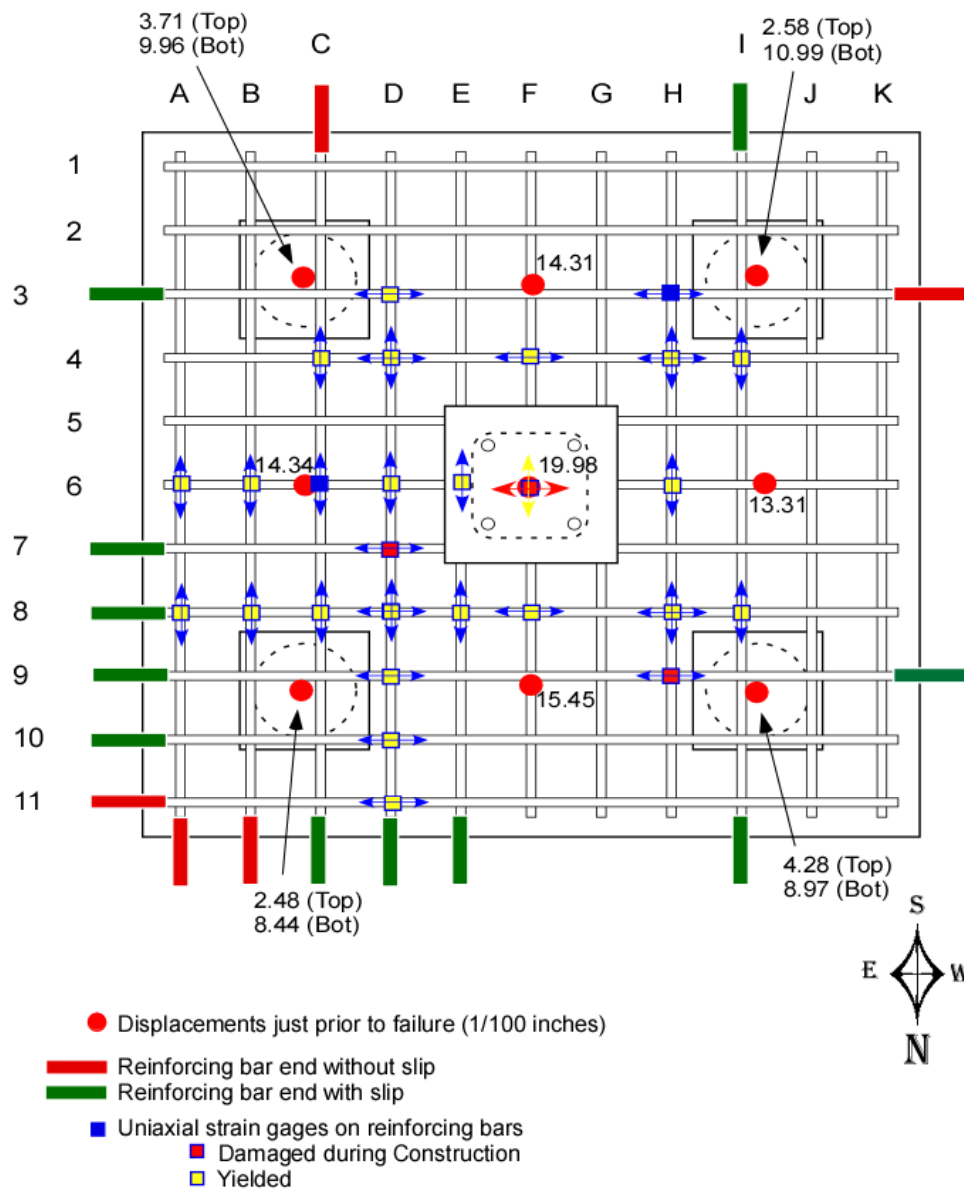


Figure 4.13: Conditions at failure for Pile Cap #4

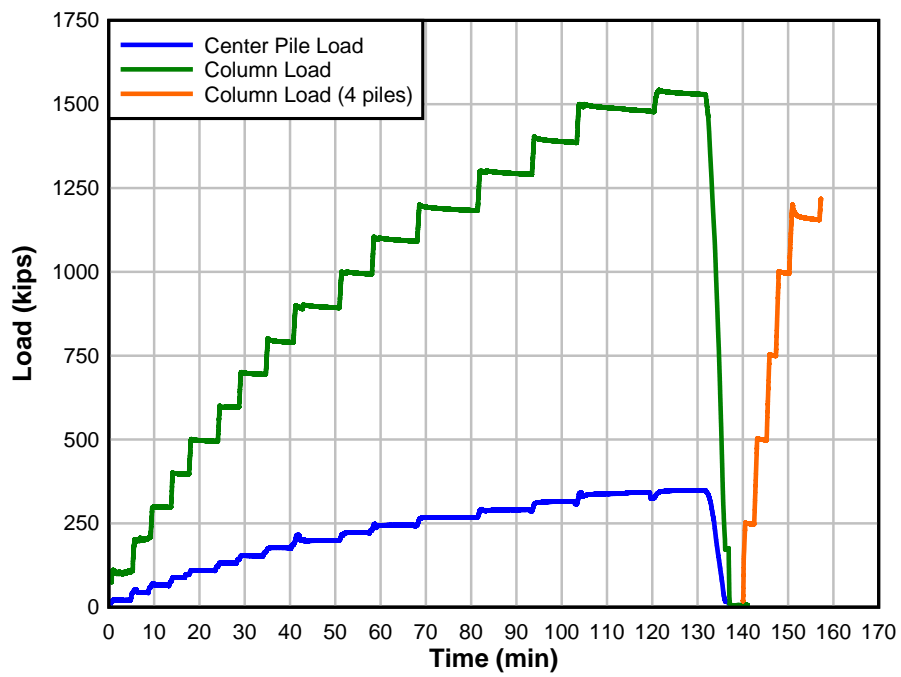


Figure 5.14: Column load vs. Time – Pile Cap #5

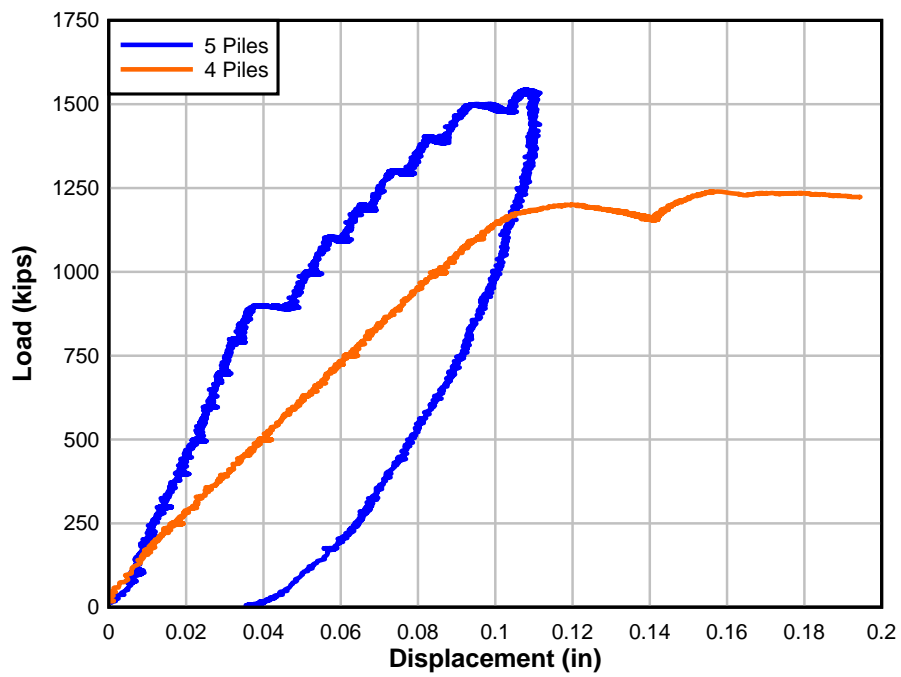


Figure 4.15: Column load vs. Centerline vertical displacement – Pile Cap #5

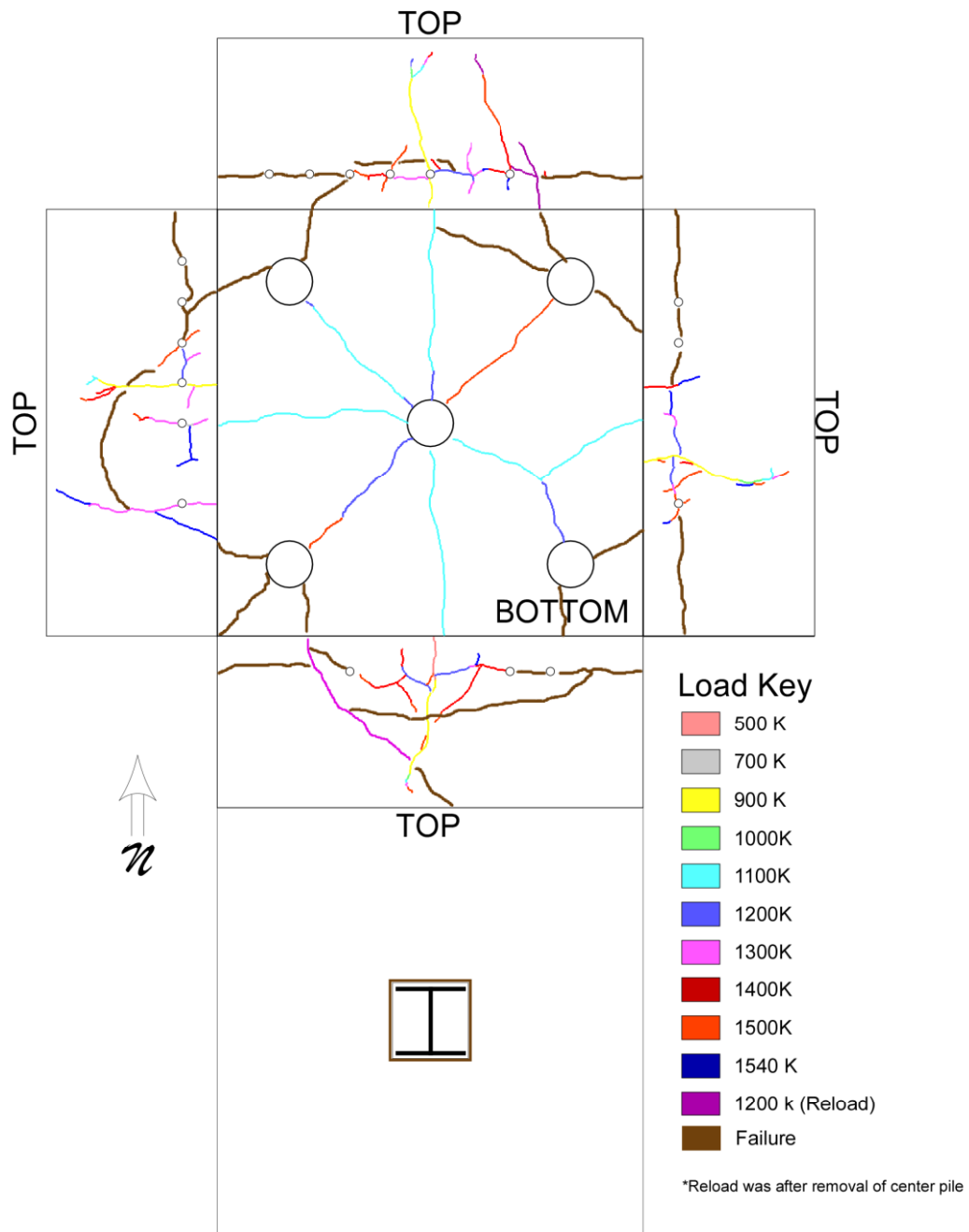


Figure 4.16: Crack maps – Pile Cap #5

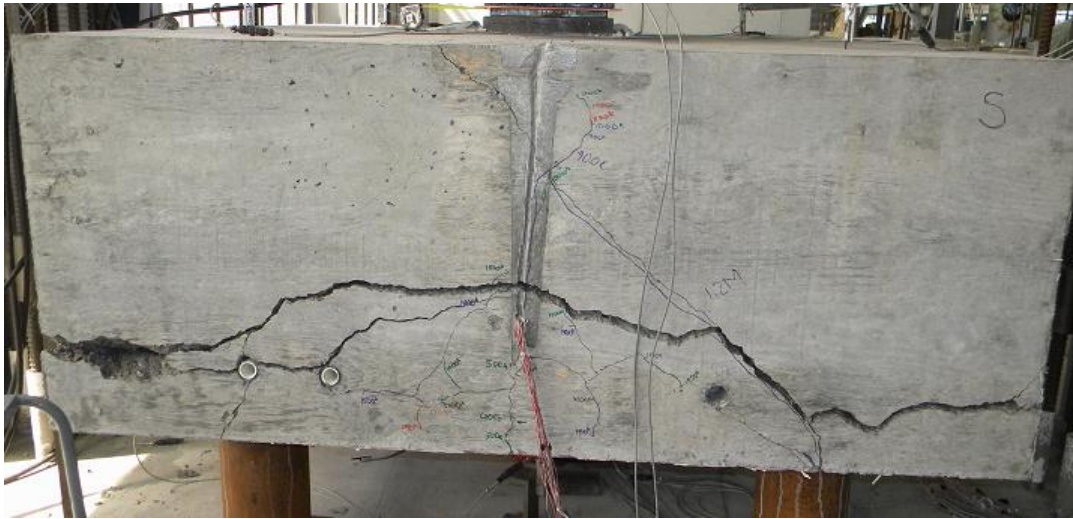


Figure 5.17a: Failure of Pile Cap #5



Figure 4.17b: Punching of 3 in. thick bearing plate at failure of Pile Cap #5

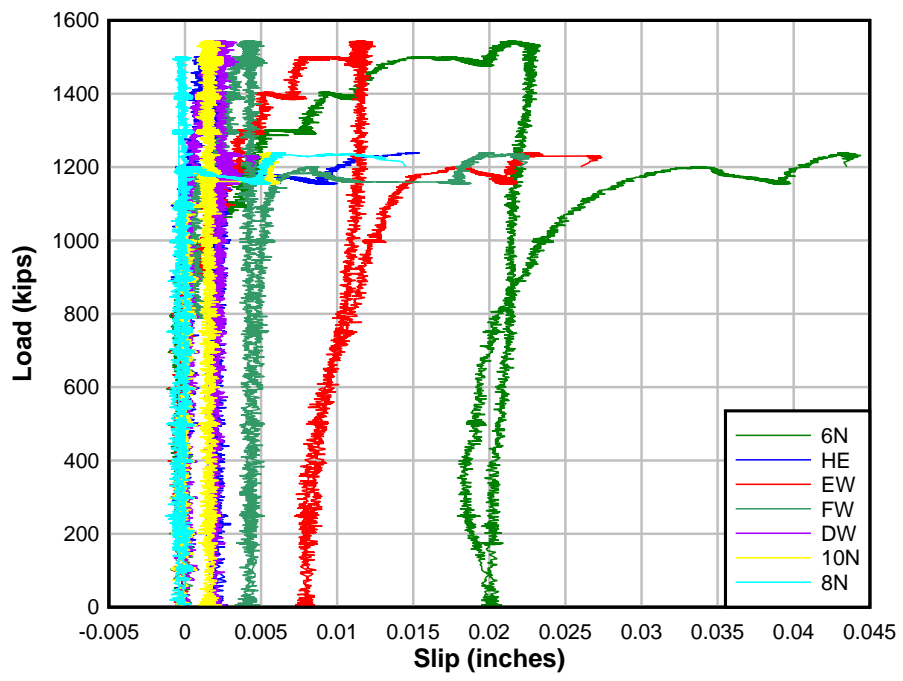


Figure 4.18: Slip of reinforcement – Pile Cap #5

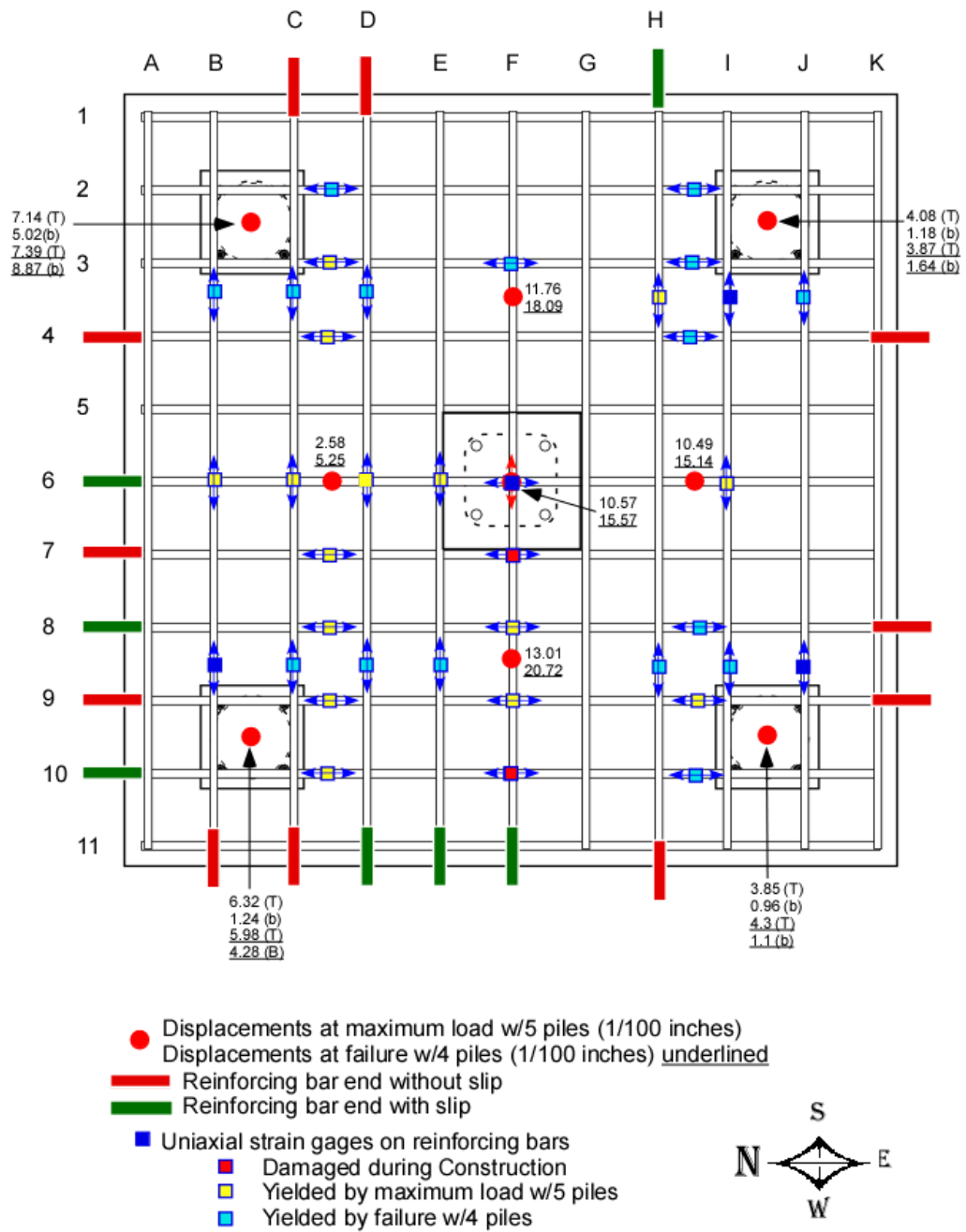


Figure 4.19: Conditions at failure for Pile Cap #5

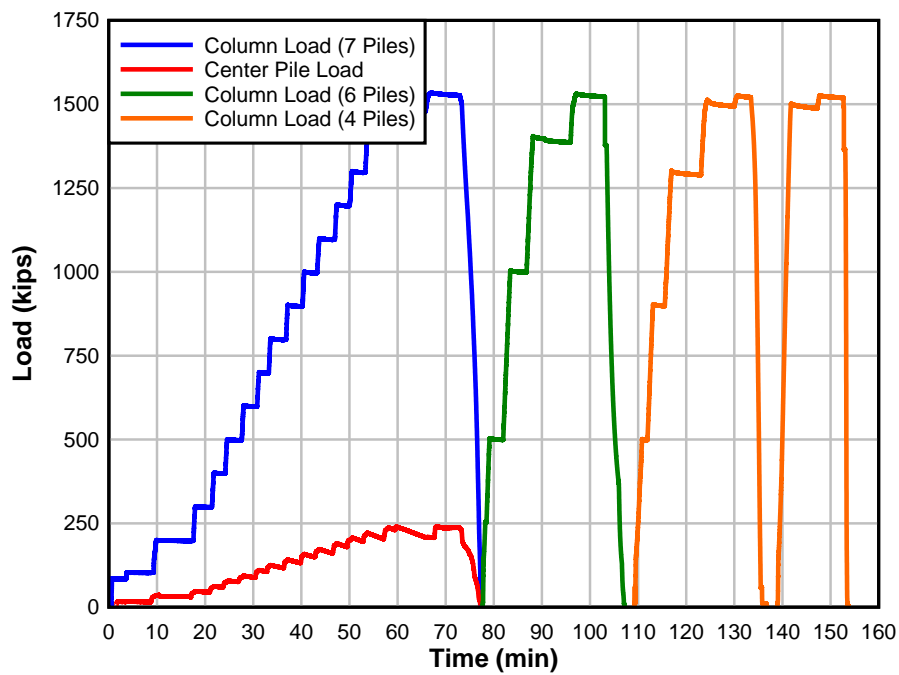


Figure 4.20: Column load vs. Time – Pile Cap #7

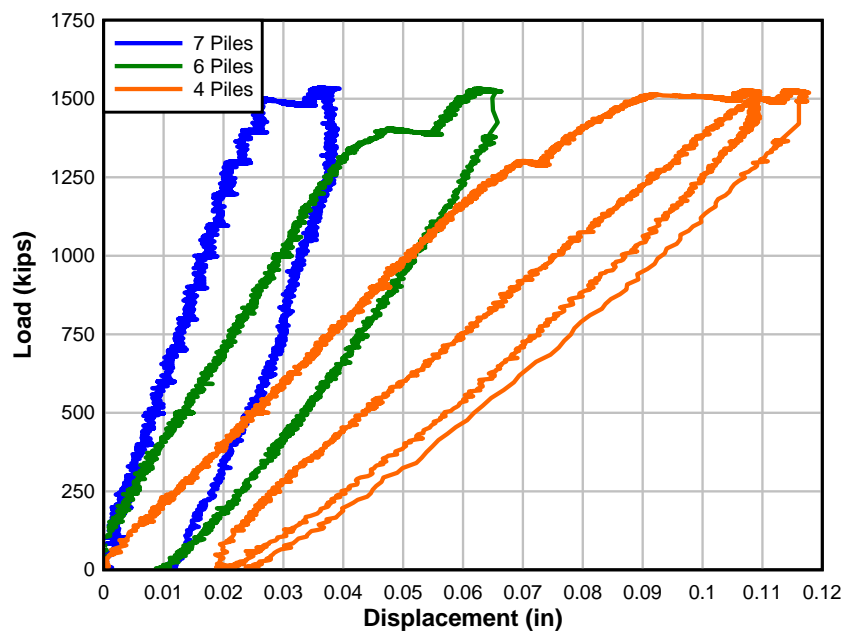


Figure 4.21: Column load vs. Centerline vertical displacement – Pile Cap #7 (note: displacement was reset to zero for different configurations)

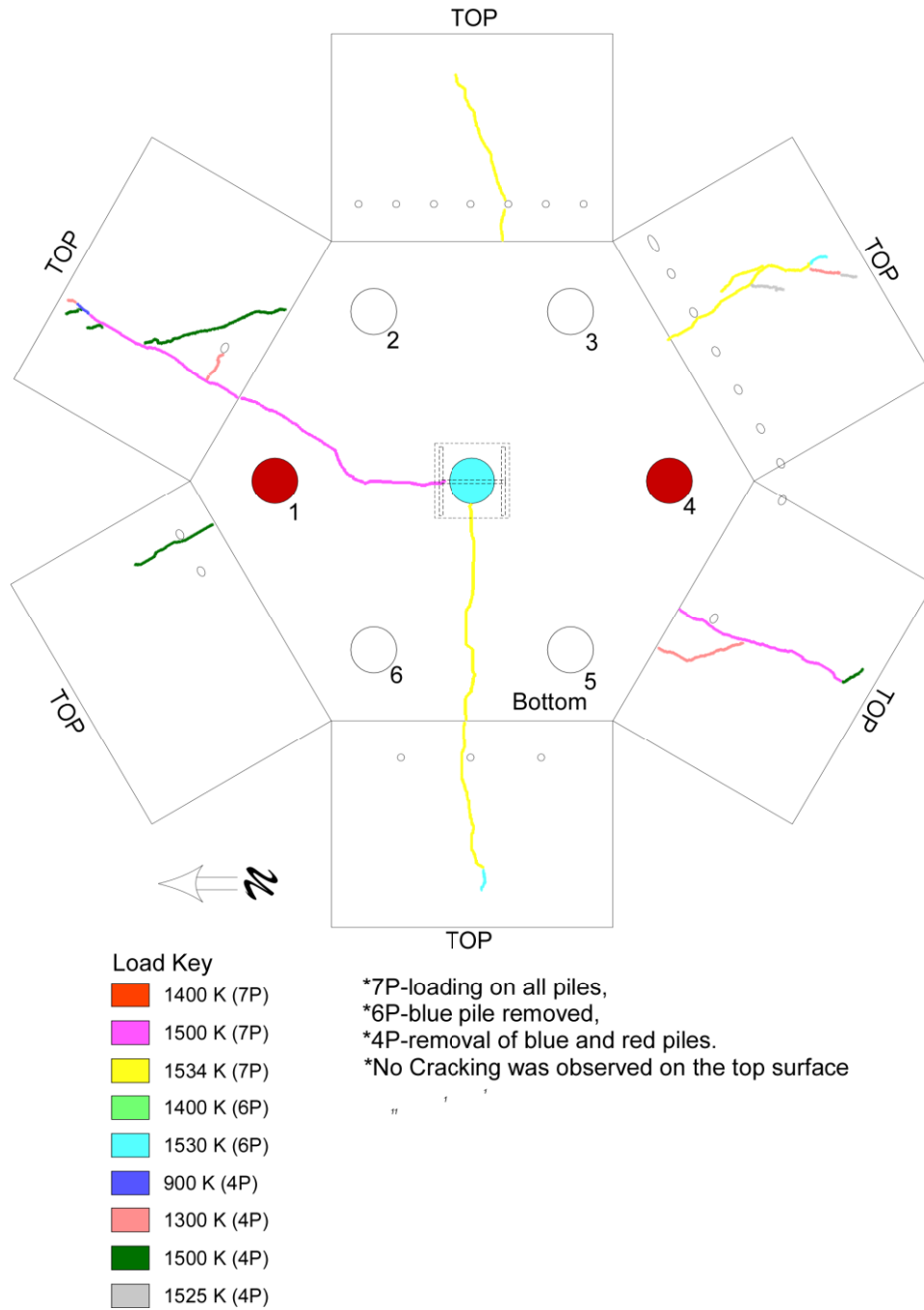


Figure 4.22: Crack maps – Pile Cap #7

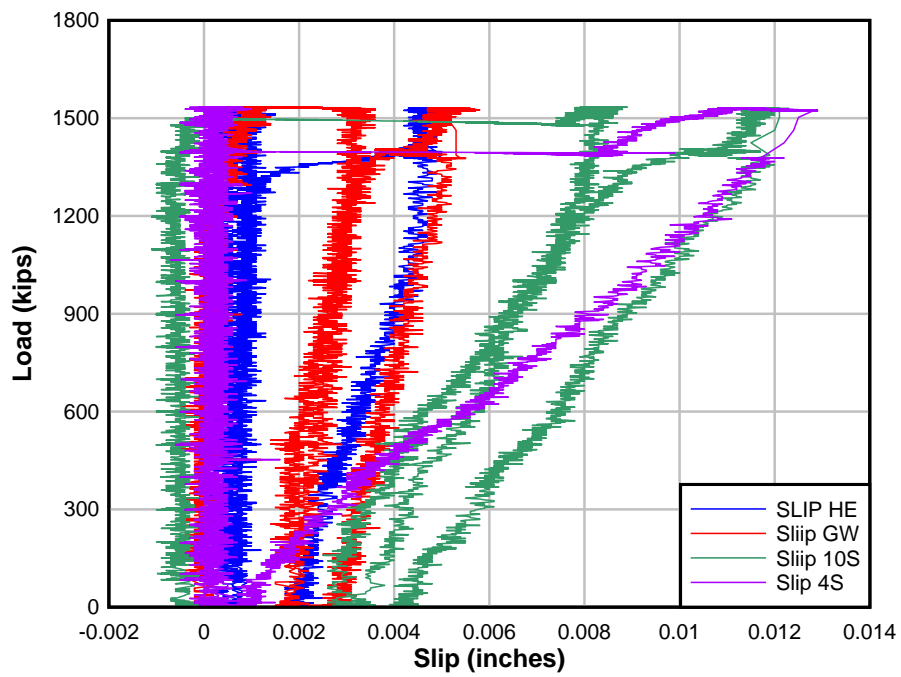


Figure 4.23: Slip of Reinforcement for Pile Cap #7 with 7 and 6 piles intact

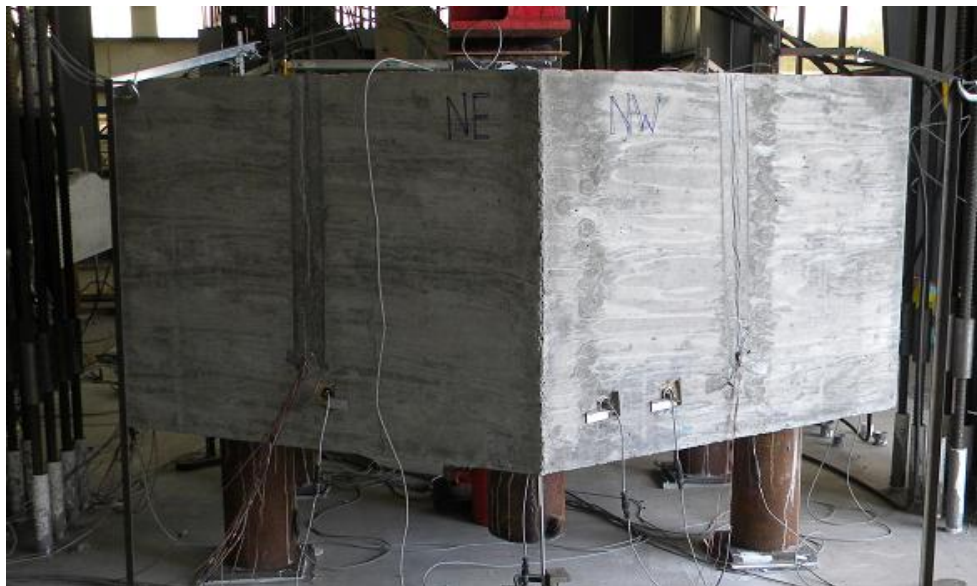


Figure 4.24: Pile Cap #7 after testing with piles 1, 4 and the center pile removed

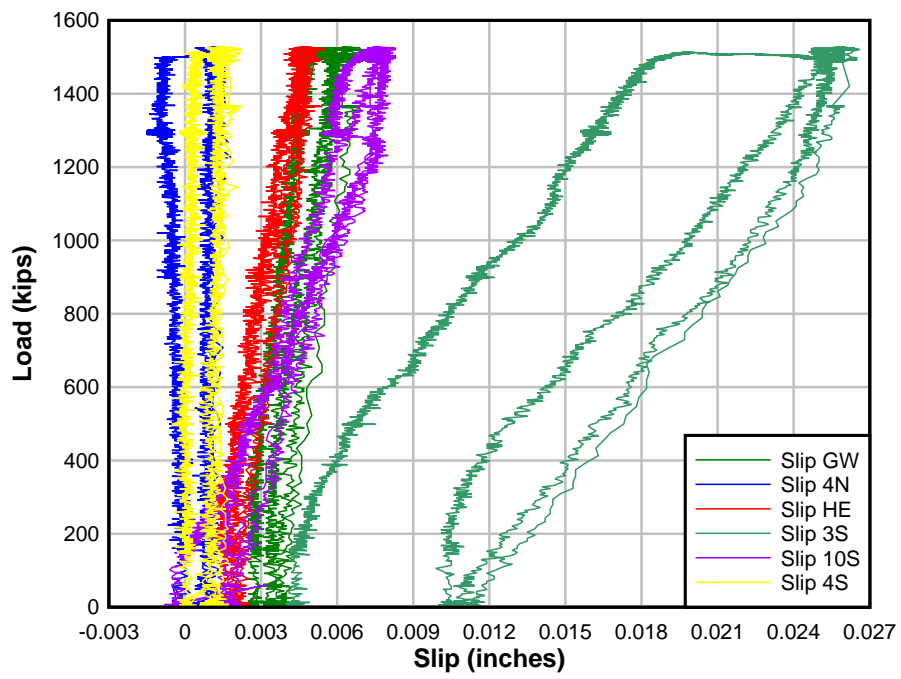


Figure 4.25: Slip of Reinforcement for Pile Cap #7 with 4 piles.

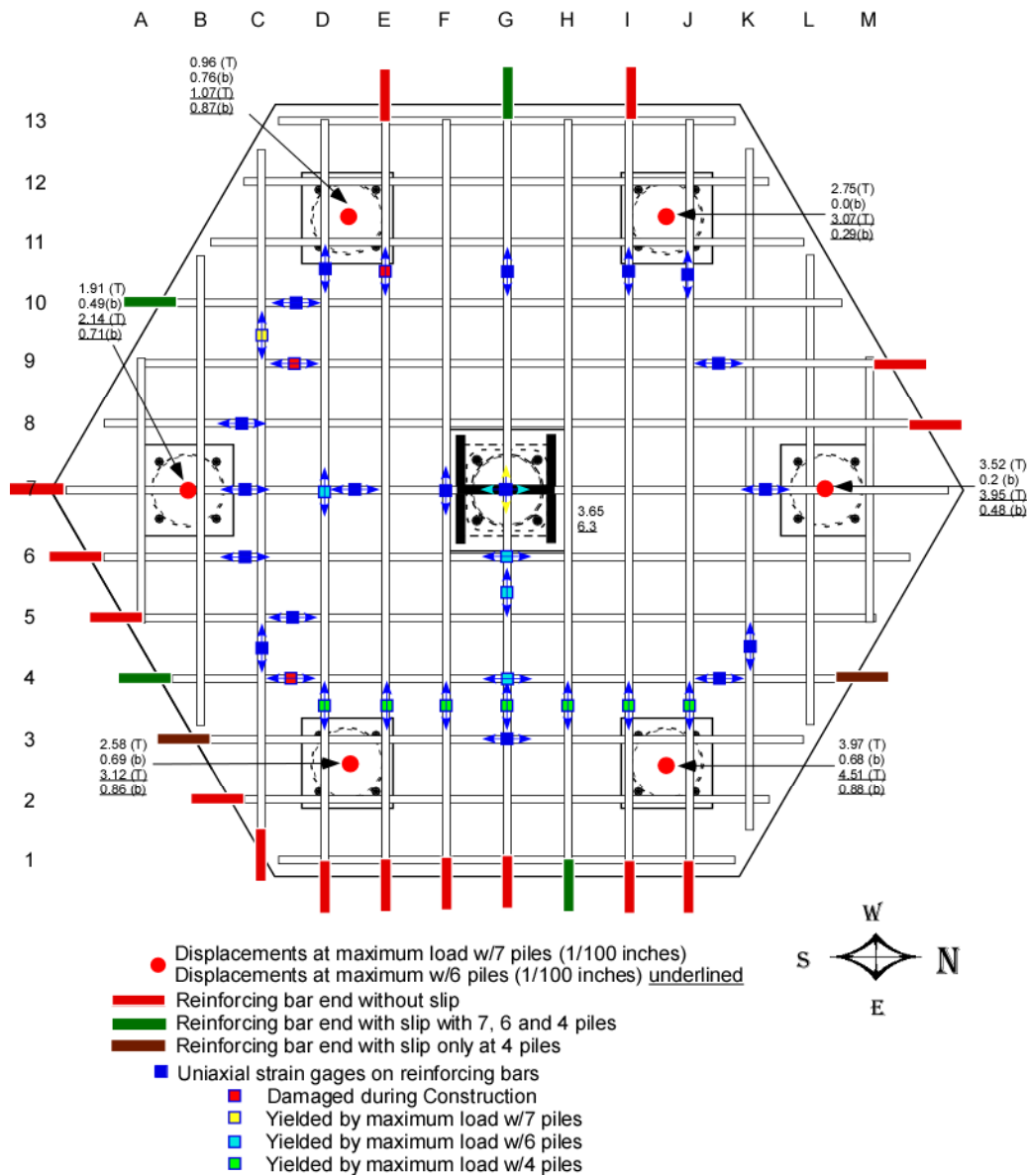


Figure 4.26: Conditions at maximum load for Pile Cap #7

5.0 ANALYSIS

Two different analysis methods were used to predict the strength of the experimental pile caps. The current ACI 318-08 design provisions provide multiple approaches for *design* of pile caps. The provisions allow for shear design in accordance with 11.11 (Provisions for slabs and footings) as well as with 15.5 (Shear in footings). Two-way shear calculations in accordance with ACI 318-08 were included for those pile caps that failed in two way shear (Pile Cap #4 and Pile Cap #5). One-way shear calculations in accordance with ACI 318-08 were made for Pile Cap #3 that failed in one-way shear. An alternative approach in ACI 318 is to use Strut-and-Tie Models (S&T) as provided in Appendix A. The following section outlines S&T models for all tested pile caps and the corresponding ultimate loads. ACI 318-08 provides reductions to concrete strengths for certain regions of the S&T model. To help guide development of rational S&T models, finite element models were developed for each of the four pile caps. Results of this study are detailed below.

5.1 Finite Element Models

Finite element analysis (FEA) of nonlinear concrete structures with disturbed stress fields is a difficult challenge. In the present study, FEA models were used to assess relative stress flow in the pile caps and were not used to predict the strength of the experimental specimens. For this reason the models were used only in the elastic range to guide S&T models. Finite element analysis results allowed for the extraction of nodal heights and approximate shapes, as well as identification of strut geometry and type.

Finite element modeling was achieved by the use of Abaqus/Standard [Hibbitt, Karlson & Sorenson 2002]. Abaqus allows users to model a wide range of geometries and materials by providing large libraries of elements types and materials models. The finite element model combines many factors including material properties, element types, mesh density and definition of boundary conditions and applied loads. The following subsections detail the FEA models used in this study.

5.1.1 Element Section Properties

FEA modeling required two main element types, one representing the concrete pile cap and the other representing the embedded reinforcing steel. The concrete pile cap was modeled using a solid element with a quadratic integration 20 node block. The reinforcing steel was modeled with truss elements and used linear integration.

5.1.2 Material Properties

Materials properties for the FEA models were considered to describe those of the test specimens. The properties for the steel reinforcement were as follows: Young's Modulus = 200000 MPa (29000 ksi), Poisson's ratio = 0.15, and plastic strain = 0.003. the yield stress of the reinforcing steel was taken as that from the coupon samples as reported in Table 3.1.

For the concrete, the Concrete Damage Plasticity (CDP) Model was used. The following properties were used: dilation angle = 31, eccentricity = 0.1, $\sigma_{b0}/\sigma_{c0} = 1.1$, $K = 0.55$, and viscosity parameter = 0.001. The dilation angle was based on recommendations by Malm [2009] for concrete subjected to both tensile and compressive stresses.

Eccentricity is a parameter affecting curvature in the stress flow and was based on a default value of 0.1. Initial equal biaxial compressive yield stress to initial uniaxial compressive yield stress (σ_b/σ_c) was set to 1.1 based on default setting of 1.16 and broad recommendation of 1.07 by Newman *et al.* [1972]. “K” represents the second stress invariant on the tensile meridian to the compressive meridian. The viscosity parameter was set at a value of .001, default is 0.0.

For the concrete compression parameters, ultimate stress was taken from day-of-test compression cylinder test results reported in Table 3.2a. The uniaxial stress strain relationship was developed using Todeschini *et al.*'s [1964] approximation. The ultimate tensile strength values were determined from testing day-of-test split cylinder tests as reported in Table 3.2b. The tensile stress-strain relationship was developed assuming yield at 50% ultimate tensile load.

5.1.3 Boundary Conditions and Loading

Boundary conditions were applied at the surface of the pile bearing plates to restrict vertical displacements while the other degrees of freedom were not restrained. Support conditions at one pile location were restricted laterally in both directions to ensure numerical stability.

Loading was applied as a hydrostatic pressure over the surface of the column bearing plate. Loads were applied in one step intervals with no less than 10 increments.

5.1.4 Assembly

The model was assembled using a solid element for the concrete portion of the pile cap. The pipe piles were not represented in the model, instead a square 30.5 cm by 30.5 cm (12 in. by 12 in.) surface was cut 12.7 cm (5 in.) into the solid elements at pile locations. These surfaces served as boundary surfaces to represent the steel pipe pile bearing. Truss elements representing the reinforcing steel were embedded into the solid. The embedment constraint rigidly attached the reinforcing steel to the surrounding concrete elements and did not allow for slip. This rigid connection is representative of test data.

The reinforcement was meshed to the same seed size as the concrete for computational purposes. Concrete meshing balanced computation efficiency and convergence. Concrete elements were taken at least twice the size of maximum aggregate size, 1.9 cm ($\frac{3}{4}$ in.) in the present case. Meshing for all specimens was between 4.1 cm. (2 inches) and 8.2 cm. (4 inches) depending on the overall size of the pile cap.

5.1.5 Finite Element Modeling Results

FEA modeling provided stress flows within the different specimens and the results were used to establish the geometry of the later S&T models (described subsequently). The stress flows provided size and shape approximations for S&T modeling. The stress tensor mapping provided evidence that the struts were in fact spreading in the middle region of the pile cap and thus should be considered as “bottle-struts.” The results of the finite element models are shown in Figs. 5.1a to Figs. 5.7f. Figures labeled principal stress tensor show stress tensors that indicate direction and magnitude of the principal stresses (both

tension and compression) while figures labeled principal compression or tension show only magnitude of the compression and tension stresses, respectively.

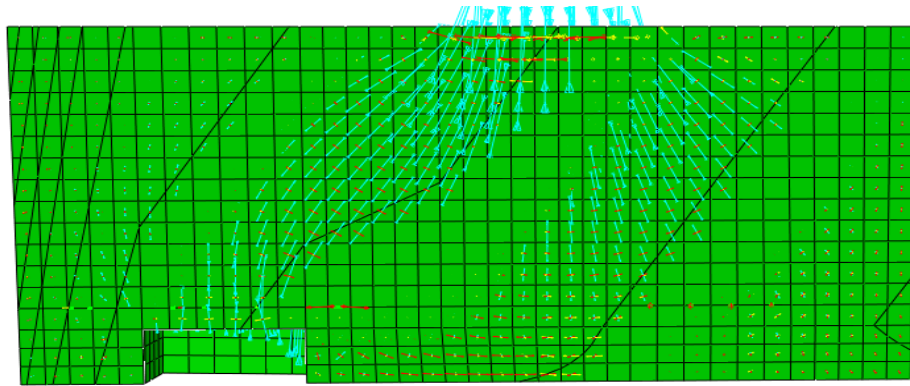


Figure 5.3a: Principal stress tensor Strut A (see Fig. 6.12) in Pile Cap #3

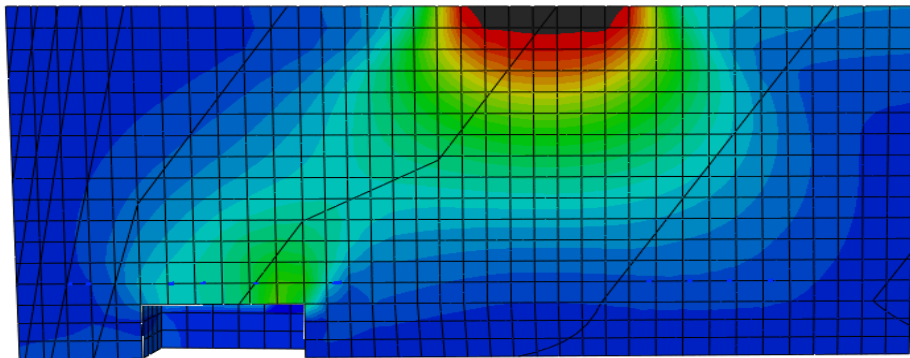


Figure 5.3b: Principal compression Strut A (see Fig. 6.12) in Pile Cap #3

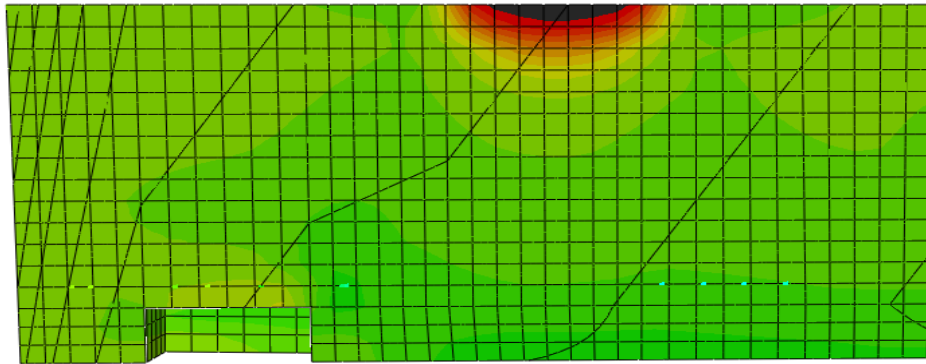


Figure 5.3c: Principal stress tension Strut A (see Fig. 6.12) in Pile Cap #3

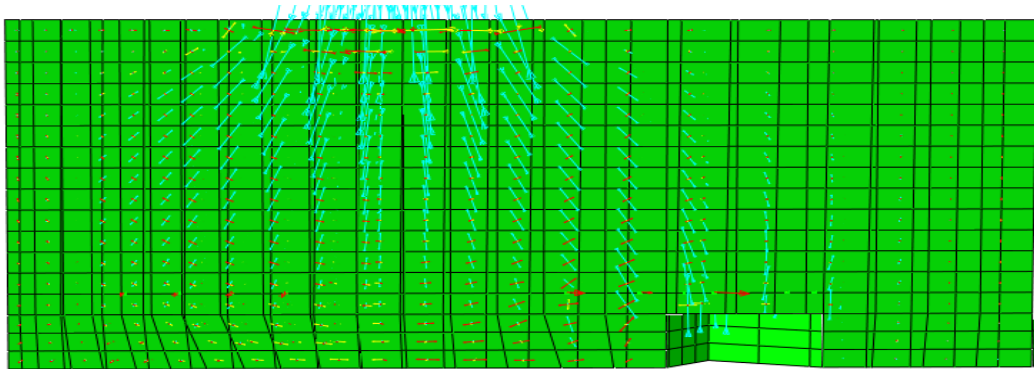


Figure 5.3d: Principal stress tensor Strut B (see Fig. 6.12) in Pile Cap #3

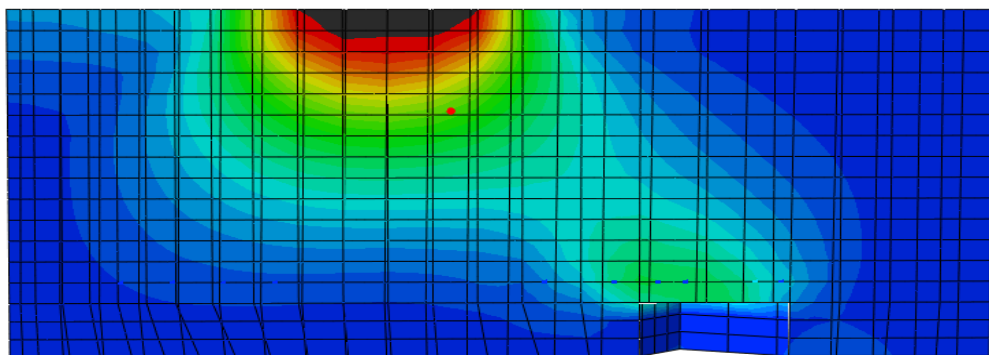


Figure 5.3e: Principal compression Strut B (see Fig. 6.12) in Pile Cap #3

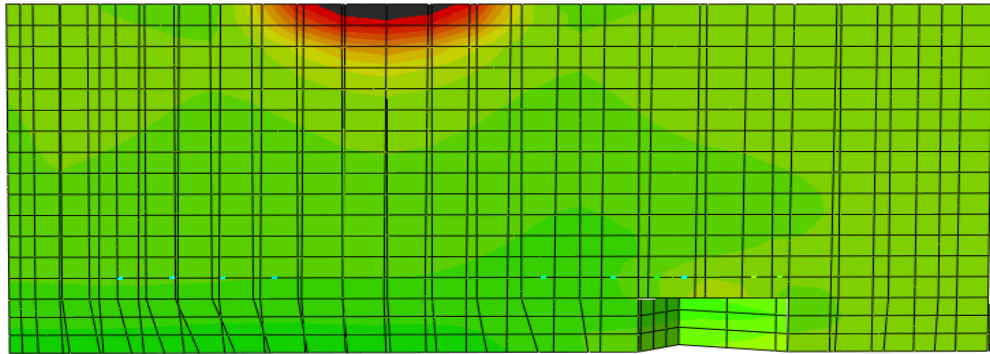


Figure 5.3f: Principal tension Strut B (see Fig. 6.10) in Pile Cap #3

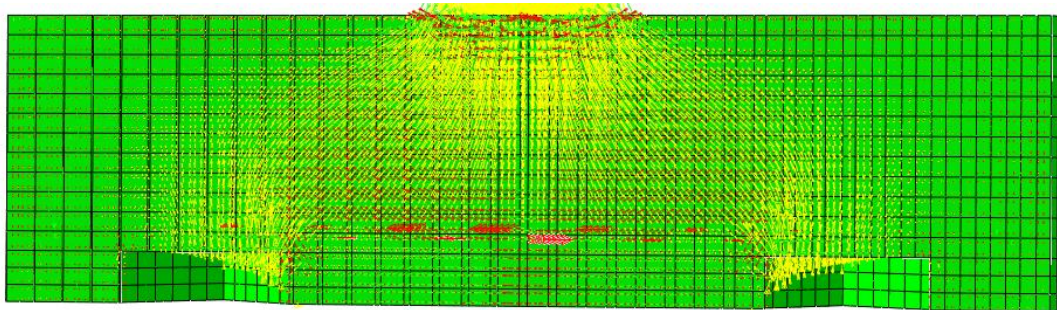


Figure 5.4a: Principal stress tensors cut along strut in Pile Cap #4

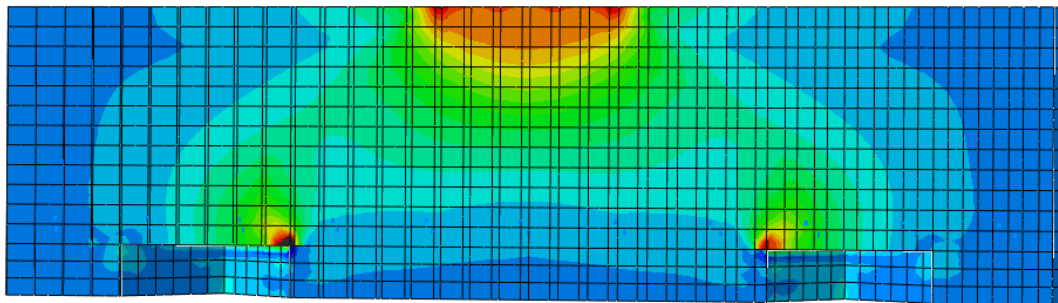


Figure 5.4b: Principal compression cut along strut in Pile Cap #4

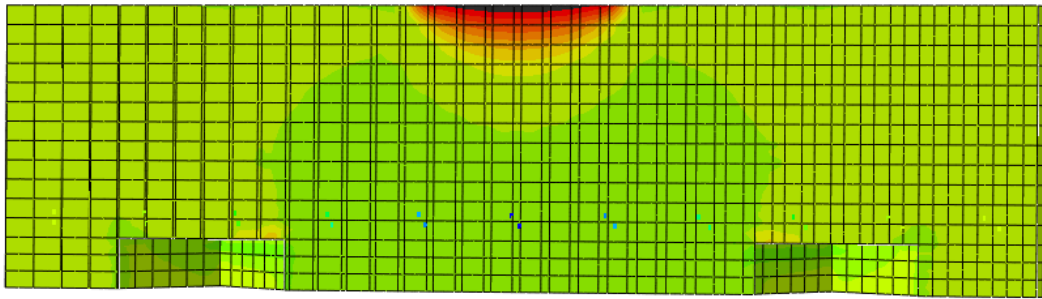


Figure 5.4c: Principal tension stress cut along strut in Pile Cap #4

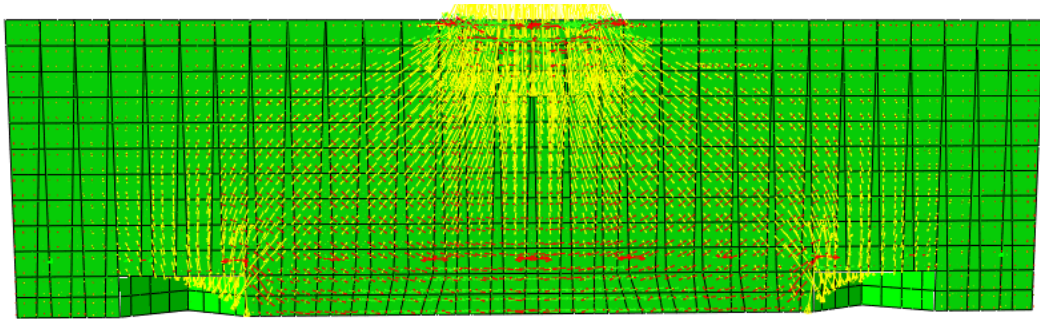


Figure 5.5a: Principal stress tensors cut along strut in Pile Cap #5

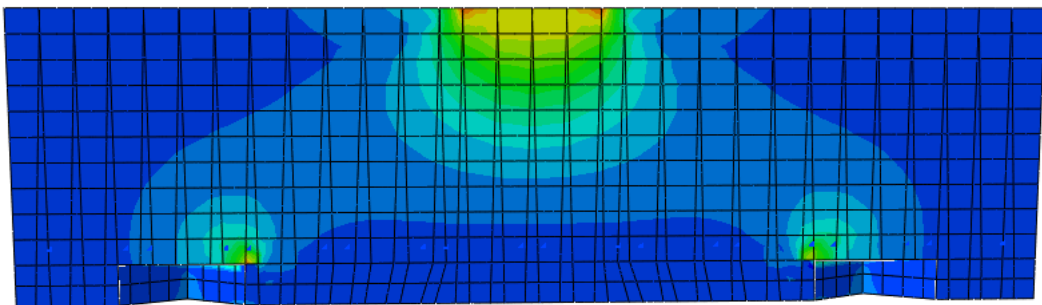


Figure 5.5b: Principal compression stresses cut along strut in Pile Cap #5

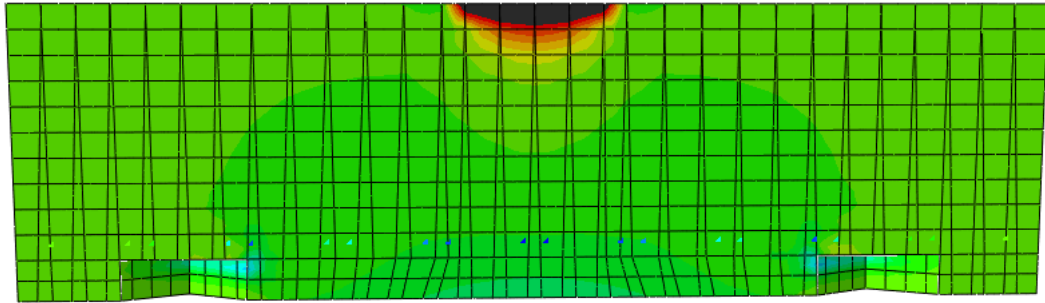


Figure 5.5c: Principal tension cut along strut in Pile Cap #5

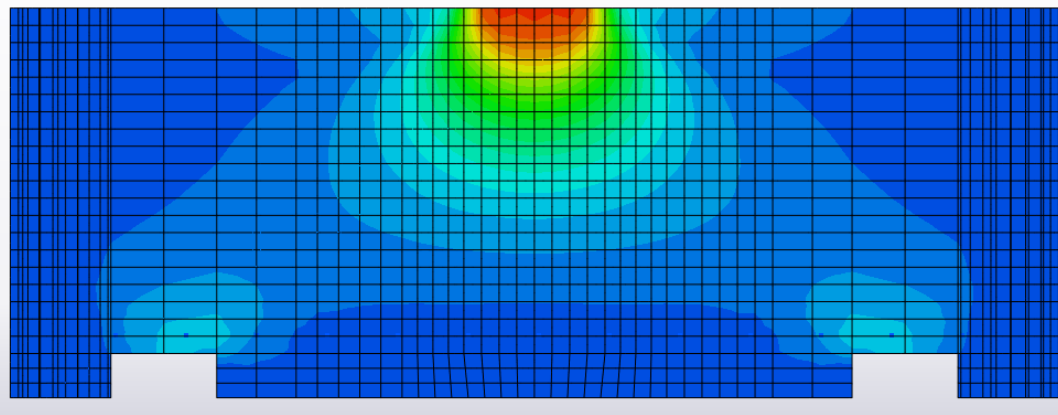


Figure 5.7a: Principal compression Strut A (see Fig. 6.14) in Pile Cap #7

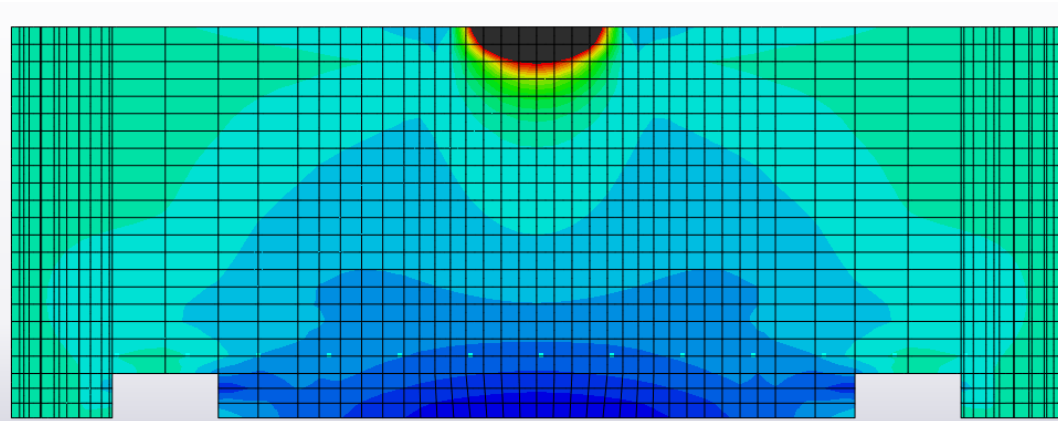


Figure 5.7b: Principal tension Strut A (see Fig. 6.14) in Pile Cap #7

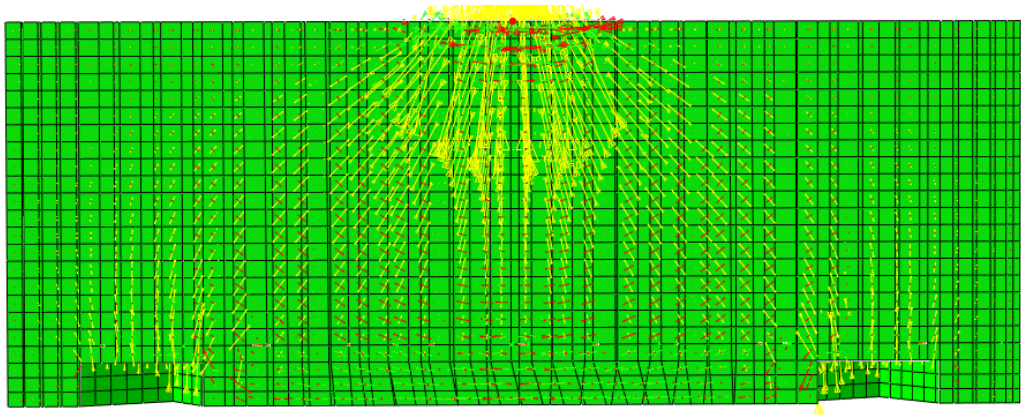


Figure 5.7c: Principal stress tensor Strut B (see Fig. 6.14) in Pile Cap #7

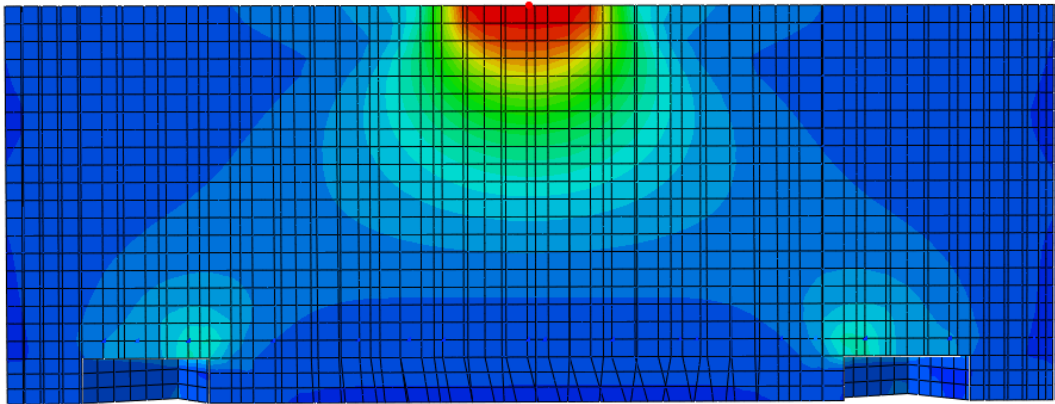


Figure 5.7d: Principal compression Strut B (see Fig. 6.14) in Pile Cap #7

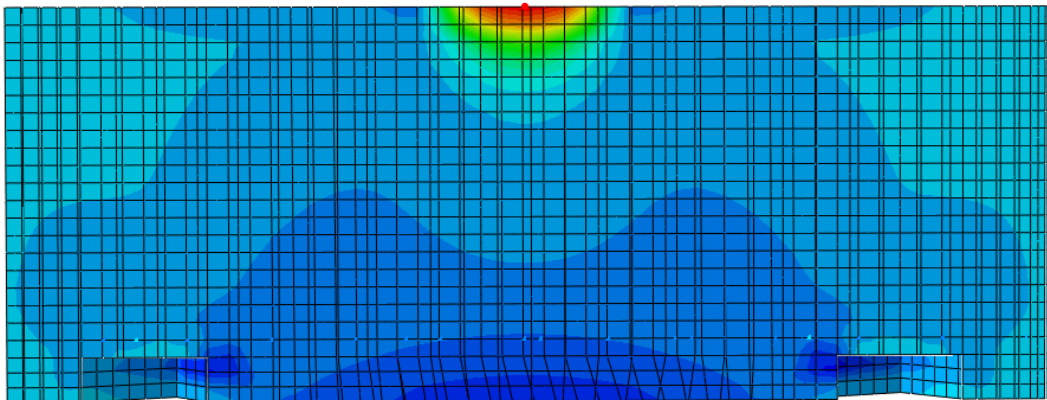


Figure 5.7e: Principal tension Strut B (see Fig. 6.14) in Pile Cap #7

5.2 Strut and Tie Models

Strut and tie models (S&T) are effective tools for designing regions with disturbed stress fields. The approach simplifies the region into an equivalent truss. The compression elements consisting of concrete are the struts while the tension elements consisting of reinforcing steel are the ties. At points of interaction, referred to as nodal zones, hydrostatic equilibrium must be met.

ACI 318-08 prescribes the strength of struts, nodal zones, and ties. The strut strength is partially dependent on the shape of the strut. Depending on the member geometry, the strut width can increase towards the mid-length. This spreading of the compression stresses results in tension stresses acting orthogonal to the compression stresses. This type of strut is referred to as a “bottle-strut”. ACI 318-08 uses a partial strength reduction factor of 0.75 for bottle struts if adequately reinforced and 0.6 if it is not reinforced. The effective compressive strength of nodes is also specified. ACI 318-08 reduces the effective compressive strength of nodes that anchor ties. Partial strength reduction factors are 0.8 for nodes anchoring a single tie and 0.6 for nodes anchoring multiple ties.

ACI 318-08 specifies that the tie force shall be developed at a point where the centroid of the reinforcement leaves the extended nodal zone. Test data along with FEA data was examined to establish the participation of the embedded reinforcing steel as ties. Measured strain values as well as FEA results were normalized by dividing by yield strain as seen in Figs. 5.8 to 5.11. Normalized strains were compared to find the relative strains amongst reinforcement steel. As can be most clearly seen in Fig. 5.10, the reinforcing bars

located away from the pipe pile bearing plates did not carry the same amount of force as those located that were close to the bearing plates. Considering the nonuniform participation of the reinforcing steel, only those bars located within an extended nodal zone above the pipe pile bearing plates were attributed to the ties in the S&T models. The extended nodal zone was projected upward from the edges of the bearing plate assuming a 45° distribution angle up to a plane passing through the centroid of the reinforcing steel. Considering the geometry of the pile caps, ACI 318-08 anchorage requirements for the ties were not met. This was because the available anchorage lengths past the nodal faces were less than the prescribed development lengths. The development lengths computed using the simplified methods in Chapter 12 of ACI 318-08 for #7 and #8 size reinforcing bars of Grade 60 steel were 94 cm (37 in.) and 107 cm (42 in.), respectively.

5.2.1 S&T Results

Analysis of the different pile cap specimens was performed using S&T models. Each of the models and the results are described below and are reported in Table 5.1.

Pile Cap #3

The geometry of the S&T model for Pile Cap #3 is shown in Fig. 5.12. Nodal zone approximations were based on finite element modeling results. Nodes at the pipe pile bearing locations had an estimated height of 7.62 cm (3 in.) while the node at the column bearing plate had an approximate depth of 20 cm (8 in.). Based on test data, all reinforcing bars were considered to participate and were used in the idealized ties (see Fig. 4.7, Fig

5.8, and Fig. 5.9. The limiting element was Strut B at the pipe pile bearing plate node. The S&T model for Pile Cap #3 resulted in an ultimate load of 3220 kN (724 kips).

Pile Cap #4

The geometry of the S&T model developed for Pile Cap #4 is shown in Fig 5.13. Reinforcement was grouped to provide two reinforcing bars per tie, resulting in four ties. Test data as seen in Fig. 4.13, showed that at failure the reinforcing steel attributed to the ties was at yield. The assumed nodal geometries were based on the finite element model, with the pipe pile bearing plate node height of 5 cm (2in.) and the column bearing plate node height of 17.75 cm (7 in.). The controlling element for the S&T model was the tie strength. The ultimate load predicted by the S&T model for Pile Cap #4 was 2326 kN (523 kips).

Pile Cap #5

Pile Cap #5 provided a similar geometry as Pile Cap #4 and is shown in Fig.5.13. The middle pile was not considered for this assessment.. Reinforcement was grouped similar to Pile Cap #4, with just two reinforcing bars used in each tie. It assumed that the high strains in the adjacent non-anchored bar can be attributed to flexural demands. Assumed nodal heights based on the finite element model are 7.62 cm (3in.) at pipe pile bearing nodes and 23 cm (9in.) at the column bearing node. Ultimate load was controlled by yielding of ties. Ultimate capacity was found to be 2402 kN (540kips).

Pile Cap #7

The geometry of the assumed strut and tie model for Pile Cap #7 is shown in Fig.5.14. Two different strut types were considered. Nodal heights at pipe pile bearing nodes were taken as 10.2 cm (4 in.) and nodal depth at column bearing was considered 23 cm (10 in.) these are estimations taken from the finite element model. Yielding of ties 1 and 2 were the limiting factors of the design. Ultimate capacity was found to be 3411 kN (767 kips).

5.3 One-way and Two-Way Shear Models

Shear strength was also predicted using ACI 318-08 Section 11.11 (Provisions for slabs and footings) as well as with 15.5 (Shear in footings). Two-way shear calculations in accordance with ACI 318-08 were included for those pile caps that failed in two-way shear (Pile Cap #4 and Pile Cap #5). One-way shear calculations in accordance with ACI 318-08 were made for Pile Cap #3 that failed in one-way shear.

ACI 318-08 Section 11.11 prescribes the strength of a normal-weight concrete slab subjected to two-way punching shear as the lesser of:

$$V_c = (2+4/\beta) * (\sqrt{f'_c}) * b_0 d$$

$$V_c = (\alpha d / b_0 + 2) * (\sqrt{f'_c}) * b_0 d$$

$$V_c = 4 * (\sqrt{f'_c}) * b_0 d$$

where d is the depth of the member, b_0 is the perimeter of the critical section, f'_c is the concrete compressive strength, β is the ratio of the long side of the column to the short side of the column (1 for square columns), and α is 40 for interior columns. This equation was used to evaluate the strength of Pile Caps #4, #5, and #7 with the critical section taken at $d/2$ from the face of the column bearing plate. Pile caps #4 and #5 both exhibited two-way punching shear failures. Pile Cap #7 was not tested to failure due to limitations of the present laboratory setup. For the analysis of Pile Caps #5 and #7, the center pile was ignored. The computed two-way punching shear strengths for the specimens are reported in Table 5.1. The predicted two-way punching shear strength for Pile Cap #4 was conservative, but for Pile Cap #5 was unconservative. This indicates that the present design provisions may not apply to the large-size pile cap specimens considered in this study.

ACI 318-08 Section 11.2 prescribes the strength of a normal-weight concrete slab subjected to one-way shear as:

$$V_c = 2*(\sqrt{f'_c})*b_w d$$

where d is the depth of the pile cap, b_w is the width at critical section, and f'_c is the concrete compressive strength. This equation was used to evaluate the strength of Pile Cap #3 with the critical section taken at midpoint between the edge of the column bearing plate and the edge of the pipe pile bearing plate on the corner of the pile cap that failed. Pile Cap #3 exhibited a one-way shear failure along the corner with the smallest available width. The computed one-way shear strength was 195 kips which was multiplied by three (3) to account for the distribution of the applied column force to the three pipe piles and is

reported in Table 5.1. The predicted one-way shear strength for Pile Cap #3 was very conservative.

Table 5.1: Analysis Results

Specimen	S&T controlling Load (kips)	One-way shear load (kips)	Two-way shear load (kips)	Experimental failure load (kips)
Pile Cap #3	724	585	N.A.	1513
Pile Cap #4	523	N.A.	958	1234
Pile Cap #5	540	N.A.	1591	1239
Pile Cap #7	767	N.A.	2,339	N.A.

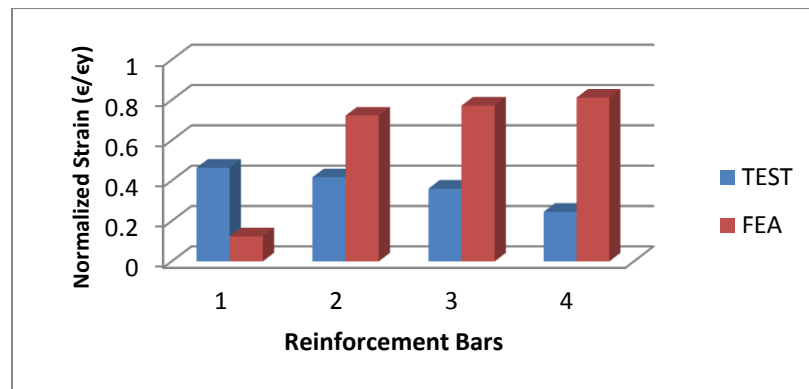


Figure 5.8: Pile Cap #3 Normalized reinforcement strain

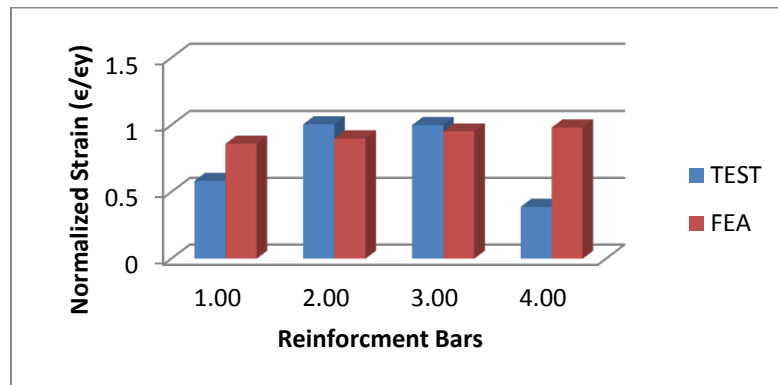


Figure 5.9: Pile Cap #3 Normalized reinforcement strain

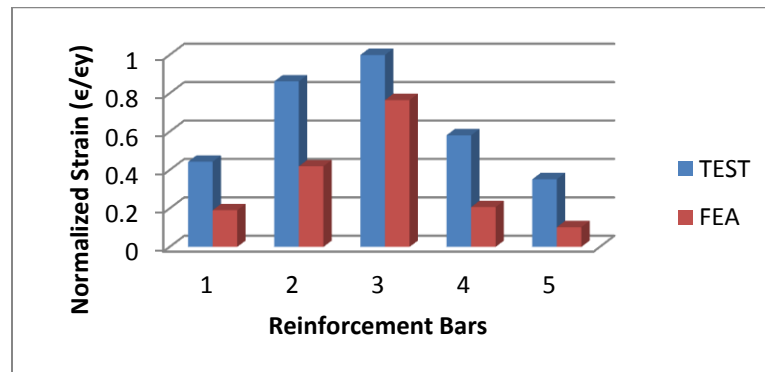


Figure 5.10: Pile Cap #4 Normalized reinforcement strain

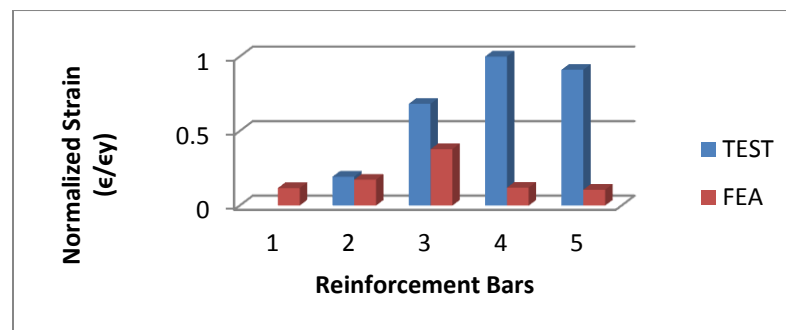


Figure 5.11: Pile Cap #5 Normalized reinforcement strain

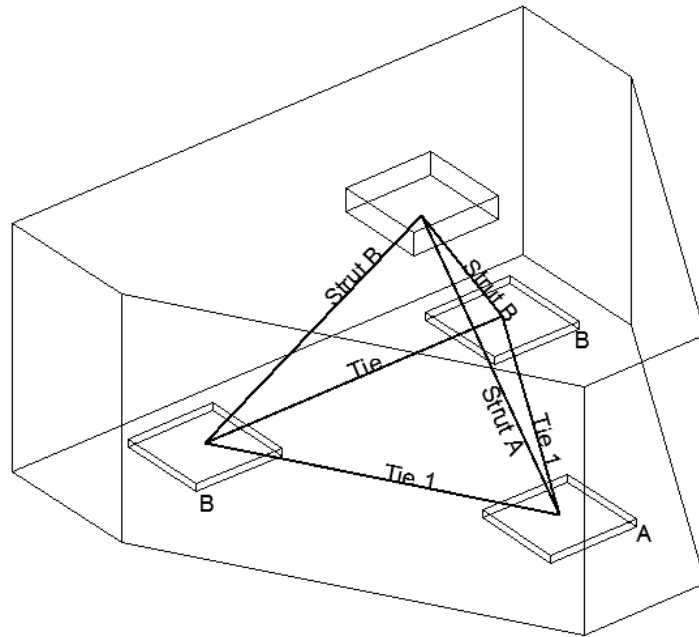


Figure 5.12: Pile Cap #3 assumed S&T geometry

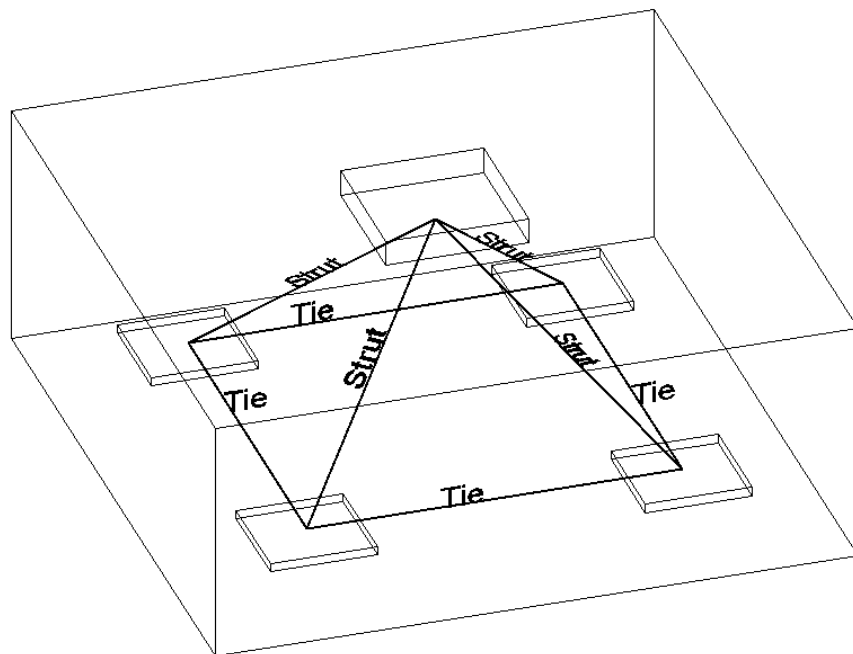


Figure 5.13: Pile Cap #4 and #5 assumed S&T geometry

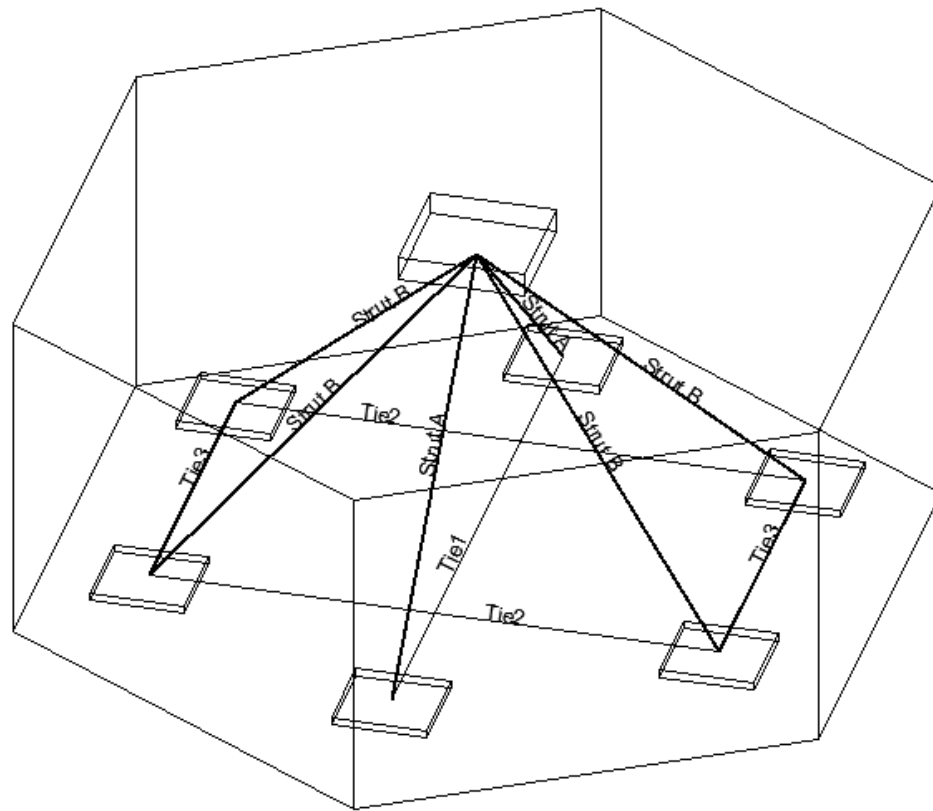


Figure 5.14: Pile Cap #7 assumed S&T geometry

6.0 SUMMARY and CONCLUSIONS

Four pile cap specimens were constructed and tested to better establish performance and ultimate strength of pile caps containing poorly detailed flexural steel. The pile cap specimens were full-size representations of in-situ pile caps used in a mid-rise hospital building. The pile cap specimens were constructed according to the available original design drawings and reinforcing steel shop drawings. Materials used to construct

the specimens were selected to represent those of the in-situ pile caps based on previously collected material samples. The tests were conducted until failure or the maximum capacity of the hydraulic loading system was achieved. ACI design methods were used to compare the predicted design strength with the measured experimental strength of the specimens. The design methods included one-way shear, two-way shear, and S&T methods. FEA models were used to guide development of the S&T models. Based on the experimental and analytical studies, the following conclusions are presented:

- The failed specimens exhibited either two-way punching shear (Pile Caps #4 and #5) or one-way shear (Pile Cap #3) failure modes.
- The failed specimens exhibited widespread yielding of the reinforcing steel at failure.
- The test specimens exhibited little relative slip between the reinforcing steel and surrounding concrete. The instrumented reinforcing bars that exhibited slip still achieved the nominal yield stress of the steel at failure.
- The one-way shear strength predicted by ACI 318 for Pile Cap #3 was very conservative. This was the only specimen that exhibited one-way shear failure.
- The two-way shear provisions in ACI 318 were found to be both conservative and unconservative for the different test specimens. The uniform applicability of the present two-way shear provisions to large-sized pile caps is uncertain.
- The S&T models considered provided quite conservative estimates of strength compared to the measured strength of the pile cap specimens.
- The predicted failure loads for most of the S&T models were limited by the tie strength due to the short available anchorage lengths. However, experimental

results showed that the reinforcing bars were able to achieve yield at the face of the nodal zone. Thus present ACI anchorage requirements appear to be conservative for such details.

- Based on the large observed conservatism of the S&T methods, experiments may be the best way to establish the available strength for an existing pile cap with poor flexural details.

REFERENCES

- Abaqus, Hibbit, Karlsson & Sorenson, Inc., ABAQUS/Standard [2002] version 6.3, USA
- ACI Committee 318, "Building Code requirements for Structural Concrete (ACI 318-08) and Commentary," *American Concrete Institute*, Farmington Hills, Michigan. 2008
- ACI Committee 318, "Building Code requirements for Structural Concrete (ACI 318-05) and Commentary," *American Concrete Institute*, Farmington Hills, Michigan. 2005
- ACI Committee 318, "Building Code requirements for Structural Concrete (ACI 318-99) and Commentary," *American Concrete Institute*, Farmington Hills, Michigan. 1999
- Adebar, P., D. Kuchma, and M. Collins, "Strut-and-Tie Models for the Design of Pile Caps: An Experimental Study," *ACI Structural Journal*, V.87, No 1, (1990), pp. 81-92
- Adebar, P., Z. Zhou, "Bearing Strength of Compressive Struts Confined by Plain Concrete." *ACI Structural Journal*. V.90 (1993), pp. 534-41.
- Adebar, P., Z. Zhou. "Design of Deep Pile Caps by Strut-and-Tie Models." *ACI Structural Journal*. V.96 No.4 (1996), pp. 437-48.
- Adebar, P. "Discussion of "An Evaluation of Pile Cap Design Methods in Accordance with the Canadian Design Standard." *Canadian Journal of Civil Engineering*. V. 31. (2004), pp. 1123-126.
- Ahmad, S., A. Shah, S. Zaman. "Evaluation of the Shear strength of Four Pile Cap Using Strut and Tie Model (STM)." *Journal of Chinese Institute of Engineers*, V.32 No.2 (2009), pp. 243-49.
- Breno, S. "Factors Affecting Strength of elements designed using Strut and Tie Models." *ACI Structural Journal*. V.104, No.3 (2007), pp. 267-77.
- Cavers, W., G. Fenton. "An Evaluation of Pile Cap Design Methods in Accordance with the Canadian Design Standard." *Canadian Civil Engineering*. 31. (2004): 109-19. Print.
- Cavers, W., G. Fenton. "Reply to the Discussion by P. Adebar on "An Evaluation of Pile Cap Design Methods in Accordance with the Canadian Design Standard". *Canadian Civil Engineering*. V. 31. (2004), pp. 1127-129.
- CSA, "Design of Concrete Structure for Buildings," *Canadian Standards Association*, Mississauga, Ont. 2004
- CSRI, "Design Handbook," *Concrete Reinforcing Steel Institute*, Schaumburg, Ill.

REFERENCES (Continued)

- Gogate, A., G. Sabnis. "Design of Thick Pile Caps." *ACI Journal*. V.77 No.1, (1980), pp. 18-22.
- Gu, Q., C. Sun, S. Peng. "Experimental Study of Deep Four-Pile Caps with Different Reinforcement Layouts Based on 3D Strut and Tie Analogy" *Key Engineering Materials*, V.400-402. (2009), pp. 917-22.
- Malm, P. "Predicting Shear Type Crack Initiation and Growth in Concrete with Non-Linear Finite Method" *Department of Civil and Architectural Engineering, Royal Institute of Technology*, Thesis, Stockholm, Sweden, 2009
- Newman, M., N. Newman. "Failure Theories and Design Criteria for Plain Concrete," *Solid Mechanics and Engineering Design*, Wiley-Interscience, NewYork, (1972) pp. 83/1-83/33.
- Park, J., D. Kuchma, R. Souza. "Strength Predictions of Pile Caps by a strut-and-tie model approach." *Canadian Journal of Civil Engineering*. V.35. (2008) pp. 1399-413.
- Sherwood, E., A. Lubell, E. Bentz, and M. Collins. "One-Way Shear Strength of Thick Slabs and Wide Beams." *ACI Structural Journal*, V. 103, No.6 (2006), 794-802.
- Souza, R., D. Kuchma, J. Park, Bittencourt. "Adaptable Strut-and Tie Model for Design and Verification of Four-Pile Caps." *ACI Structural Journal*, V.106, No.2 (2009), pp. 142-50.
- Suzuki, K., K. Otsuki, T. Tsubata. "Influence of Bar Arrangement on Ultimate Strength of Four-Pile Caps." *Transactions of the Japan Concrete Institute*. 20. (1998), pp. 195-202.
- Suzuki, K., K. Otsuki, T. Tsuchiya. "Influence of Edge Distance on Failure Mechanism of Pile Caps." *Transactions of the Japan Concrete Institute*. 22. (2000), pp. 361-68.
- Suzuki, K., K. Otsuki. "Experimental Study on the Corner Shear Failure of Pile Caps." *Transactions of the Japan Concrete Institute*. 23. (2002) pp. 303-10.
- Todeschini, Bianchini, Kesler, "Behavior of Concrete Columns Reinforced with High Strength Steels" *ACI Journal, Proceedings*, (1964) V. 61, No.6, pp. 707-716.

APPENDICES

APPENDIX A – Original Design Drawings

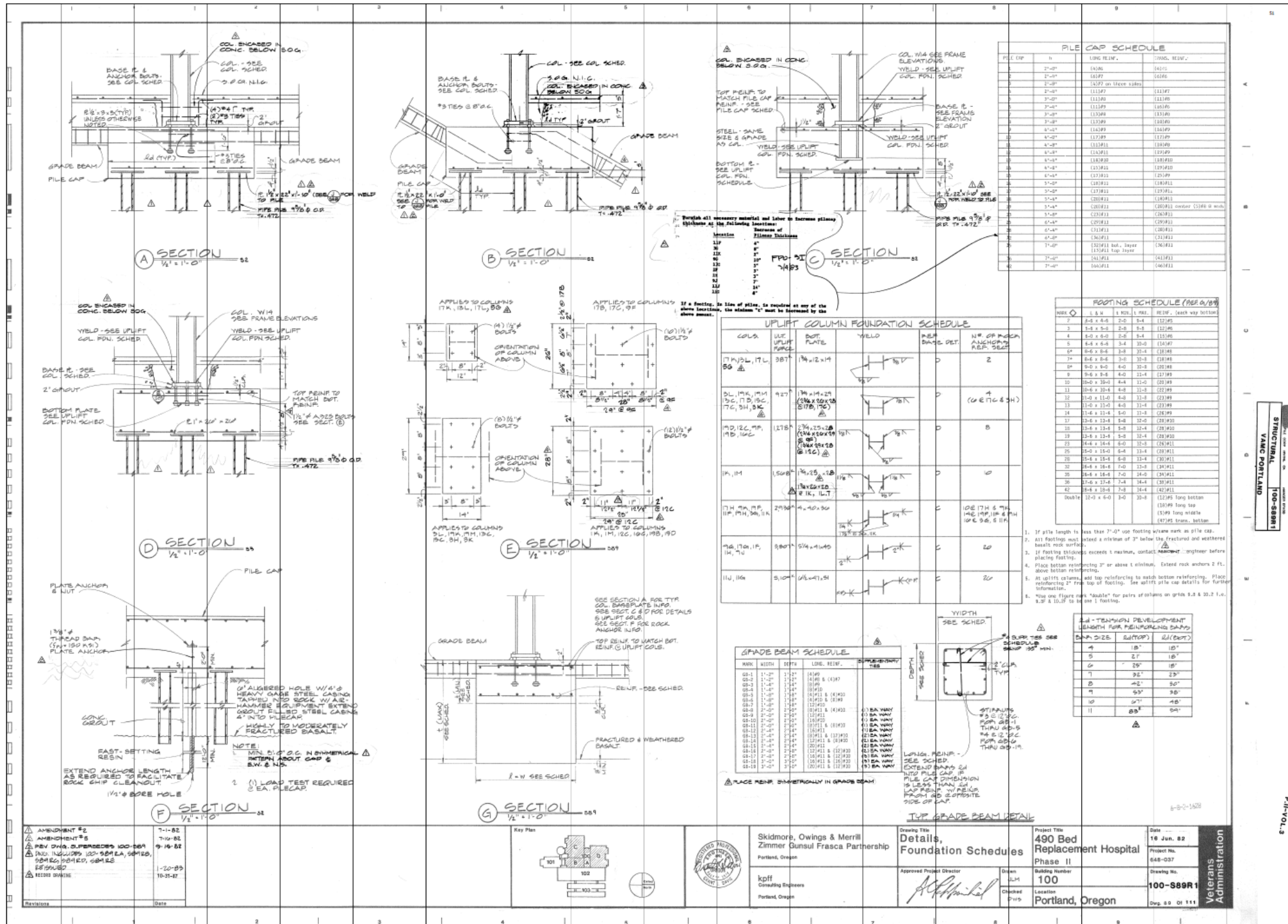


Figure A.2: Original Design Drawing (2 of 3)

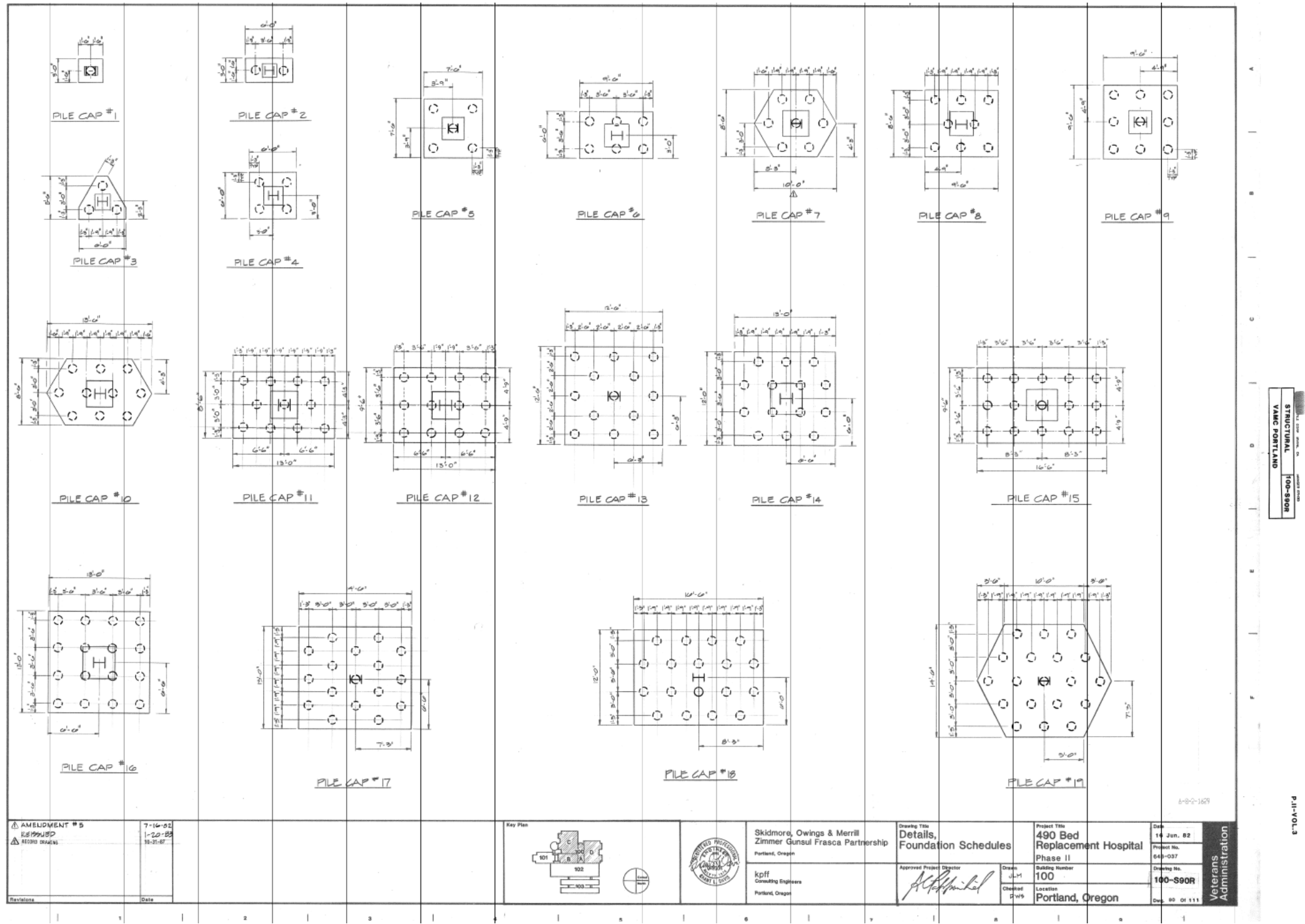


Figure A.3: Original Design Drawing (3 of 3)

APPENDIX B – Shop Drawings of In situ Pile Caps

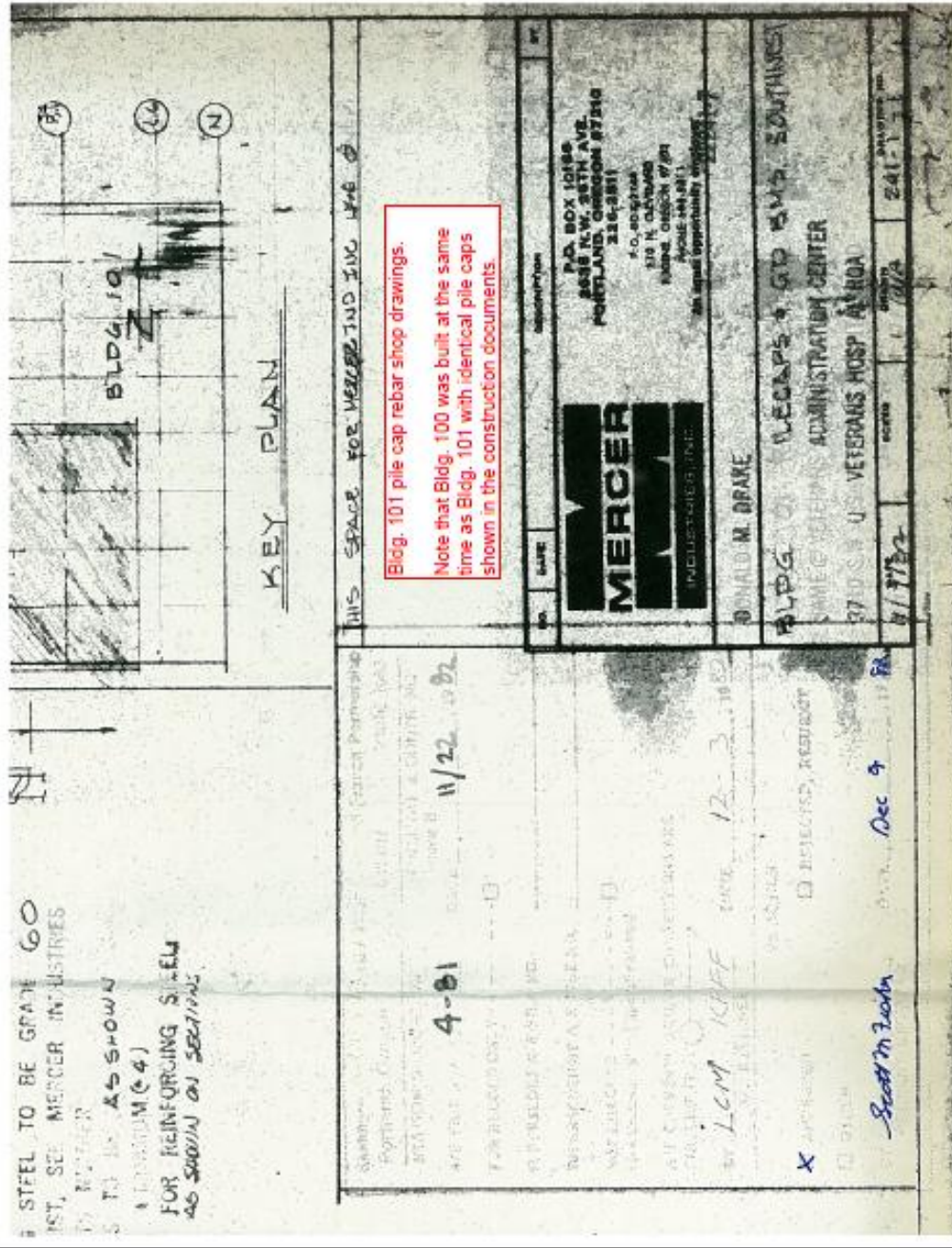


Figure B.1: Shop Drawings of In-Situ Pile Caps (1 of 4)

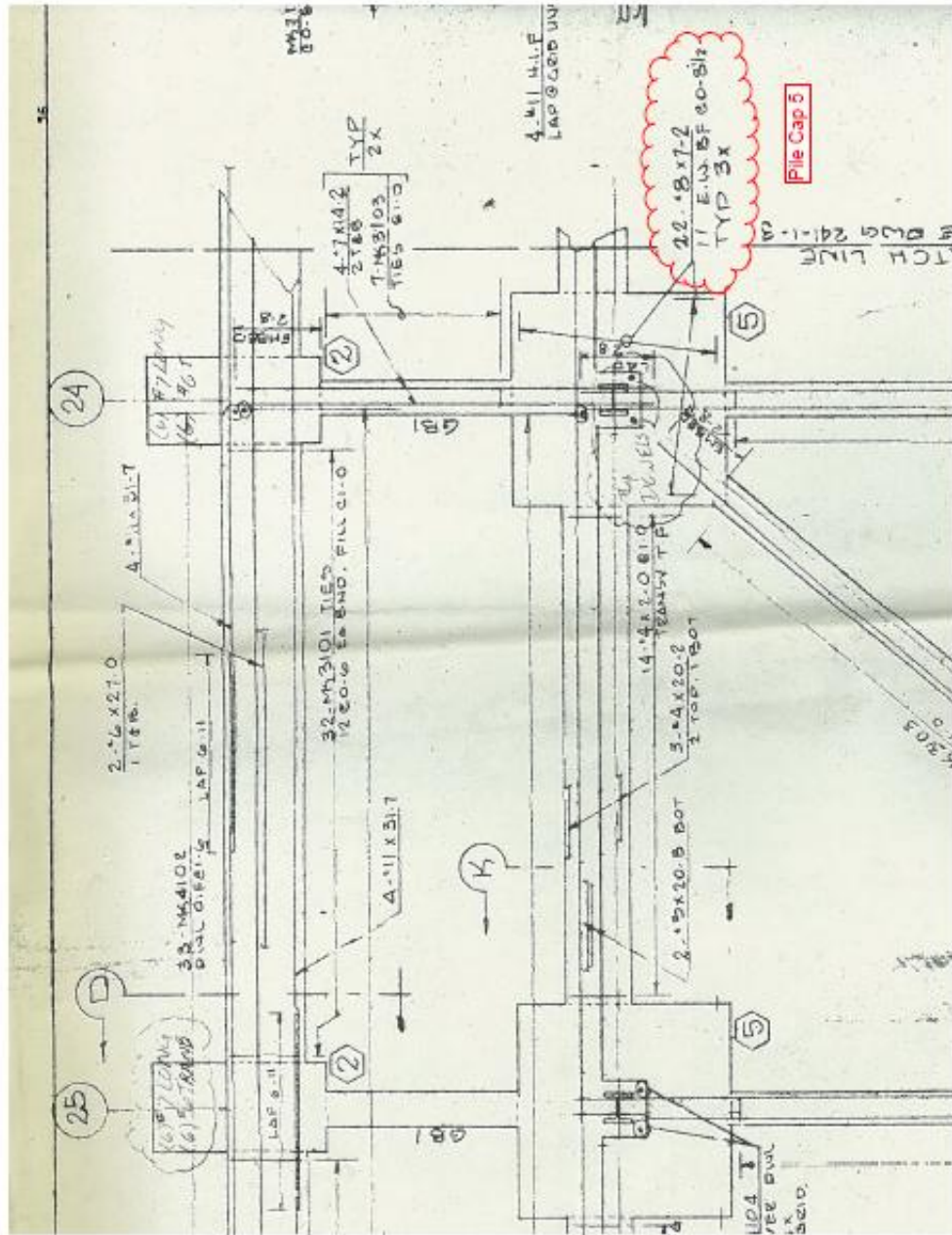


Figure B.3: Shop Drawings of In-Situ Pile Caps (3 of 4)

APPENDIX C – Concrete Mix Design for In situ Pile Caps

NORTHWEST TESTING LABORATORIES

CONCRETE MIX DESIGN

Mix # 203

3"
slump

4,000 p.s.i. concrete
6.0 sacks cement per cubic yard
3/4" maximum sized aggregate
Water Reducing Agent

<u>Material</u>	<u>Pounds Saturated Surface Dry</u>	<u>Corrected For Average Moisture*</u>
Cement (Type I-II) (Kaiser)	564	564
Sand (42%)	1,330	1,400 (5%)
Gravel: #4 to 3/4"	1,908	1,925 (1%)
Water (28.3 Gals.)	236	17.9 gals.
Zeecon	6.0 oz/100# cement	33.8 oz.

Laboratory results on the above design:

Unit Weight	149.6 lbs./cu.ft.
Slump	3 inches
Natural Air Content	2.5 %
Water Per Cement Ratio	4.72 gal./sack

Compressive strength of cylinders obtained in the laboratory on this concrete mix design:

Average at 7 Days	3960 p.s.i.	<small>Drawings/product literature checked before submission by qualified employees of Donald M. Company for accuracy, compliance with Contract requirements</small>
	4170 p.s.i.	
Average at 14 Days	5410 p.s.i.	
Break at 28 Days	6860 p.s.i.	
	6950 p.s.i.	
	7080 p.s.i.	
Average at 28 Days	<u>6963</u> p.s.i.	WDT 11/24/82 Authorized Reviewer Date

Concrete Supplier: Western Pacific Construction Materials Co.
Project: VAMC-Portland, Oregon
Architect: SOM-ZGF
Contractor: Donald M Drake Co.
Report Number: 257622
Date: October 26, 1982

*These are only average moisture corrections and actual moisture corrections should be made by the concrete plant at all times when batching concrete.

Figure C.1: Concrete Mix Design for In-Situ Pile Caps (1 of 5)

NORTHWEST TESTING LABORATORIES

CONCRETE MIX DESIGN

Mix # 741

4,000 p.s.i. concrete
 6.0 sacks cement per cubic yard
 3/4" maximum sized aggregate
 Water Reducing Agent

4" Slump

<u>Material</u>	<u>Pounds Saturated Surface Dry</u>	<u>Corrected For Average Moisture*</u>
Cement (Type I-II) (Kaiser)	564	564
Sand (42%)	1,321	1,390 (5%)
Gravel: #4 to 3/4"	1,895	1,915 (1%)
Water (29.3 Gals.)	244	18.6 gals.
Zeecon	6.0 oz/100# cement	33.8 oz.

Laboratory results on the above design:

Unit Weight	149.0 Lbs./cu.ft.
Slump	4 "
Natural Air Content	2.5 %
Water Per Cement Ratio	4.88 Gals./Sack

Compressive strength of cylinders obtained in the laboratory on this concrete mix design:

Average at 7 Days	4350 p.s.i.
	4390 p.s.i.
Average at 14 Days	5550 p.s.i.
Break at 28 Days	7330 p.s.i.
	6970 p.s.i.
	7400 p.s.i.
Average at 28 Days	7233 p.s.i.

The drawings/product literature has been checked before submission by technically qualified employees of Donald M. Drake Co. for accuracy, completeness and compliance with Contract requirements.

WDS 11/24/82
 Authorized Reviewer Date

Concrete Supplier: Western Pacific Construction Materials Co.
 Project: VAMC-Portland, Oregon
 Architect: SOM-ZGF
 Contractor: Donald M Drake Co.
 Report Number: 257623
 Date: October 26, 1982

*These are only average moisture corrections and actual moisture corrections should be made by the concrete plant at all times when batching concrete.

Figure C.2: Concrete Mix Design for In-Situ Pile Caps (2 of 5)

NORTHWEST TESTING LABORATORIES

CONCRETE AGGREGATE DATA

GRAVEL

Fine:
(3/4" - #4)

<u>Screen Size</u>	<u>Percent Retained</u>	<u>Percent Passing</u>	<u>ASTM Percent Passing</u>
1"	0	100	100
3/4"	6.6	93.5	90-100
1/2"	32.0	68.0	--
3/8"	50.4	49.6	20-55
#4	98.9	1.1	0-10
Pan	100	0	--

Specific Gravity (SSD) = 2.68
Absorption, % = 2
Moisture 2.1 (as received)

Concrete Sand:

<u>Screen Size</u>	<u>Percent Retained</u>	<u>Percent Passing</u>	<u>ASTM Percent Passing</u>
#4	3.5	96.5	95-100
#8	17.9	82.1	80-100
#16	32.3	67.7	50-85
#30	49.8	50.2	25-60
#50	80.1	19.9	10-30
#100	97.2	2.8	2-10
Pan	100	0	

Specific Gravity (SSD) = 2.58
Absorption, % = 3.8
Fineness Modulus = 2.81
Moisture 7.3 (as received)

The drawings/product literature have been
 checked before submission by techn-
 qualified employees of Donald M. Davis
 Company for accuracy, completeness &
 compliance with Contract requirements.
 WDS 11/29/82
 Authorized Reviewer Already Submitted Date

Figure C.3: Concrete Mix Design for In-Situ Pile Caps (3 of 5)

-- SAMPLE DATA --
AND
LABORATORY TEST REPORT

Oregon State HIGHWAY DIVISION Materials Section
Form 73-3880

Page 1 of 1 pages
Data Sheet No.: 6589
LABORATORY REPORT NUMBER
82 0281

AGGREGATE BITUMINOUS MIXTURE

Project: W Bankrupt / Sellwood Br. Prefix No.: 26-1012

Contract No.: 9183 County: MULT

Res. Engr.: Barnhart F.A. Proj. No.:

Tested by: C.H. Baird Sampled by: J. F. Zee Date Sampled: 1-12-82

Field Control Test Number: 14888

SIEVE ANALYSIS	
Sieve Size	Percent Passing
10/4	100
40/10	91
200/10	57
Fracture	32
Pl	1
LL	0
S.E.	
Moisture	
Retention	
Extracted A/C	FM = 6.76
Total A/C	

REGULATE SIZE: BRAND AND GRADE OF ASPHALT: TYPE MIX:
3/4" #4

REQUIRED USE: PCC

TRUCK OR GRAVEL LOCATION AND SOURCE NUMBER:
Willamette River near Ross Island
26-100-1

LEAD AGENCY: Willamette Downtown Plant

REMARKS, INSTRUCTIONS, OR SPECIAL DATA:
yearly Regualification
shipped 1-14-82

INDICATE TEST REQUIRED: Each sample requires separate data sheet. List additional projects separately.

TEST	RESULT	REMARKS
T-27	Fracture	10%
T-11	Percent Passing	40/10: 91, 200/10: 57
T-19	UNIT WT lb/ft	LOOSE: 107.1, COMPACT: 107.1
T-21	ORGANIC COLOR-PLATE NO.	(Standard #3)
T-84	Sp. Gravity, Bulk	SSD
T-85	Sp. Gravity, Bulk	2.61, SSD 2.64, Appar. 2.76, Absorp. 3.10
T-89	L.L.	
T-90	PLASTICITY INDEX	
OSHD SAND EQUIVALENT		
T-96	ABRASION GRADING	Percent Wear
T-104	SODIUM SULFATE SOUNDNESS PERCENT LOSS	
OSHD DEGRAD		
T-112	FRIABLE PARTICLES	20%
T-113	LIGHT WEIGHT PIECES	3/8: 0.07, 4-16: 0.07
T-182	ASPH. STRIP BRAND	
OSHD FINENESS FACTOR		6.68
Wood Waste		0.0

P200 0.3 %
Weight of sample = 4762.8g

FHWA Construction Engineer: Barnhart
Reg. Geologist: Eshelman
Cascade Construction Co. Inc.

Material represented by this sample Does Does not comply with specifications.
Lab Comments: NOTED
C.H. BAIRD
John C. Jentzen

Date Received: 1-14-82
Date Reported: 2-2-82
Lab Charges: 74.00

Figure C.4: Concrete Mix Design for In-Situ Pile Caps (4 of 5)

SAMPLE DATA AND LABORATORY TEST REPORT

Oregon State HIGHWAY DIVISION Materials Section
 Form 734-3880

Page of pages
 Data Sheet No.: 6390
 LABORATORY REPORT NUMBER: 82 0252

AGGREGATE BITUMINOUS MIXTURE

Project: SW Bancroft / Sellwood BT Prefix No.: 26-1012
 Location: Cascade Contract No.: 9183 County: Mult
 Submitted by: C.H. Baird Res. Engr.: Barnhart F.A. Proj. No.:
 Sampled by: J.E.Z. 11 Date Sampled: 1-12-82

No. of bags or boxes: 1 Quantity Represented: yearly Reg. L.F. Purpose of Sample: Mix Design Record Check Qualifying FIELD CONTROL TEST NUMBER:

REGGATE SIZE: Sand BRAND AND GRADE OF ASPHALT: TYPE MIX:
 UNDESIGNED USE: PCC

FRY OR GRAVEL LOCATION AND SOURCE NUMBER:
Willamette River Near Ross Island

FIELD DATA:
26-100-1
Willamette downtown plant
yearly Reg. L.F.
shipped 1-14-82

Sieve Size	Percent Passing
10/4	100
40/10	96
200/10	78
Fracture	62
PI	40
LL	13
S.S.	2
Moisture	0
Retention	0
Extracted A/C	309
Total A/C	

DICATE TEST REQUIRED: Each sample requires separate data sheet. List additional projects separately.

Test	Result	Notes
T-27	100	
St-11	96	
Fracture	78	
Fracture	60	
Fracture	32	
Fracture	27	
Fracture	2	

T-19 UNIT WT lb/ft LOOSE COMPACT
 COMB: % THIS SAMPLE % LAB. No.

T-21 ORGANIC COLOR PLATE NO. (Standard #3) 1

T-84 Sp. Gravity, Bulk 2.51 SSD 2.58 Appar. 2.70 Absorp. 2.70

T-85 Sp. Gravity, Bulk SSD Appar. Absorp.

T-89 L.L. T-90 PLASTICITY INDEX

OSHD SAND EQUIVALENT 85

T-96 ABRASION GRADING Percent Wear

T-104 SODIUM SULFATE SOUNDNESS PERCENT LOSS
 2% - 1% 1% - % Rip Rap Avg.
 1% - % % - 3/8 % 3/8 - 4 % P.A.
 4 - 8 8.3 8 - 16 9.9 16 - 30 7.7 30 - 50 7.0 P.A. 7.08

OSHD DEGRAD. Ht. in. P20 % Ref. Ht. in. P20 %
 4.0 Ref. Ht. in. P20 %

T-112 FRIABLE PARTICLES 60 Wt. Avg. %
 1% - % % - 3/8 % 3/8 - 4 % 4 - 16 %

T-113 LIGHT WEIGHT PIECES C.A. % F.A. 0.0 %

T-182 ASPH. STRIP BRAND Grade Coated
 Additive Brand %
 Brand Grade Coated

OSHD FINENESS FACTOR—1% 4, 3/8, 4, 8, 16, 30, 50, 100 2.99

Wood Waste %

11 P200 1.0 %
 wt. of sample = 9763

Additional Tests:

FHWA
 Construction Engineer
 Region Engineer
 Resident Engineer Barnhart
 District Engineer
 Geology and Soils
 Reg. Geologist Eshelman
 Files
Baird
 Cascade Construction Co. Inc.

Material represented by this sample Does Does not comply with specifications.

Lab Comments:
NOTED
C.H. BAIRD

Date Received: 1-14-82
 Date Reported: 2-2-82
 Lab Charges: 123.50

John C. Johnston WJS
 Engineer of Materials

Figure C.5: Concrete Mix Design for In-Situ Pile Caps (5 of 5)

APPENDIX D – Concrete Core Strengths for In Situ Pile Caps

Carlson Testing, Inc.

Bend Office (541) 330-9155
 Geotechnical Office (503) 601-8250
 Eugene Office (541) 345-0289
 Salem Office (503) 589-1252
 Tigard Office (503) 684-3460

March 15, 2011
 T1103993

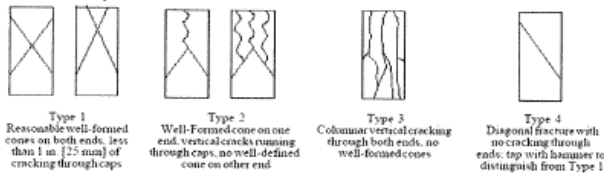
Degenkolb Engineers – Kent Yu
 707 SW Washington Street, Suite 600
 Portland, OR 97205

Re: VA Medical Center – Building 100 (Structural Pile Test)
 3710 SW US Veterans Hosp Rd – Portland, OR
Compressive Strength of Drilled Concrete Cores (ASTM C42)

As requested, Carlson Testing Inc. has completed compression testing on four (4) specimens extracted from the above-mentioned project. Samples were obtained by core drilling on February 25, 2011 by your representative. Core specimens were placed into sealed bag on February 25, 2011 at 12:00 P.M. prior to testing. Core results are as follows:

Register #98047 Specimen number	1	2	3
Age of Specimen (days)	5	5	5
Date and Time tested	3/2/11	3/2/11	3/2/11
Nominal Maximum Aggregate Size (in.)	3/8"-0	3/8"-0	3/8"-0
Length of Specimen as Received (in.)	9.00	6.50	9.00
Length of specimen prior to capping (in.)	7.10	5.30	7.20
Length of specimen after capping (in.)	7.30	5.50	7.40
Direction of load in respect to placement	P	P	P
Moisture condition at time of testing	D	D	D
Average diameter of core specimen (in.)	3.71	3.71	3.71
Length to diameter ratio (l/d) *	1.97	1.48	1.99
Applied load at specimen failure (lbs.)	72077	75071	67052
Specimen area (sq.in.)	10.80	10.80	10.80
Uncorrected unit (psi)	6673	6951	6208
Strength correction factor *	---	0.96	---
Corrected unit psi (psi)	6670	6670	6210
Type of Fracture	4	3	3
Density lb/ft ³	N/R	N/R	N/R

*P - Perpendicular * Strength correction factor applied when length to diameter ratio is less than 1.75
 L - Parallel N/R - Not Requested



Core Specimen Location

Specimen No. 1	CC-PC-1 SOUTH FACE OF PILE CAP AT GRID LINES M/16
Specimen No. 2	CC-PC-2 EAST FACE OF PILE CAP AT GRID LINES M/16
Specimen No. 3	CC-PC-3 EAST FACE OF PILE CAP AT GRID LINES M/15

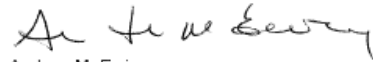
Figure D.1: Concrete Core Strengths for In-Situ Pile Caps (1 of 3)

Page 2 of 2
T1103993
March 15, 2011

Our reports pertain to the material tested/inspected only. Information contained herein is not to be reproduced, except in full, without prior authorization from this office. Under all circumstances, the information contained in this report is provided subject to all terms and conditions of CTI's General Conditions in effect at the time this report is prepared. No party other than those to whom CTI has distributed this report shall be entitled to use or rely upon the information contained in this document.

If there are any further questions regarding this matter, please do not hesitate to contact this office.

Respectfully submitted,
CARLSON TESTING, INC.



Andrew M. Ewing
Project Manager

eah

cc: Degenkolb Engineers – Kent Yu

kyu@degenko1b.com

Figure D.2: Concrete Core Strengths for In-Situ Pile Caps (2 of 3)

Carlson Testing, Inc.

Bend Office (541) 330-9155
 Geotechnical Office (503) 601-8250
 Eugene Office (541) 345-0289
 Salem Office (503) 589-1252
 Tigard Office (503) 684-3460

March 16, 2011
 T1103993
 Permit N^o N/A

LAB REPORT

DATES COVERED: March 2, 2011

PROJECT: VA Medical Center – Building 100 (Structural Pile Test)
 ADDRESS: 3710 SW US Veterans Hosp Rd – Portland, OR

REPORT OF 6X12 CONCRETE SPLIT TENSILE TEST SPECIMENS

Register Number	Date Received	Date Tested	Average Diameter	Average Length	Total Load	Area	Unit PSI	Remarks
98047	02/25/2011	03/02/2011	5.69	11.00	54,000	196.53	550	CC-PC-4 East south face of pile cap at grid line M/15. Estimates 85% core fracture.

Our reports pertain to the material tested/inspected only. Information contained herein is not to be reproduced, except in full, without prior authorization from this office. Under all circumstances, the information contained in this report is provided subject to all terms and conditions of CTI's General Conditions in effect at the time this report is prepared. No party other than those to whom CTI has distributed this report shall be entitled to use or rely upon the information contained in this document.

If there are any further questions regarding this matter, please do not hesitate to contact this office.

Respectfully submitted,

CARLSON TESTING, INC.


 Andrew M. Ewing
 Project Manager

JT/ks

cc: Degenkolb Engineers – Kent Yu

kyu@degenkolb.com

Figure D.3: Concrete Core Strengths for In-Situ Pile Caps (3 of 3)

APPENDIX E – Concrete Mix Design for Pile Cap Specimens



April 11, 2011

Mr. Michael Dyson
Oregon State University

Project: Pile Caps
Subject: Product Submittal

I would like to submit the following product for the above project.

031-40B150AM 4000 p.s.i. @ 28 Days Concrete

The above concrete mix design was prepared by an OSHD certified concrete control technician in accordance with the project specifications. The proposed mix design will meet strength specifications when handled, placed, and tested in accordance with current ASTM and ACI standards and recommended practices.

We request the inclusion of Knife River on the distribution list for cylinder tests from the testing laboratory.

Materials proportions, production records, and product performance data submitted are solely intended for verification of submitted materials and not to be distributed to non-contract related parties. If I can be of further assistance, please call.

Sincerely,

Mike Stephens
Ready Mix Sales
Mid Valley Division
(cell) 541-740-7072

Enclosures
xc: Office Files
Linda Zulauf
Dan Simmons

<input checked="" type="checkbox"/> REVIEWED	<input type="checkbox"/> MAKE CORRECTIONS NOTED
<input type="checkbox"/> REJECTED	<input type="checkbox"/> REVISE AND RESUBMIT
THIS REVIEW DOES NOT RELIEVE CONTRACTOR FROM COMPLIANCE WITH THE REQUIREMENTS OF THE DRAWINGS AND SPECIFICATIONS. THIS REVIEW IS ONLY FOR GENERAL CONFORMANCE WITH THE DESIGN CONCEPT OF THE PROJECT AND GENERAL COMPLIANCE WITH THE INFORMATION GIVEN IN THE CONTRACT DOCUMENTS. CONTRACTOR IS RESPONSIBLE FOR: CONFIRMING AND CORRELATING ALL QUANTITIES AND DIMENSIONS; SELECTING FABRICATION PROCESSES AND TECHNIQUES OF CONSTRUCTION; COORDINATING HIS WORK WITH THAT OF ALL OTHER TRADES, AND PERFORMING HIS WORK IN A SAFE AND SATISFACTORY MANNER.	
04/11/11	JDN
DATE	DEGENKOLB ENGINEERS BY

Due to limited compressive strength testing history, suggest casting extra cylinders to allow monitoring of strength gain and in case curing extends past 28-days to achieve required day of test strength.

Mid Valley Division * P.O. Box 1126 * Corvallis, OR 97339 * 541-752-3428 * (fax) 541-752-5415

Figure E.1: Concrete Mix Design for Pile Cap Specimens (1 of 3)



Mix ID Number: 031-40B150AM

Concrete Mix Design

MIX DESIGN QUANTITIES

Material	Product/Source	SG	Weight	Volume	Mass	Volume
Cement	Cal/Portland, Type I-II	3.15	750 lb	3.82 ft ³	445 kg	0.141 m ³
Fly Ash	None	2.25	0 lb	0.00 ft ³	0 kg	0.000 m ³
Water(Total)	Well/Corvallis R-Mix Plant 1	1.00	267 lb	4.28 ft ³	158 kg	0.158 m ³
3/4-#4 Round PCC	Corvallis (Builders Supply)	2.80 *	1775 lb*	10.94 ft ³	1053 kg*	0.405 m ³
PCC Sand	Corvallis (Builders Supply)	2.58 *	1153 lb*	7.16 ft ³	684 kg*	0.265 m ³
Admixtures	Grace	1.00	26.41 lb	0.42 ft ³	15.66 kg	0.016 m ³
Total Mix Weight (Mass):			3971 lb		2355 kg	
Air(Entrap/Entrain)			1.5 %	0.41 ft ³		0.015 m ³
Total Mix Volume:				27.00 ft ³		1.000 m ³

ADMIXTURES

Product	ProductName/Type	SG	Dosage Rate	Dosage (English)	Dosage (Metric)
Mid-Range Water Reducer	Grace Daracem 55	1.00	8.00 oz/cwt**	60.0 oz/cy**	2320.3 mL/m ³ **
Non-Chloride Accelerator	Grace Daraset 200	1.00	45.00 oz/cwt**	337.5 oz/cy**	13051.6 mL/m ³ **
Hydration Stabilizer	Grace Recover	1.00	1.00 oz/cwt**	7.5 oz/cy**	290.0 mL/m ³ **
Add'l Fibers			lb/cy**	0.0lb/cy**	0.0 kg/m ³ **

MIX DESIGN PROPERTIES

Aggregate Properties		ODOT# ^A	SG	Abs	FM	Unit Weight	
3/4-#4 Round PCC	2003-0.750-000#4-001	22-001-2	2.60	2.6		99.3 pcf	1591 kg/m ³ Dry Rodded
PCC Sand	2003-00000-0SAND-001	22-001-2	2.58	3.8	3.05		
Plastic Properties:		Slump:	4.0 ±	1.0 inch		100 ±	25 mm
		Air Content:	1.5 ±	1.5 %			
		Unit Weight (Wet):	147.1 pcf			2355 kg/m ³	
Design Properties:		Required Strength (f_c):	4000 psi @ 3 days			28 MPa @ 3 days	
		Total Cementitious:	750 lb	7.08 Sack		444.84 kg	
		Fly Ash %:	0.0 %				
		w/c Ratio***:	0.39 (Incl Admix)				

Project: PILE CAPS
 Contractor: OSU
 Comments:

Footnotes: *SSD Weights and SG. ** Admixture dosage rate will be adjusted according to manufacturer's recommendations to accommodate varying field conditions. *** This is a design w/c ratio and production w/c ratio may vary as recognized by industry standards such as ASTM C 94. ^AODOT Source #.

Submitted By: MIKE STEPHENS Date Submitted: 4/11/2011
 Designed By: DAN SIMMONS CCT

Figure E.2: Concrete Mix Design for Pile Cap Specimens (2 of 3)

STANDARD SUBMITTAL SUMMARY - COMPRESSIVE

Report Date: 3/5/2010

KNIFE RIVER CONSULTANTS
 10000 Highway 99, Suite 100
 Sacramento, CA 95828
 (916) 486-1000

PLANT NAME: Corvallis Reside Plant 1
 MIX ID: 031-408150AM
 DESIGN STRENGTH: 4000 PSI
 DESIGN AGE: 3 DAYS

Date Sampled	Time Sampled	Lab	Lab ID Number	Test Type	% AIR	SLUMP	W/C Ratio	7 Day Avg.	28 Day Avg.	3 Test Avg.
10/31/06	10:30	MHI-CIV	06-C28250	Field	1.6	5.00	0.39	4920	6020	
10/6/08	11:20	PEI	06-C20020	Field		3.50		5270	6250	
Average					1.60	4.25	0.39	5100	6140	
Standard Deviation						1.06		247	163	
Coefficient Of Variation								4.9	2.7	
Average 7:28 Day Ratio										83
Number of Tests								2	2	2

Figure E.3: Concrete Mix Design for Pile Cap Specimens (3 of 3)

APPENDIX F – Experimental Data for All Pile Cap Specimens

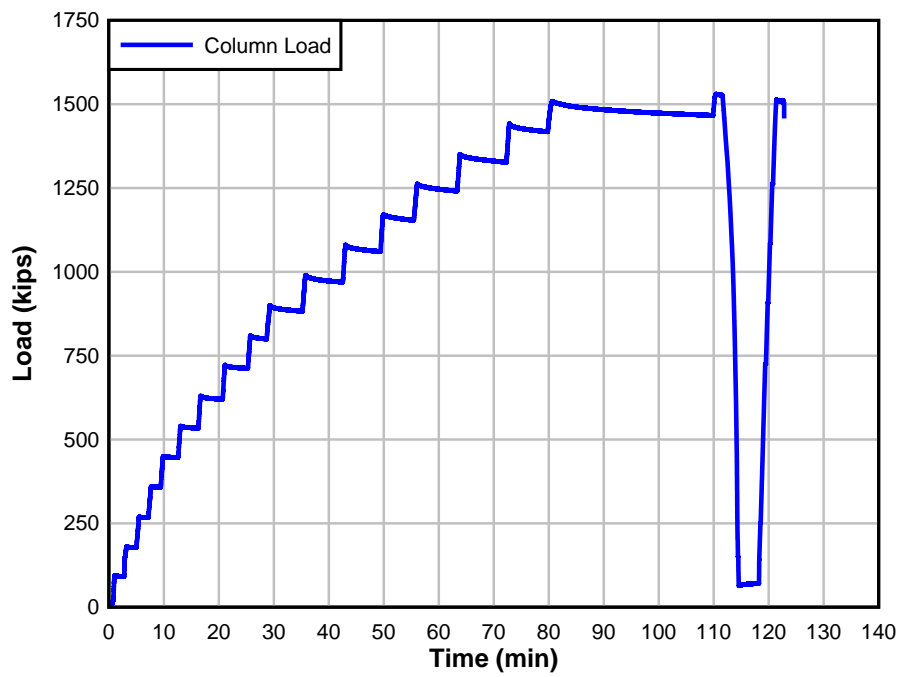


Figure F3.1: Column Loading – Pile Cap #3

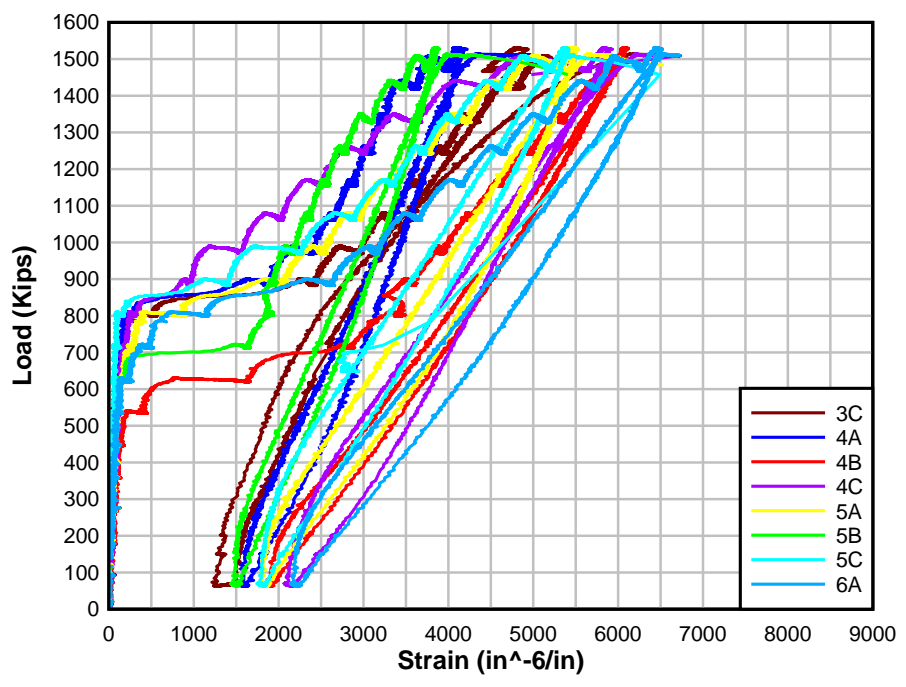


Figure F3.2: Column load vs. Strain (1 of 4) – Pile Cap #3

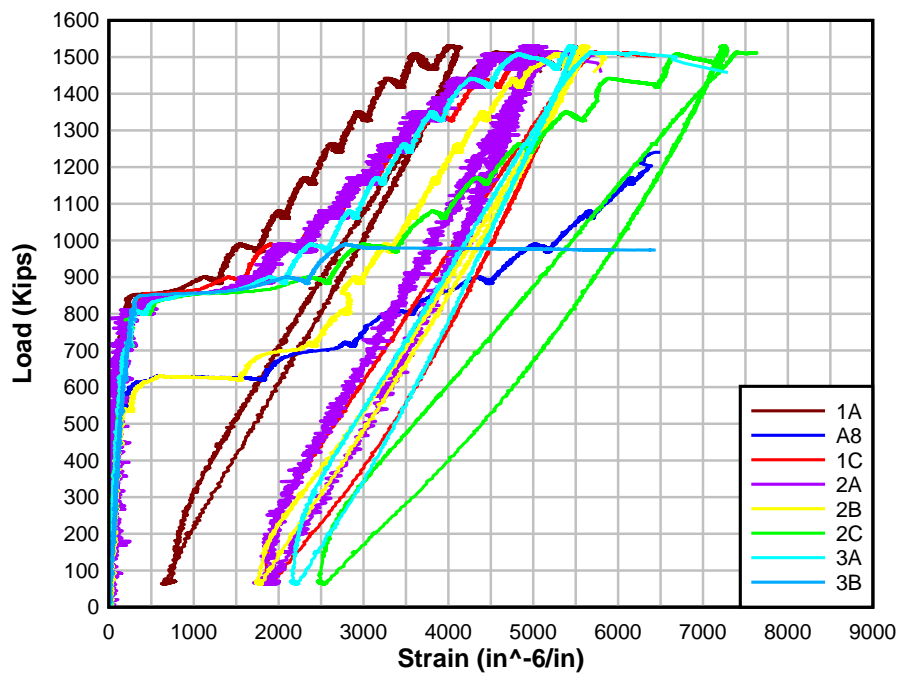


Figure 3.3: Column load vs. Strain (2 of 4) – Pile Cap #3

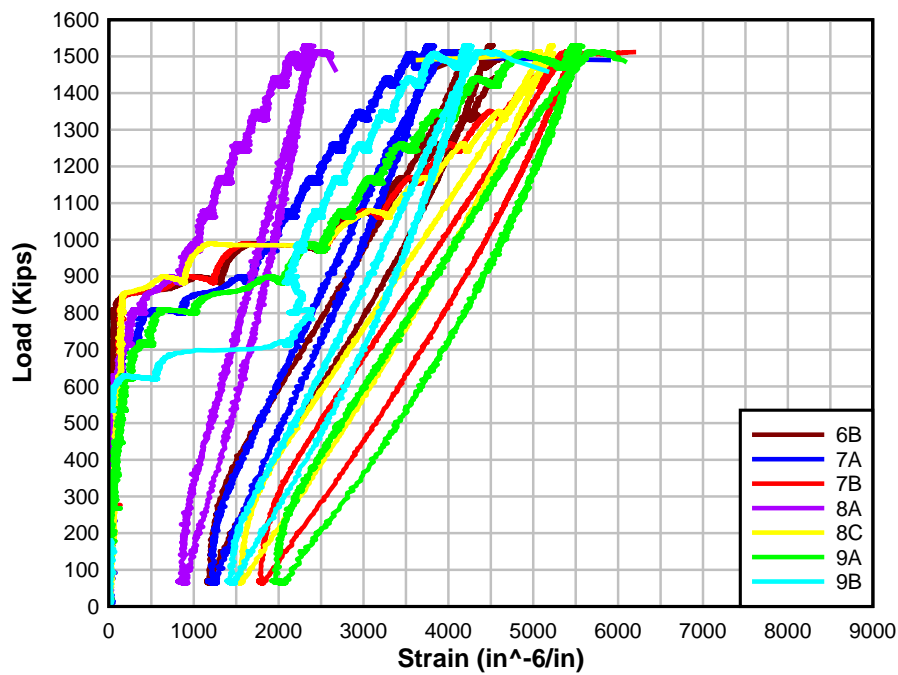


Figure F3.4: Column load vs. Strain (3 of 4) – Pile Cap #3

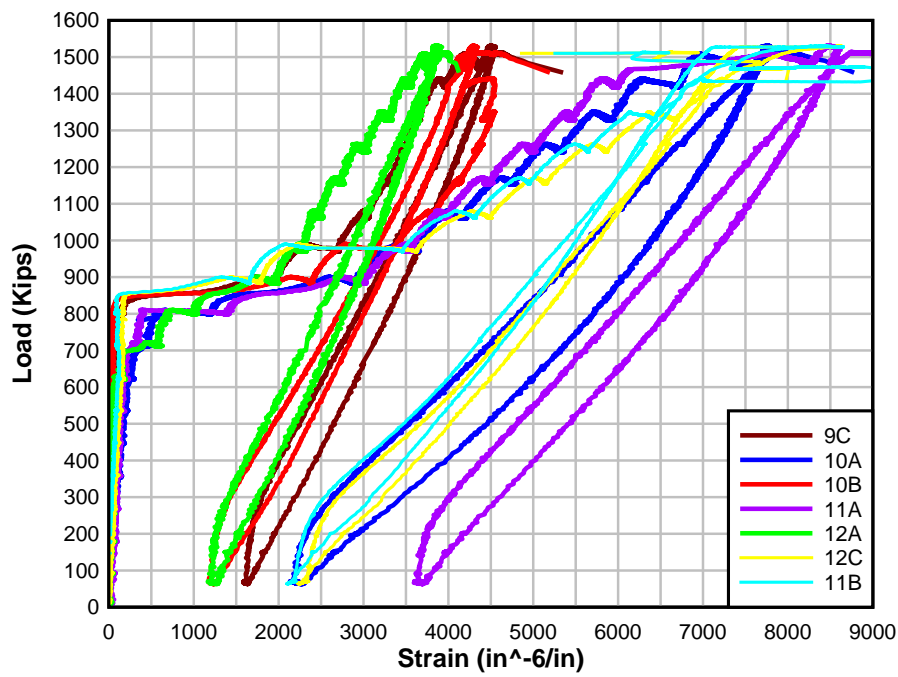


Figure F3.5: Column load vs. Strain (4 of 4) – Pile Cap #3

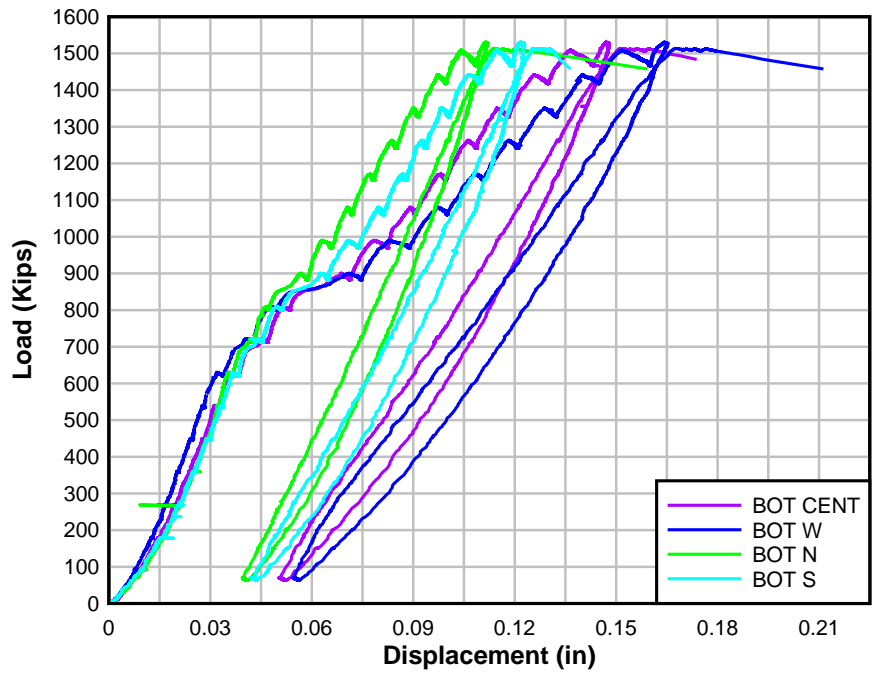


Figure F3.6: Column load vs. Displacement (1 of 2) – Pile Cap #3

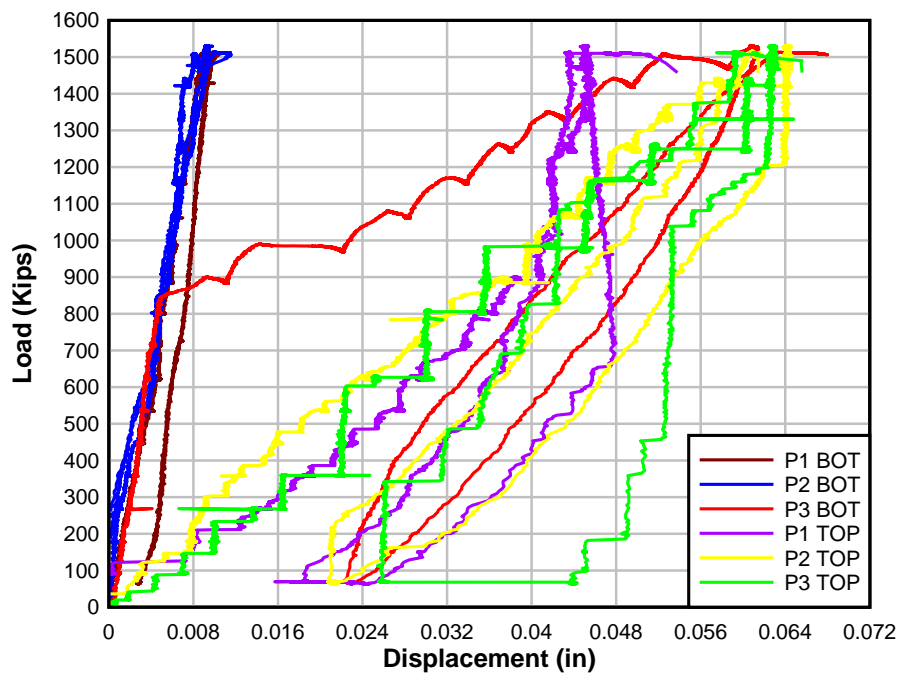


Figure F3.7: Column load vs. Displacement (2 of 2) – Pile Cap #3

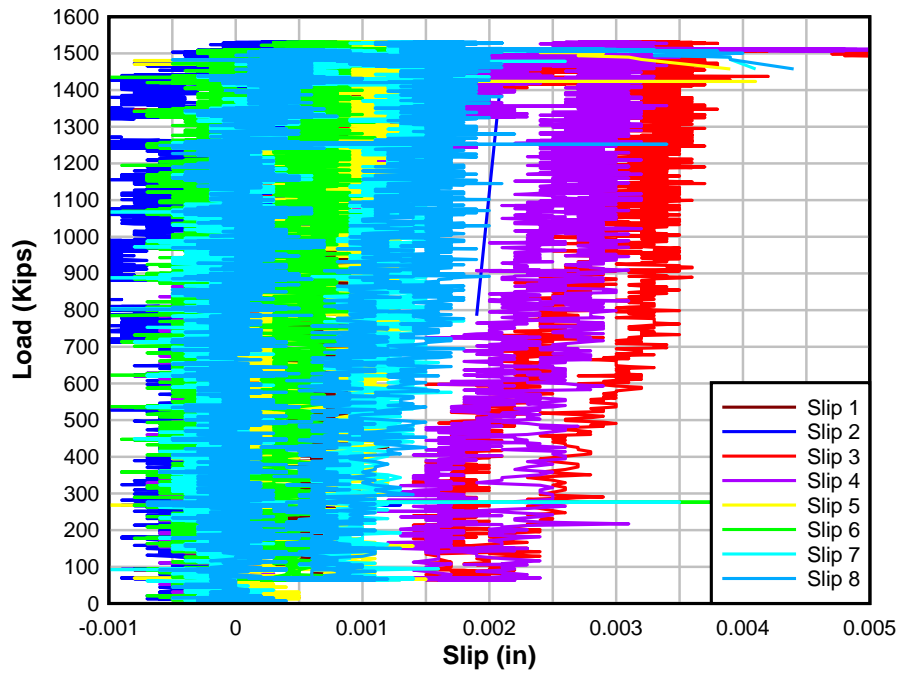


Figure F3.8: Column load vs. Slip (1 of 2) – Pile Cap #3

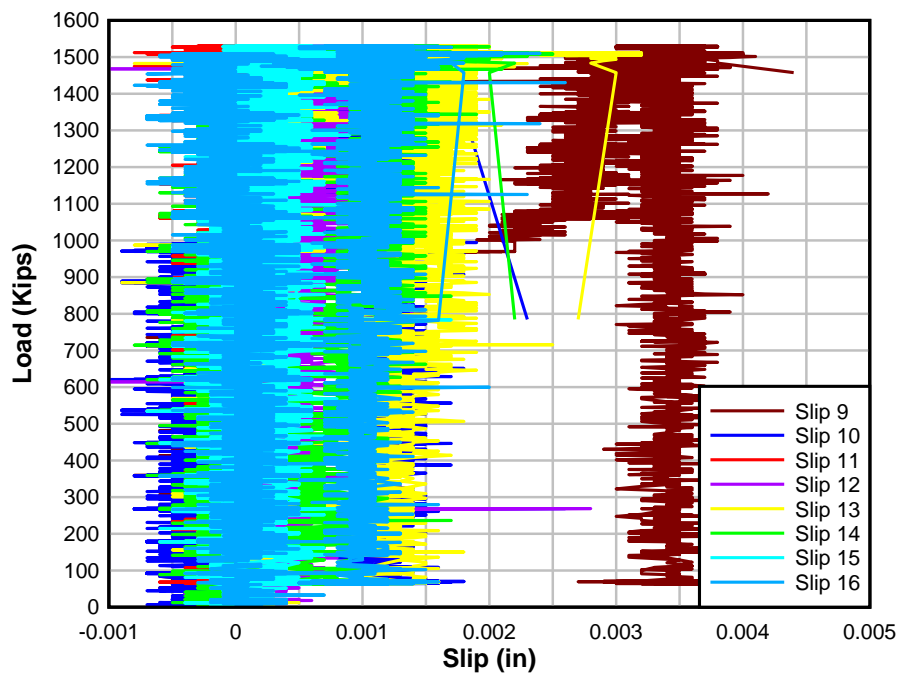


Figure F3.9: Column load vs. Slip (2 of 2) – Pile Cap #3

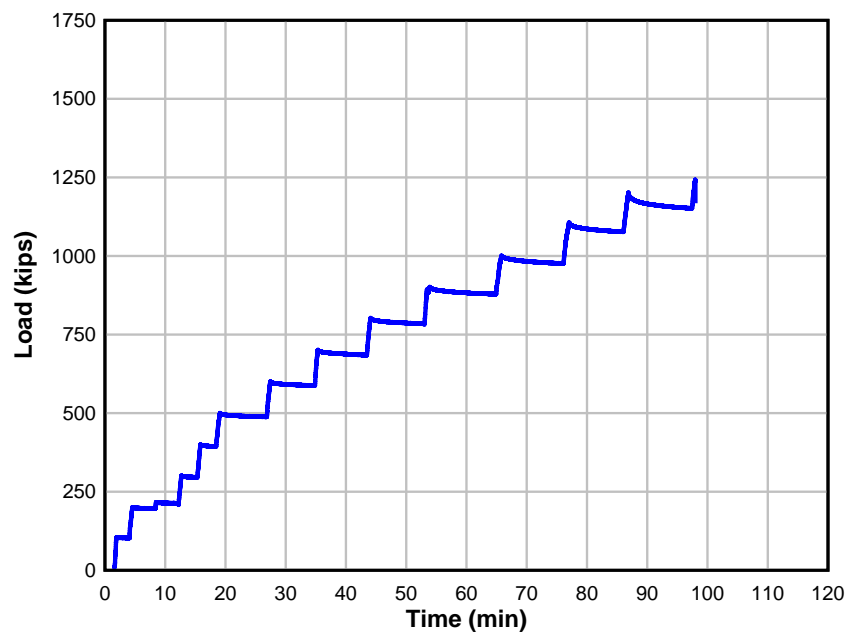


Figure F4.1: Loading – Pile Cap #4

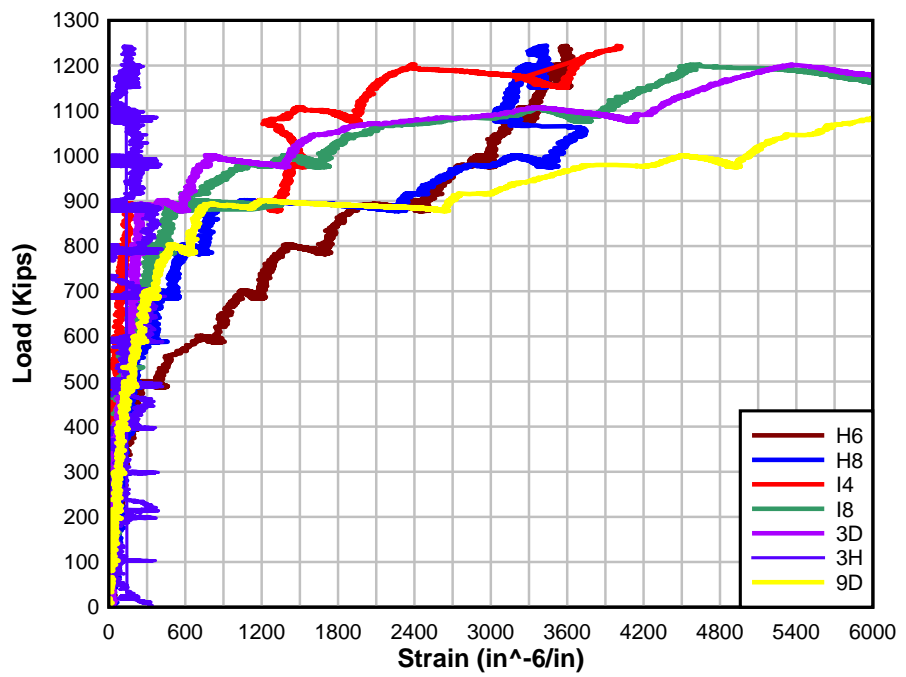


Figure F4.2: Column load vs. Strain (1 of 4) – Pile Cap #4

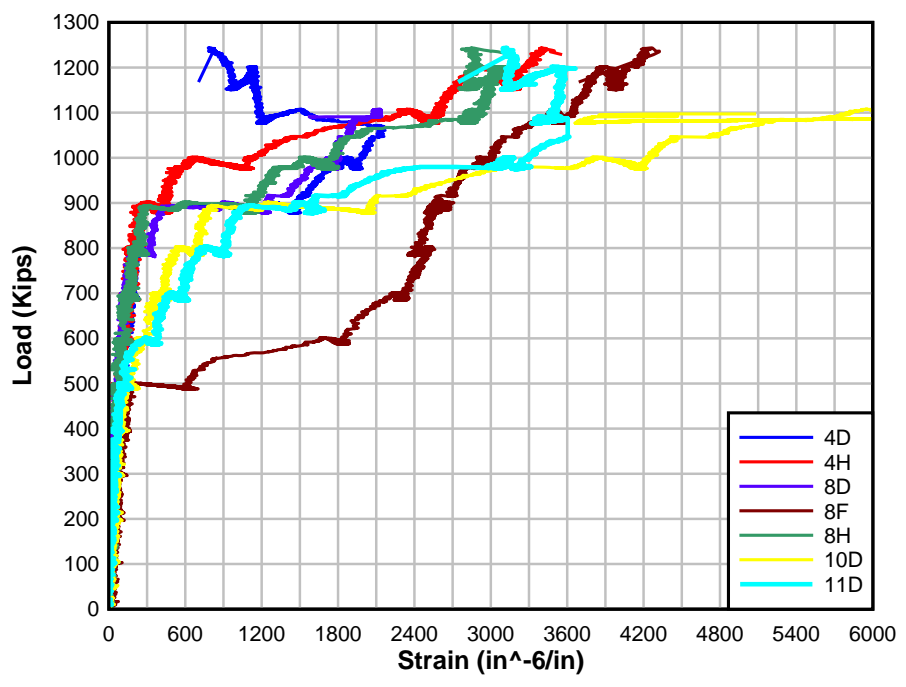


Figure F4.3: Column load vs. Strain (2 of 4) – Pile Cap #4

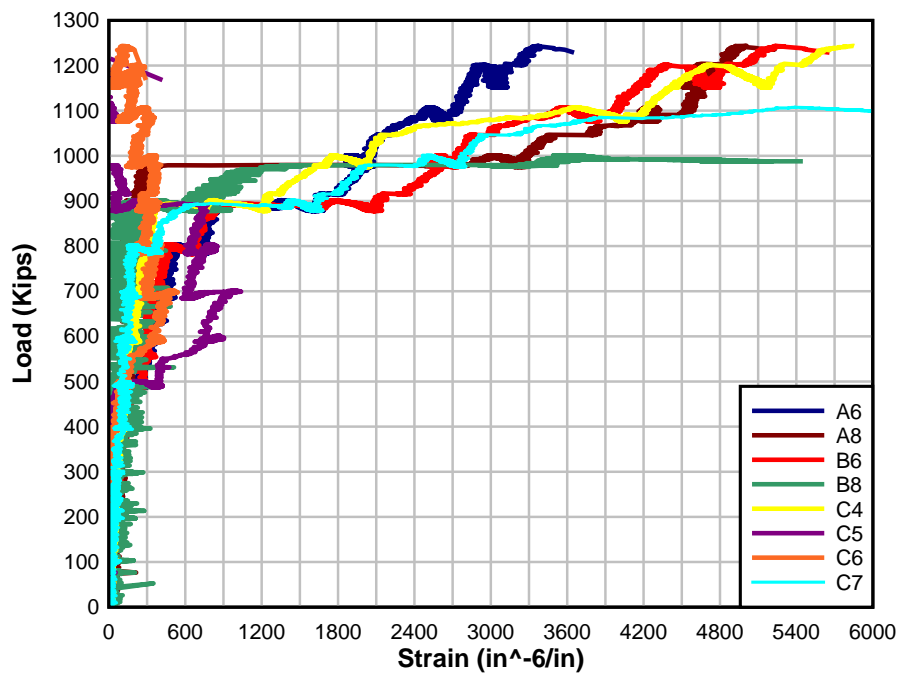


Figure F4.4: Column load vs. Strain (3 of 4) – Pile Cap #4

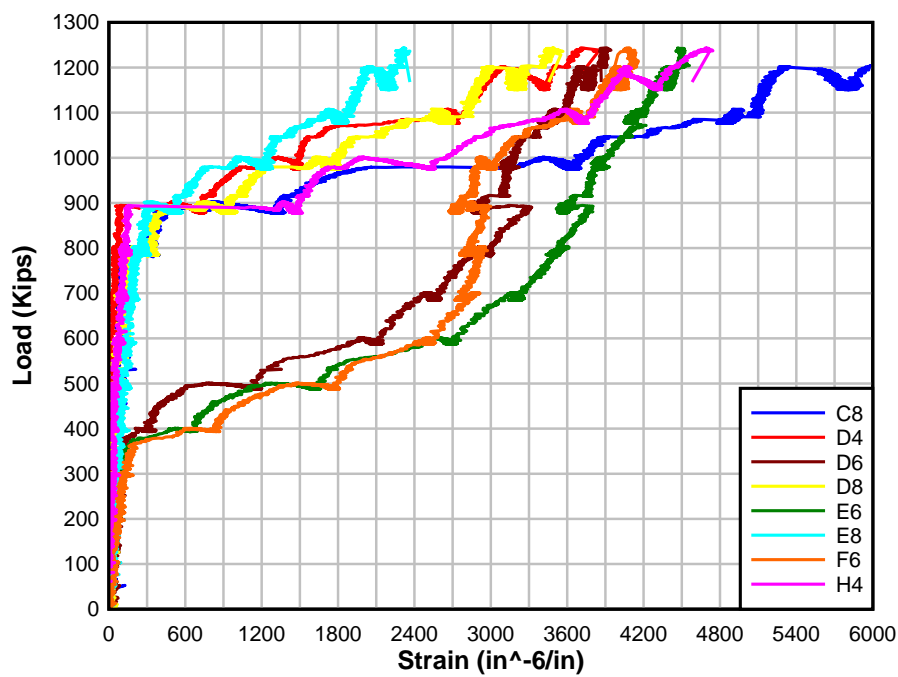


Figure F4.5: Column load vs. Strain (4 of 4) – Pile Cap #4

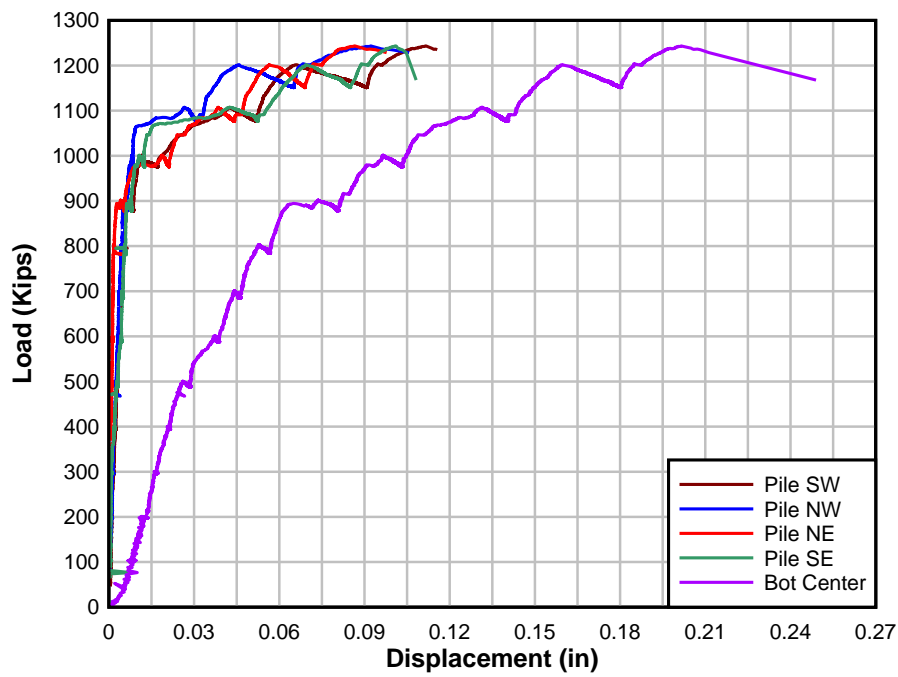


Figure F4.6: Column load vs. Displacement (1 of 2) – Pile Cap #4

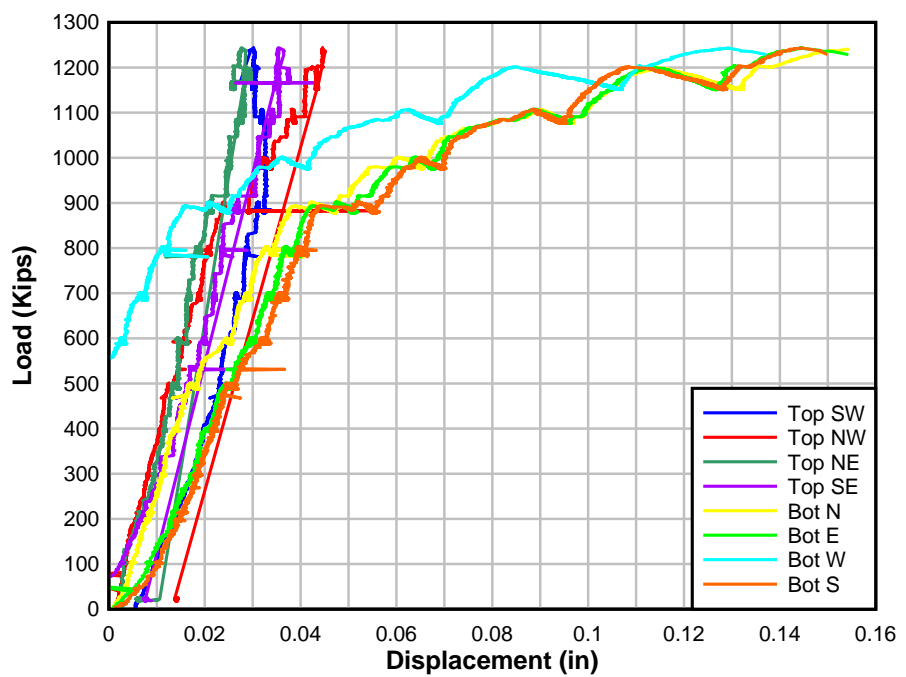


Figure F4.7: Column load vs. Displacement (2 of 2) – Pile Cap #4

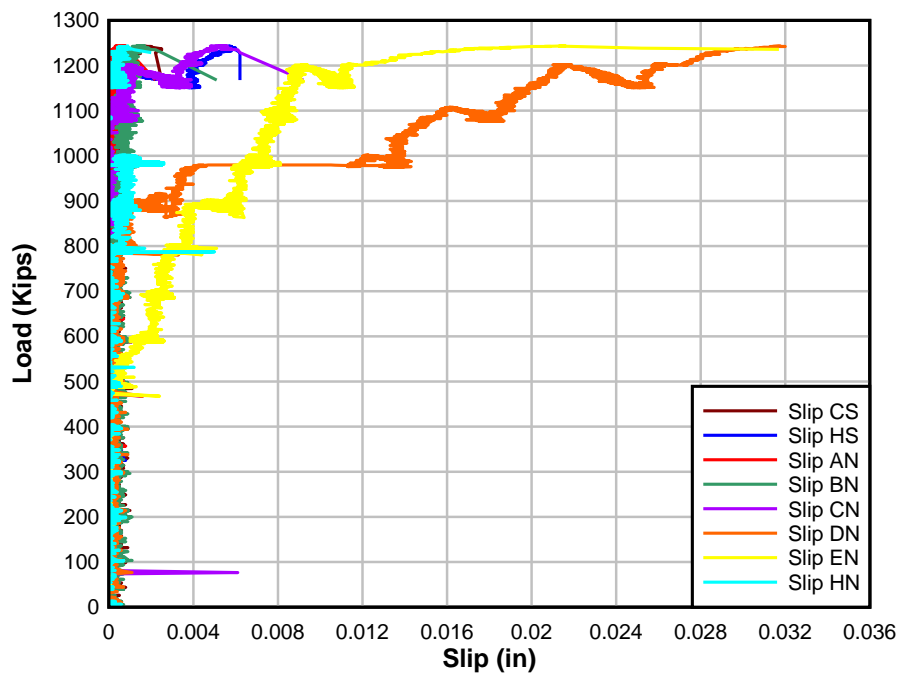


Figure F4.8: Column load vs. Slip (1 of 2) – Pile Cap #4

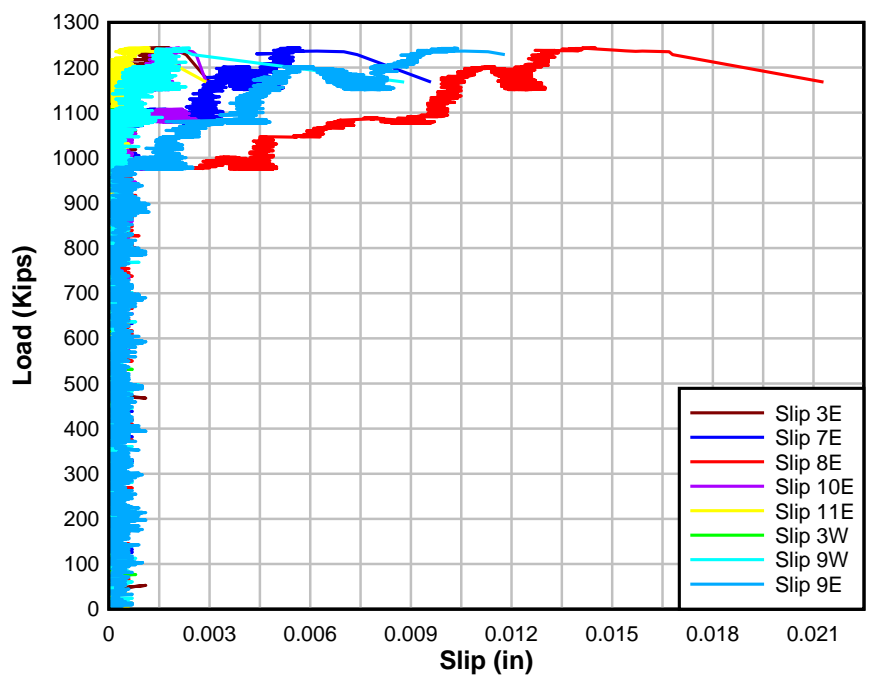


Figure F4.9: Column load vs Slip (1 of 2) – Pile Cap #4

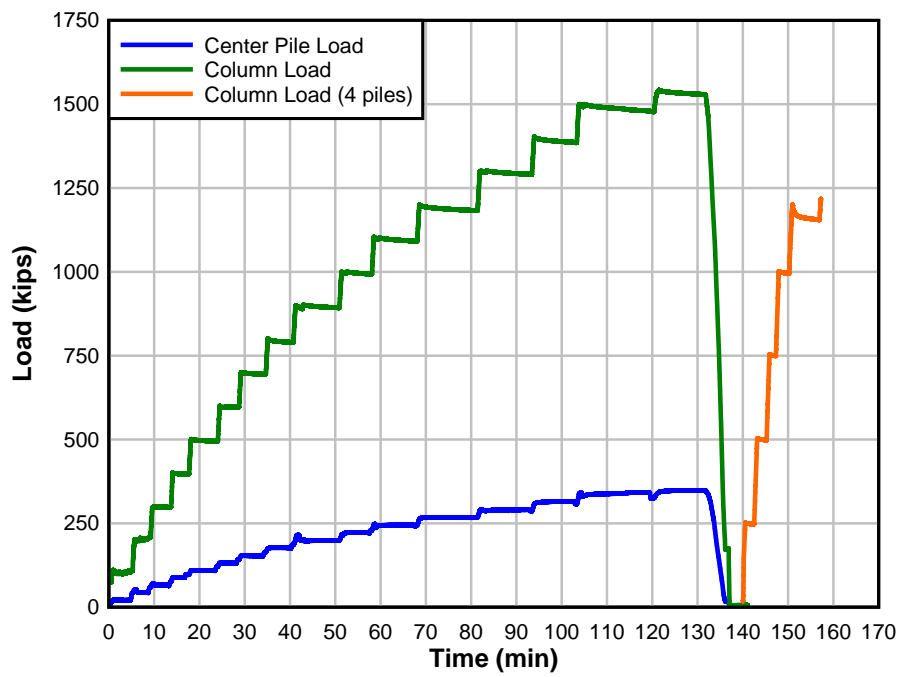


Figure F5.1: Loading – Pile Cap #5

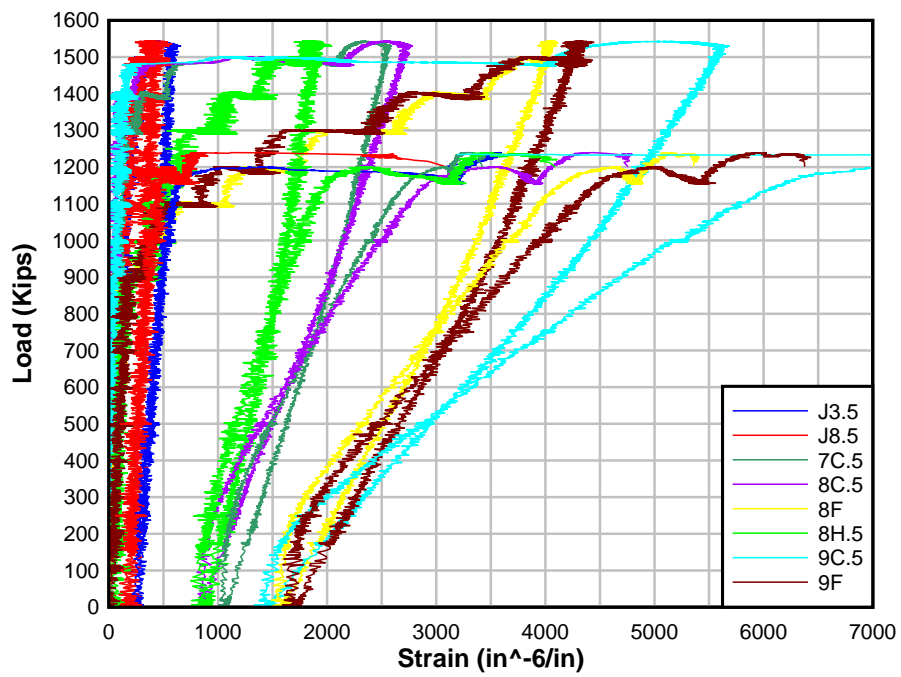


Figure F5.2: Column load vs. Strain (1 of 4) - Pile Cap #5 (5 piles)

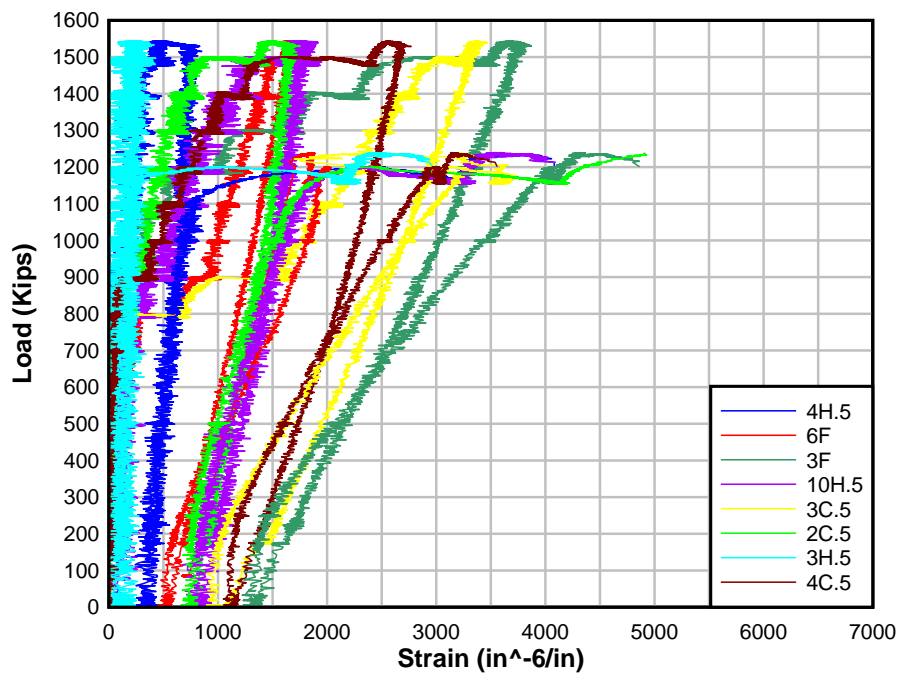


Figure F5.3: Column load vs. Strain (2 of 4) – Pile Cap #5 (5 piles)

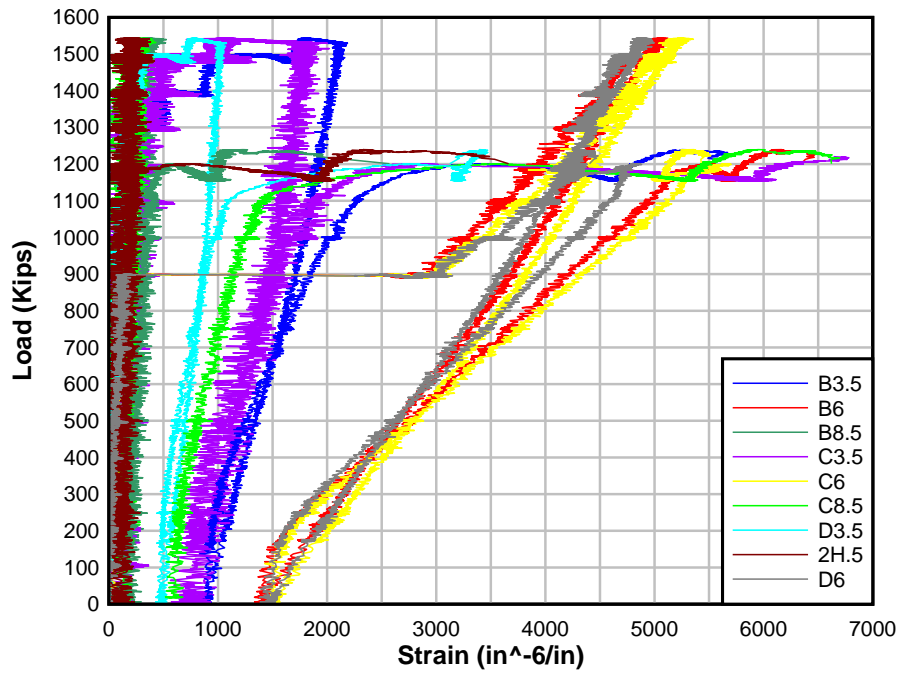


Figure F5.4: Column load vs. Strain (3 of 4) – Pile Cap #5

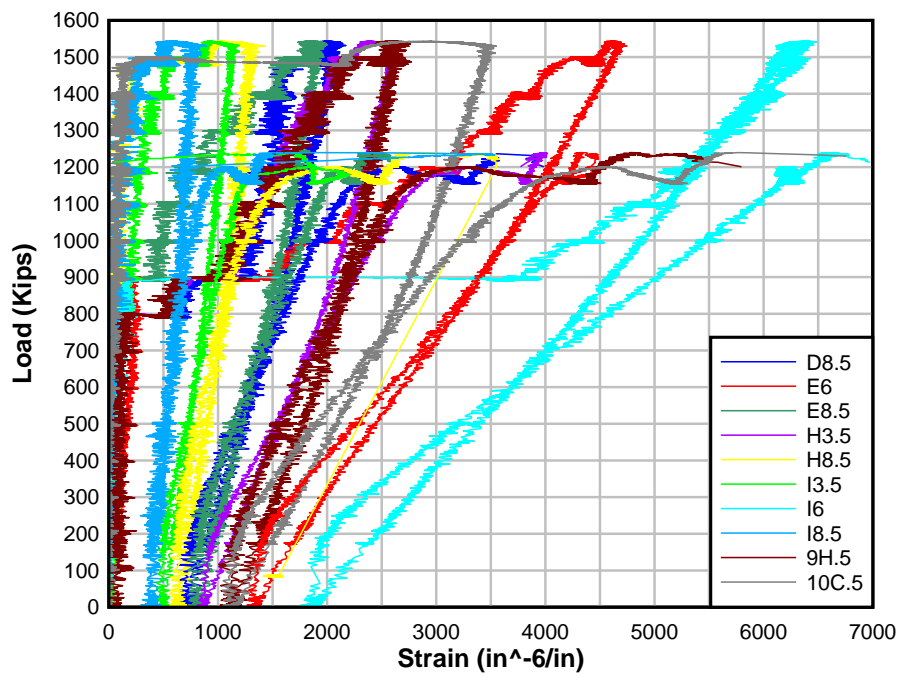


Figure F5.5: Column load vs. Strain (4 of 4) – Pile Cap #5

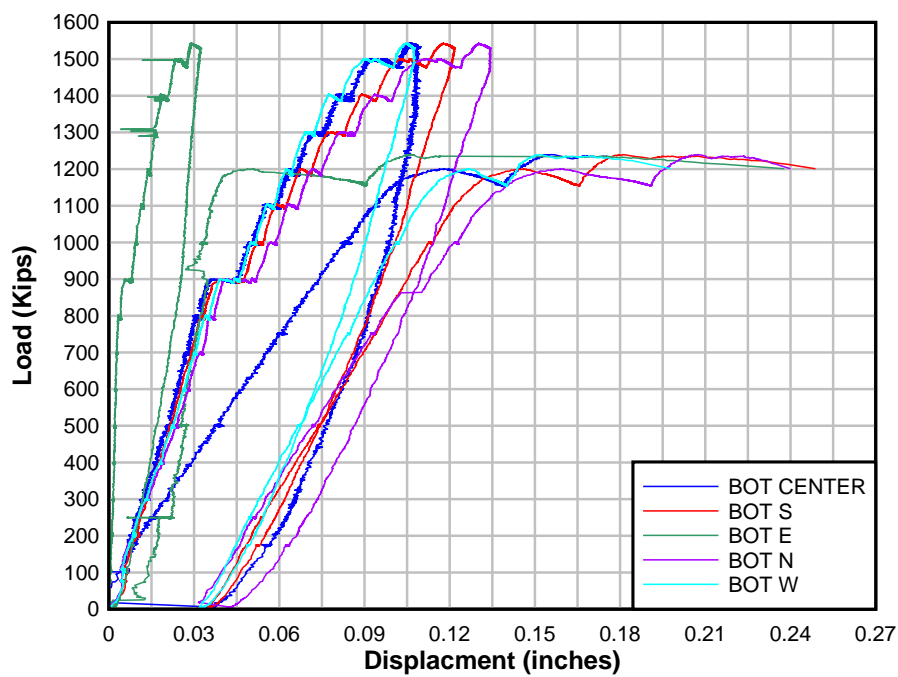


Figure F5.6: Column load vs. Displacement (1 of 2) – Pile Cap #5

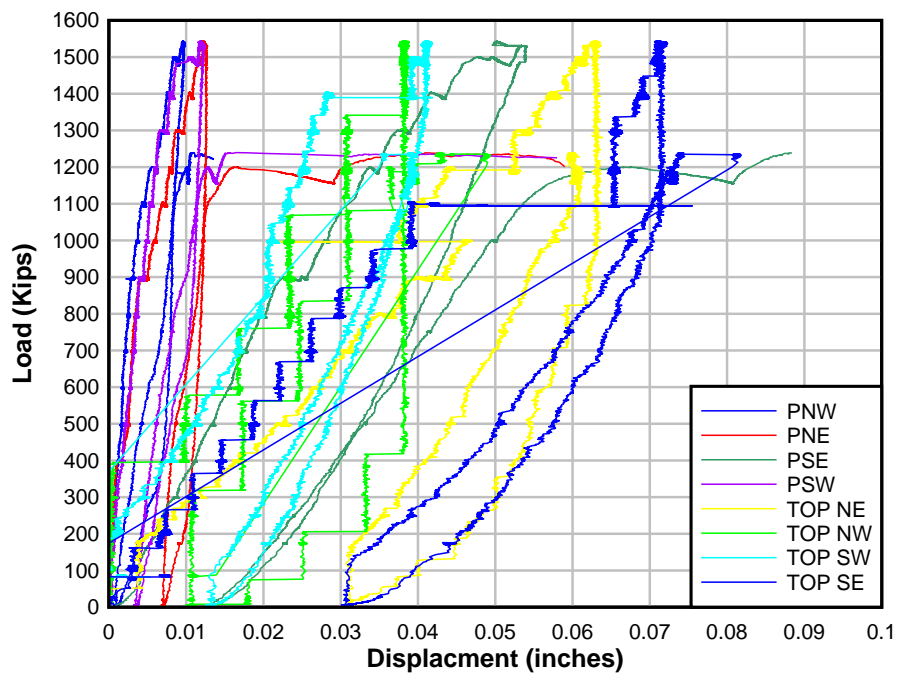


Figure F5.7: Column load vs. Displacement (2 of 2) – Pile Cap #5

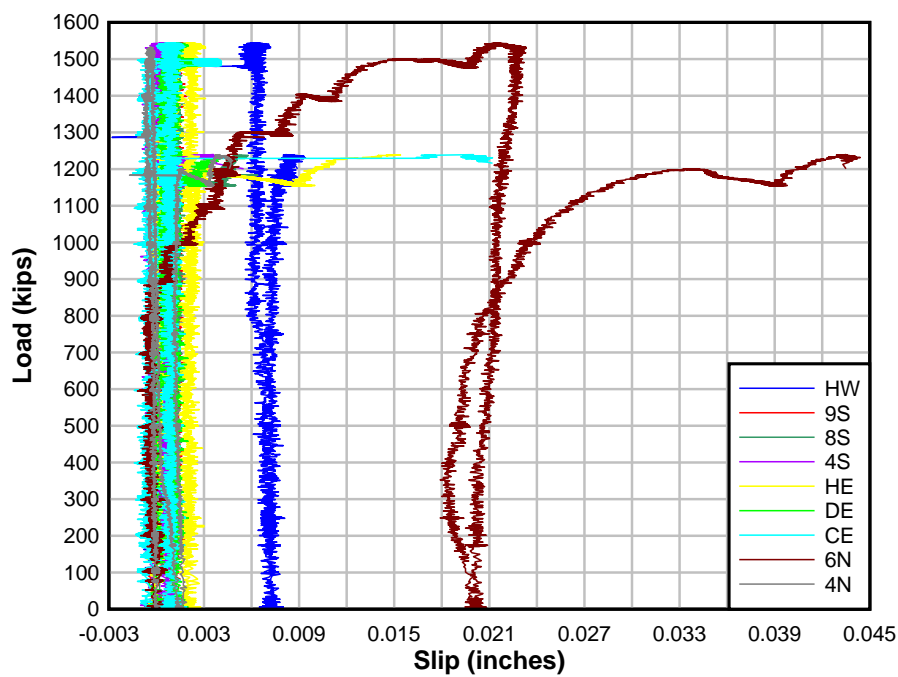


Figure F5.8: Column load vs. Slip (1 of 2) – Pile Cap #5

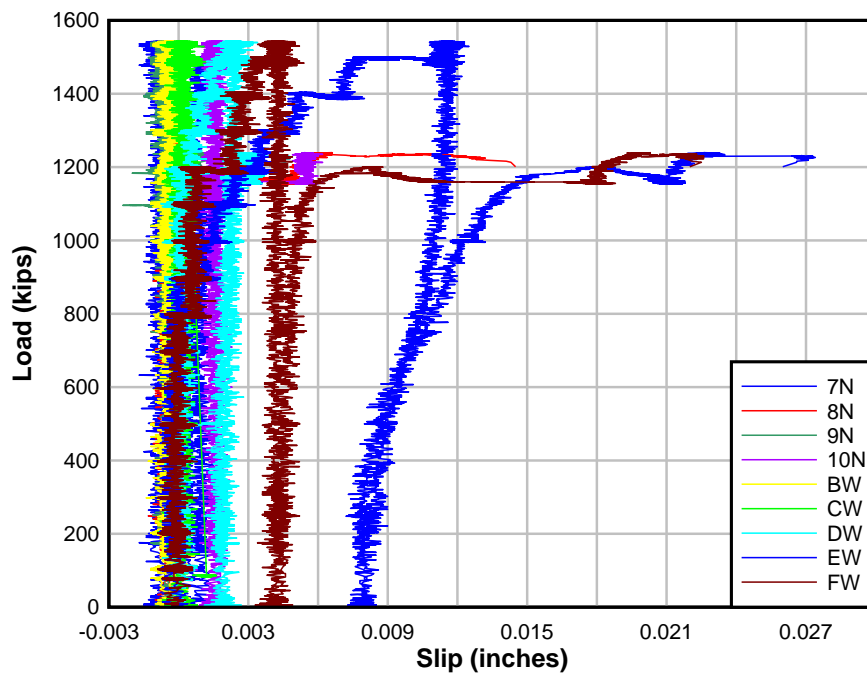


Figure F5.9: Column load vs. Slip (2 of 2) – Pile Cap #5

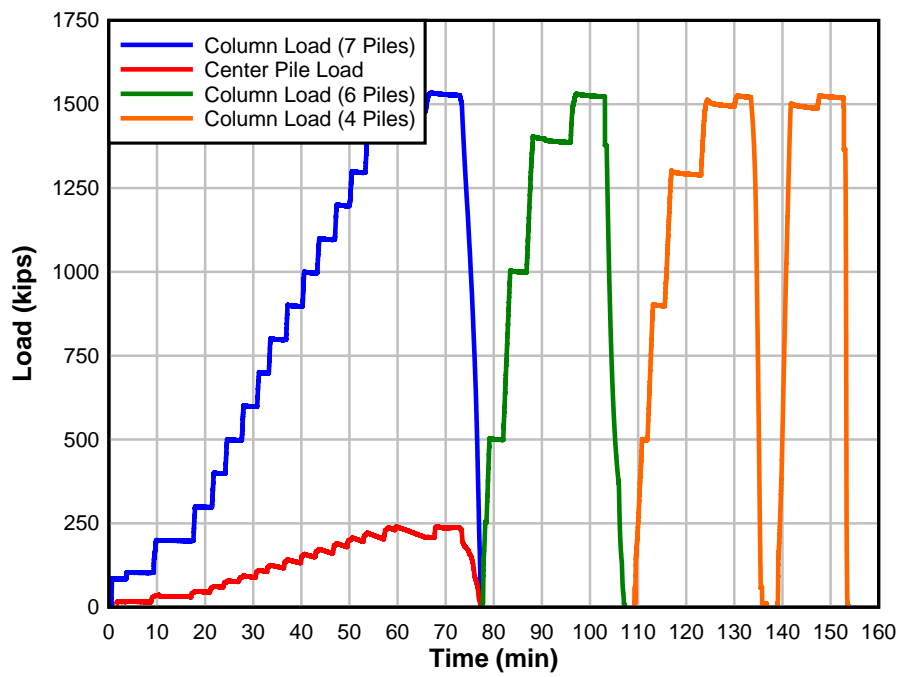


Figure F7.1: Column Load vs. Time – Pile Cap # 7

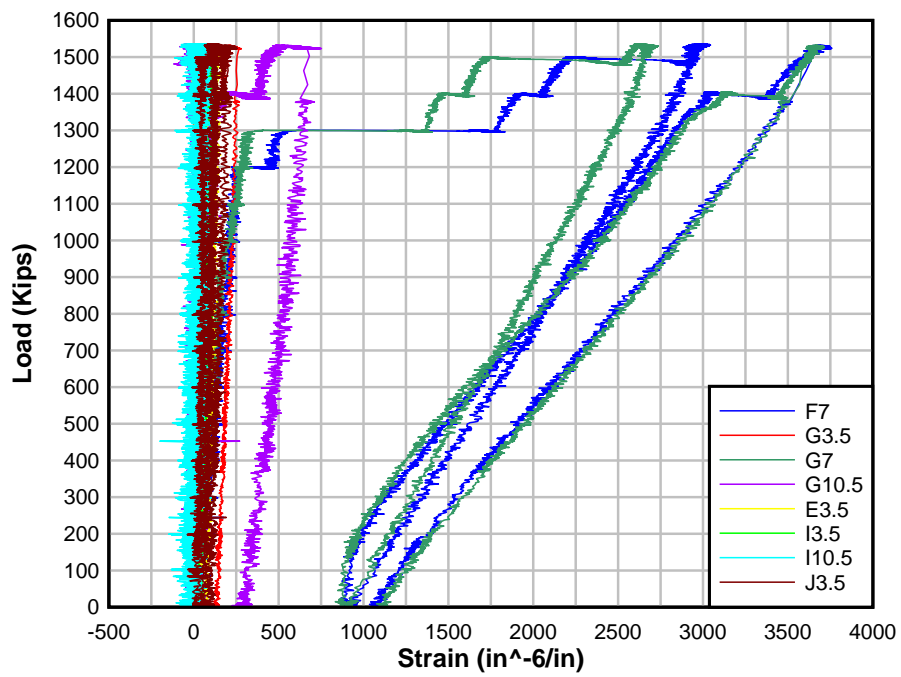


Figure F7.2: Column load vs. Strain (1 of 4) – Pile Cap #7 (7 and 6 piles)

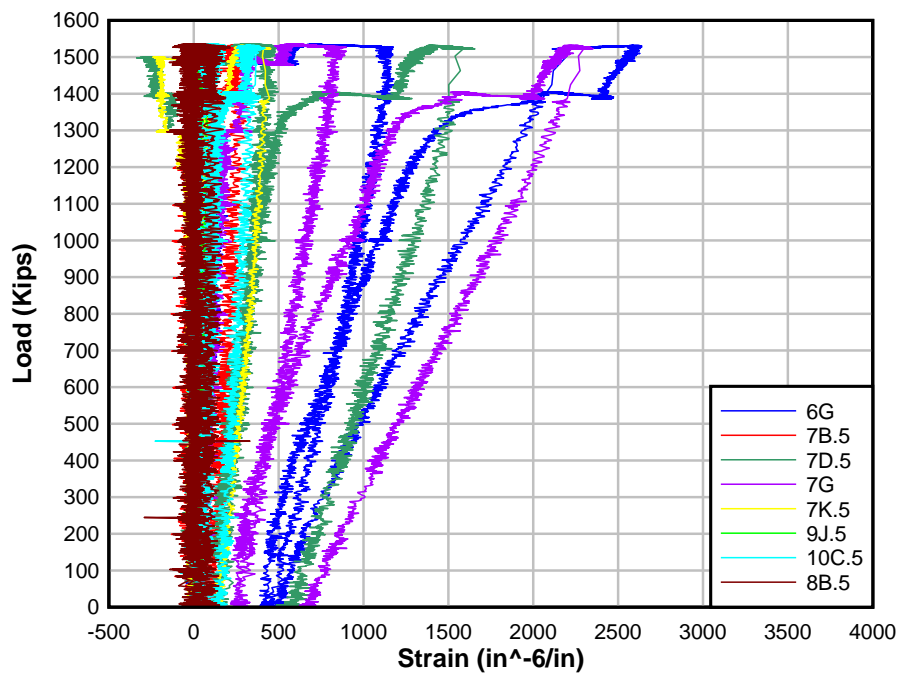


Figure F7.3: Column load vs. Strain (2 of 4) – Pile Cap #7 (7 and 6 piles)

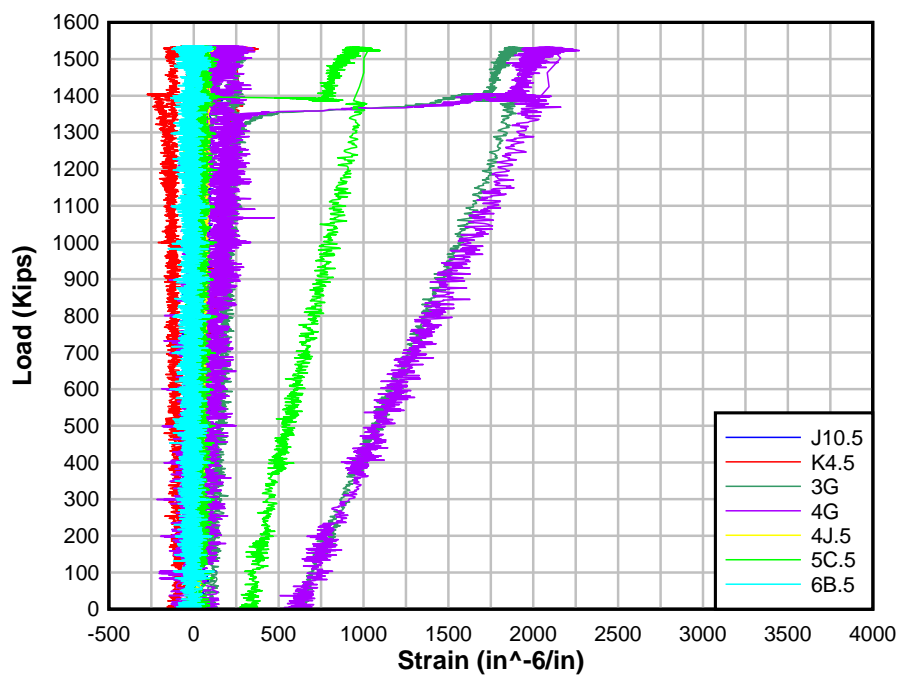


Figure F7.4: Column load vs. Strain (3 of 4) – Pile Cap #7 (7 and 6 piles)

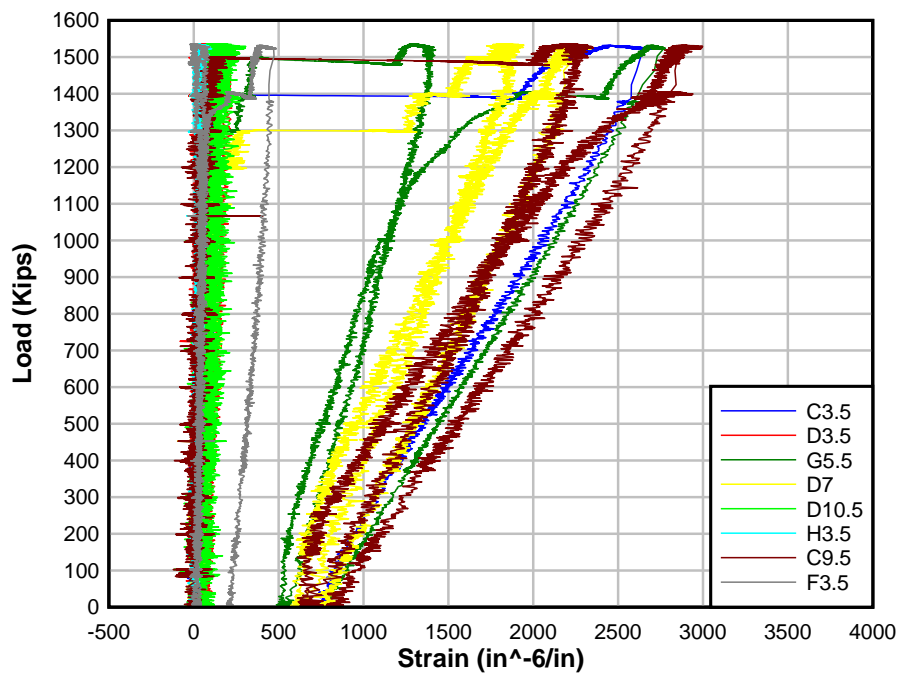


Figure F7.5: Column load vs. Strain (4 of 4) – Pile Cap #7 (7 and 6 piles)

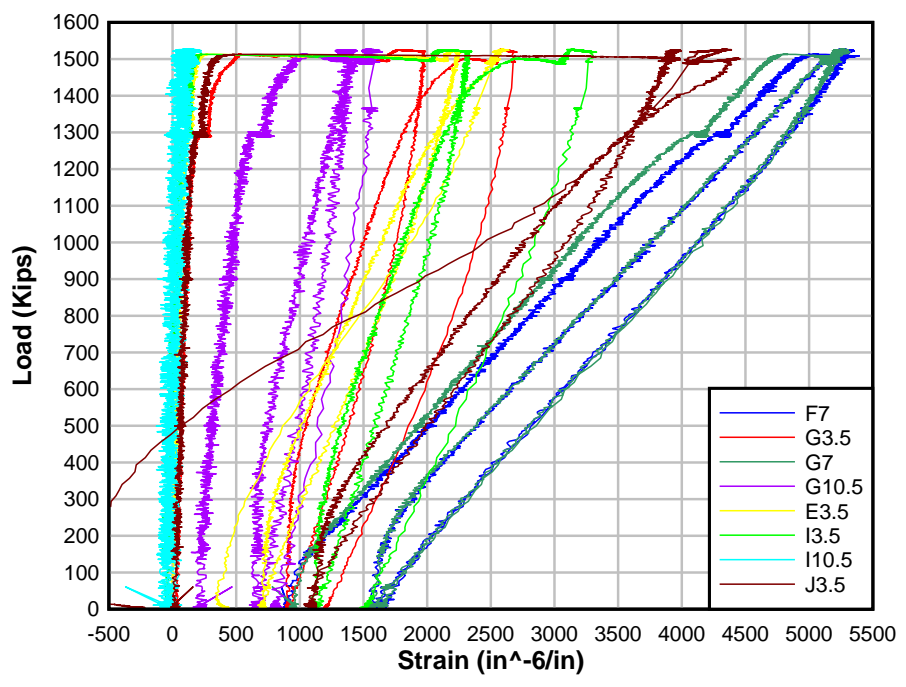


Figure F7.6: Column load vs. Strain (1 of 4) – Pile Cap #7 (4 Piles)

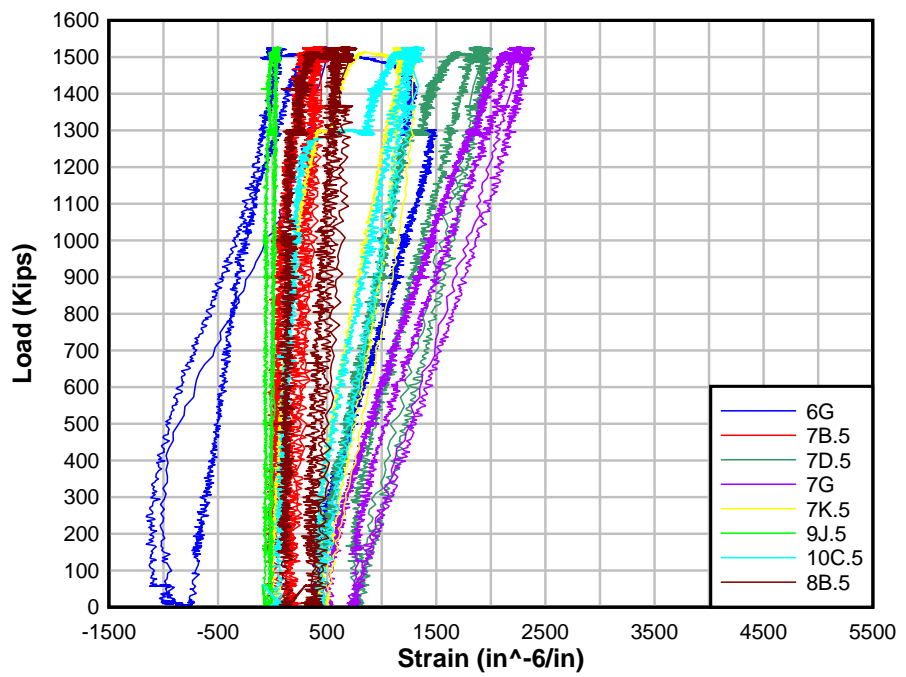


Figure F7.7: Column load vs. Strain (2 of 4) – Pile Cap #7 (4 Piles)

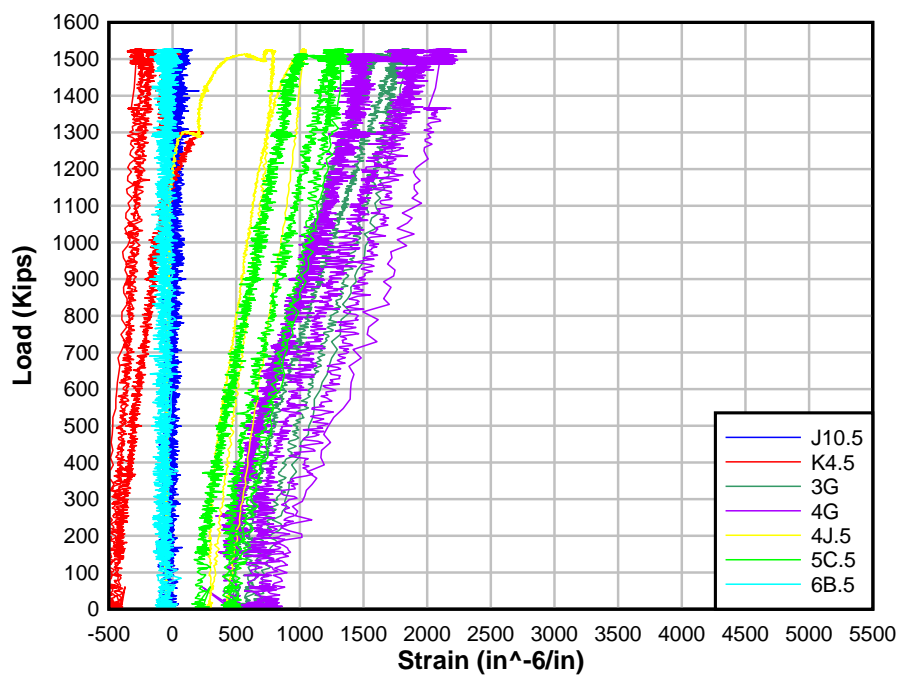


Figure F7.8: Column load vs. Strain (3 of 4) – Pile Cap #7 (4 Piles)

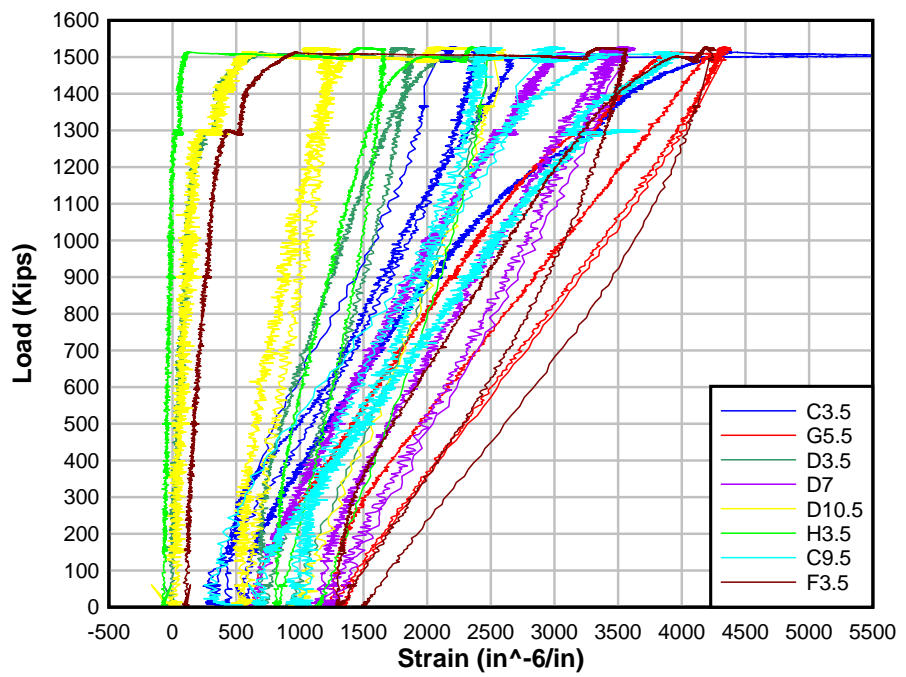


Figure 7.9: Column load vs. Strain (4 of 4) – Pile Cap #7 (4 Piles)

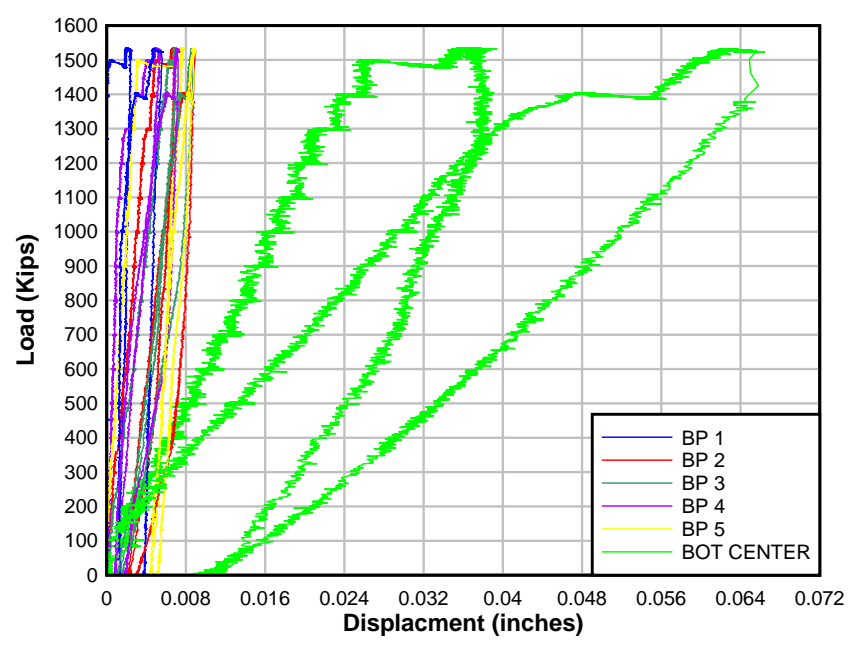


Figure F7.10: Column load vs. Displacements (1 of 2) – Pile Cap #7 (7 and 6 Piles)

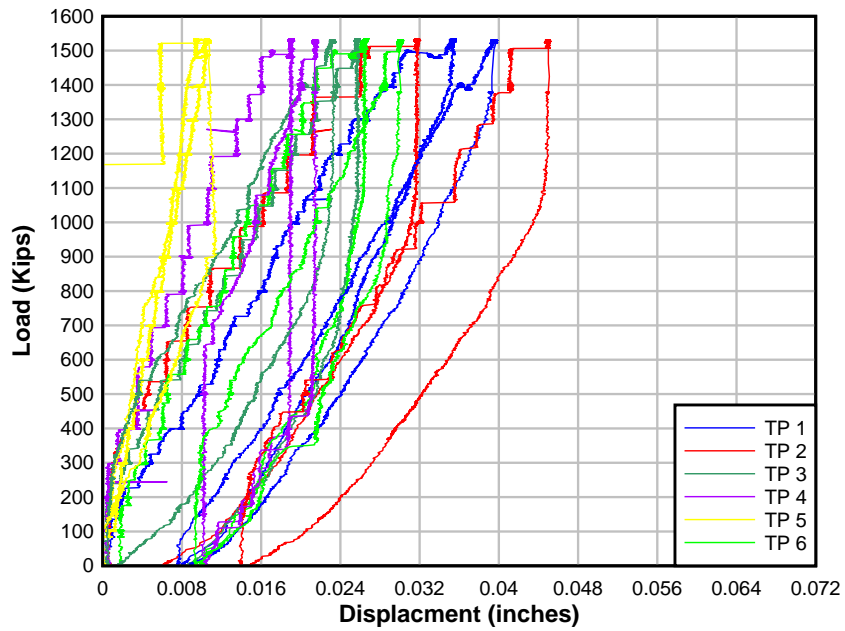


Figure F7.11: Column load vs. Displacement (2 of 2) – Pile Cap #7 (7 and 6 Piles)

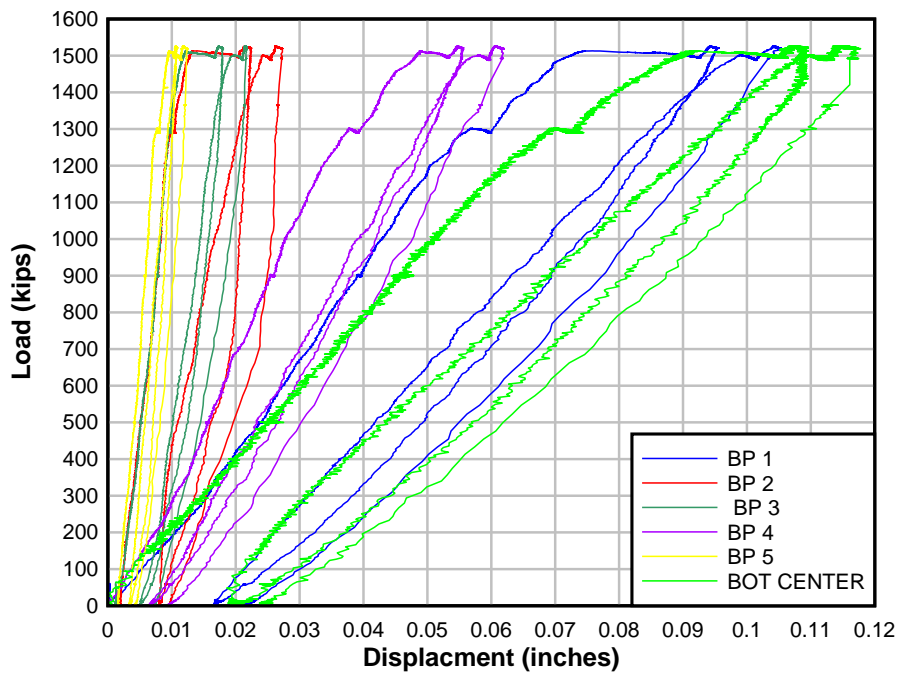


Figure F7.12: Column load vs. Displacement (1 of 2) – Pile Cap #7 (4 Piles)

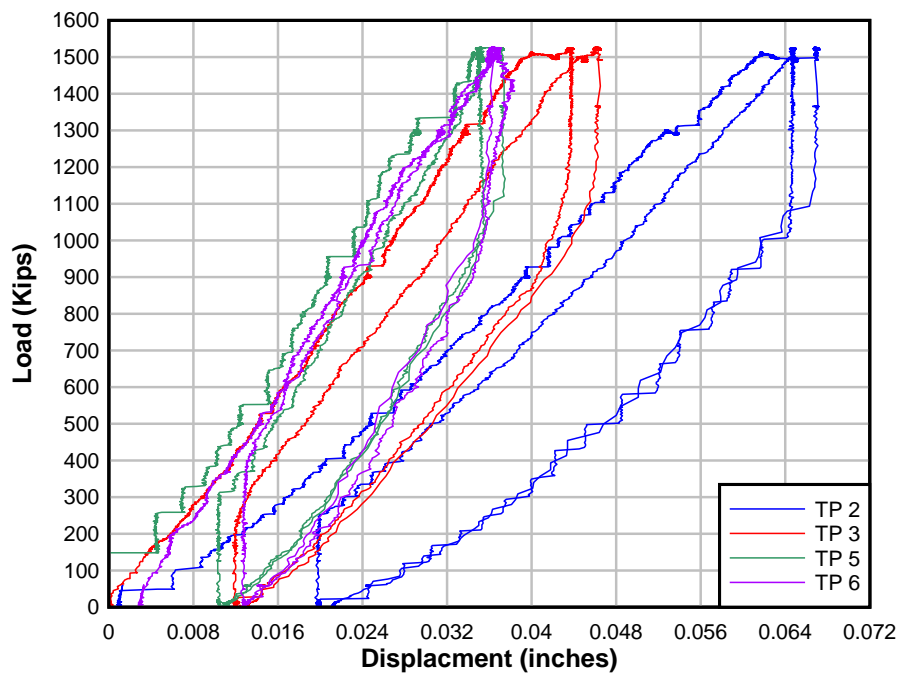


Figure F7.13: Column load vs. Displacement (2 of 2) – Pile Cap #7 (4 Piles)

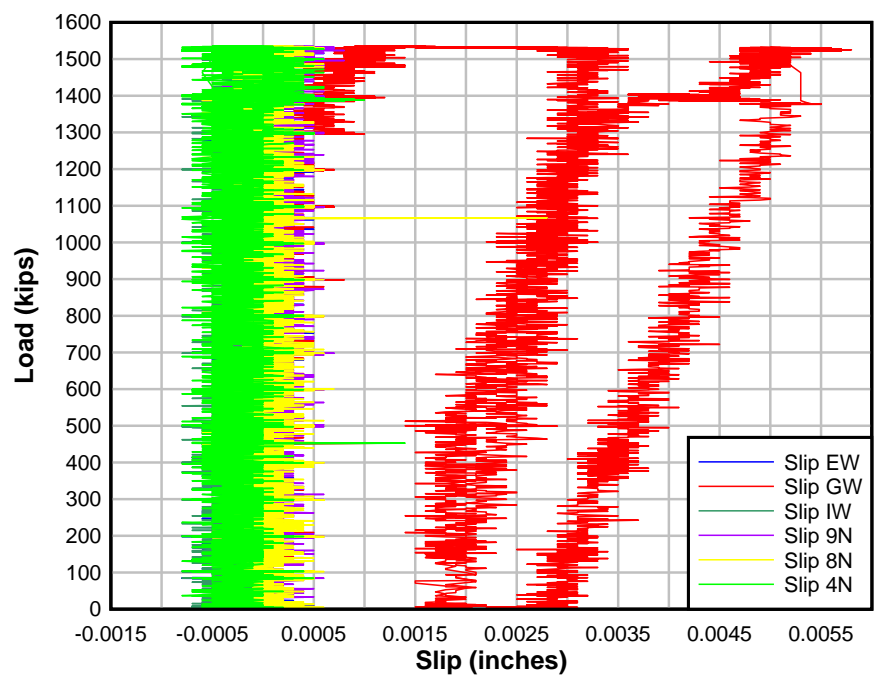


Figure F7.14: Column load vs. Slip (1 of 3) – Pile Cap #7 (7 and 6 Piles)

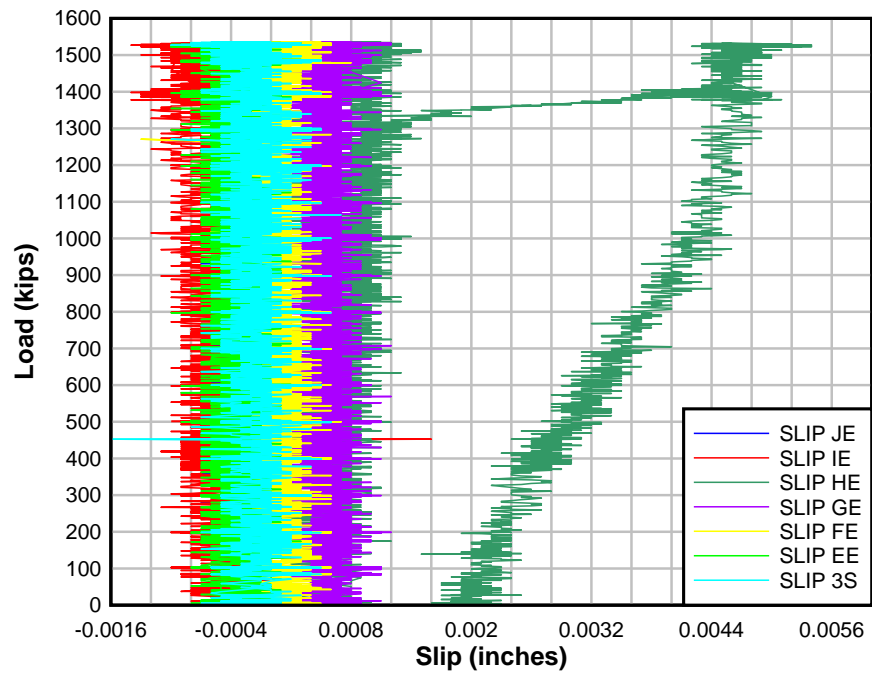


Figure F7.15: Column load vs. Slip (2 of 3) – Pile Cap #7 (7 and 6 Piles)

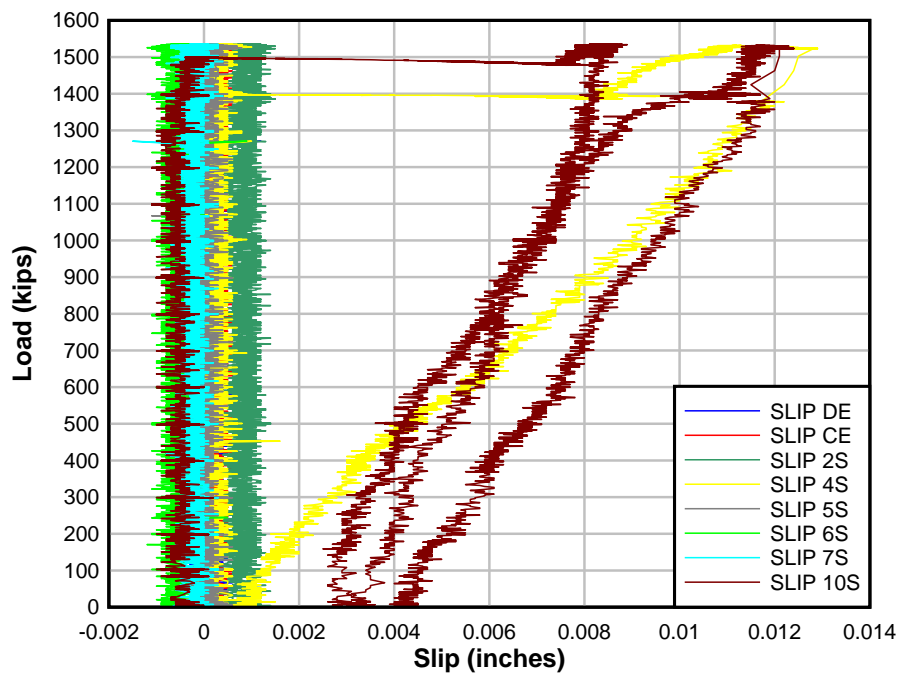


Figure F7.16: Column load vs. Slip (3 of 3) – Pile Cap #7 (7 and 6 Piles)

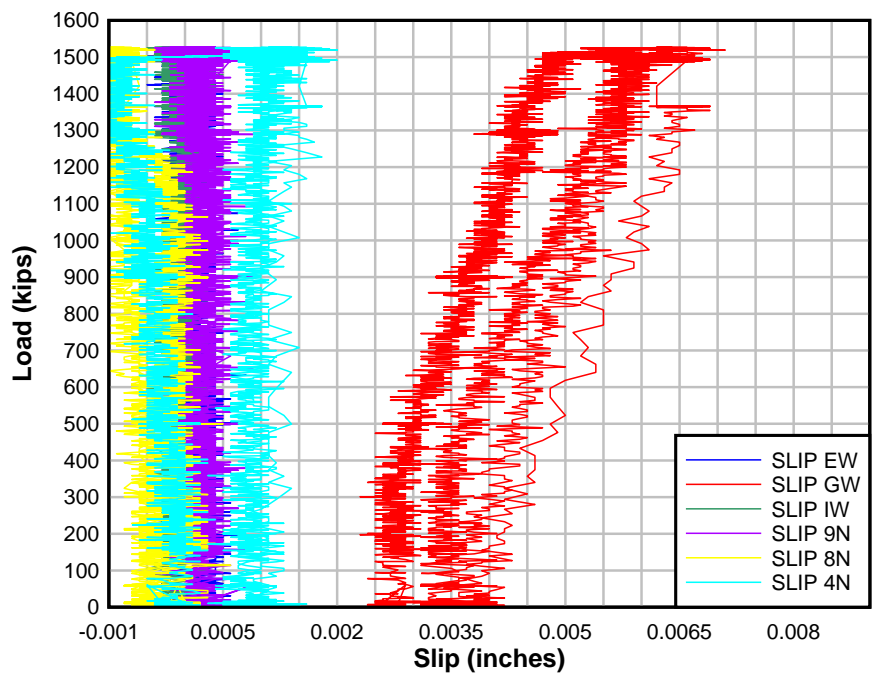


Figure F7.17: Column load vs. Slip (1 of 3) – Pile Cap #7 (4 Piles)

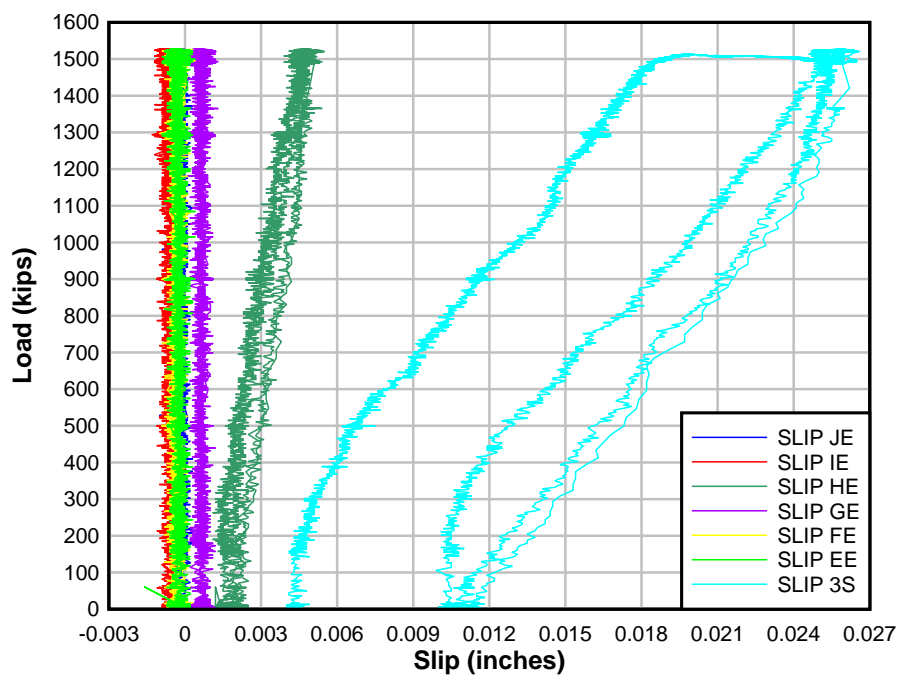


Figure F7.18: Column load vs. Slip (2 of 3) – Pile Cap #7 (4 Piles)

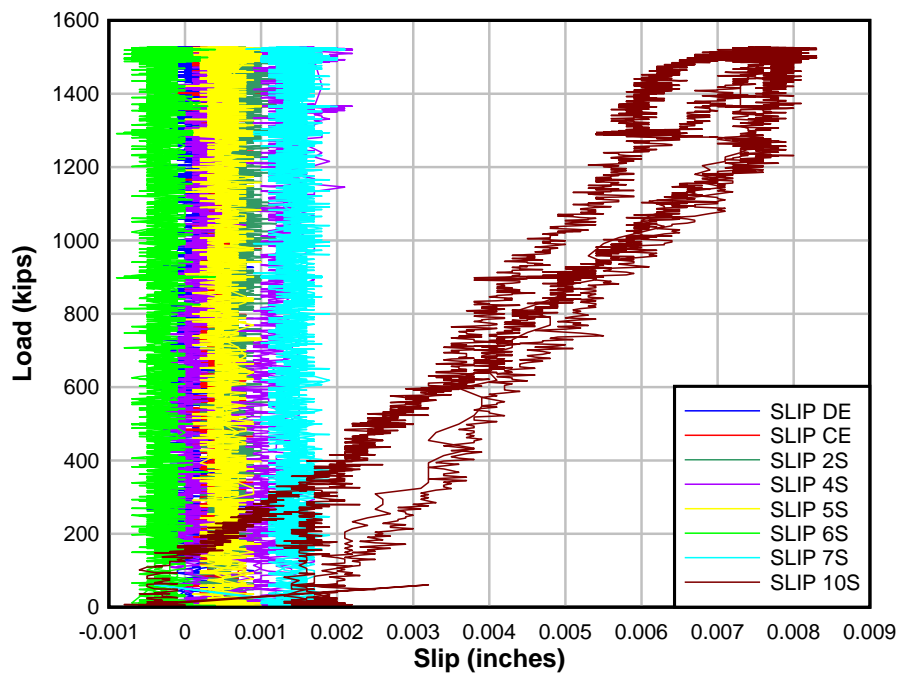


Figure F7.19: Column load vs. Slip (3 of 3) – Pile Cap #7 (4 Piles)

